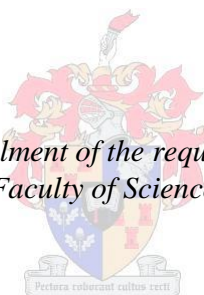


Development and Implementation of a Flow injection analyser with chemiluminescence for detection of sub-nanomolar Fe in seawater

by
Raimund Rentel

*Thesis presented in fulfilment of the requirements for the degree of
Master of Science in the Faculty of Science at Stellenbosch University*



Supervisor: Prof. Alakendra N. Roychoudhury
Co-supervisor: Dr Eva Bucciarelli

December 2014

Declaration

By submitting this thesis electronically, I declare that the entirety of the work contained therein is my own original work, that I am the authorship owner thereof (unless to the extent explicitly otherwise stated) and that I have not previously in its entirety or in part submitted it for obtaining any qualification.

Signature:

Date: 15 August 2014

Abstract

Iron is an essential micronutrient for all phytoplankton and is found in seawater at picomolar-level concentrations. For the first time in South Africa, a technique that utilizes a flow injection analyser (FIA) coupled with a chemiluminescence reaction has been developed for the analysis of Fe in seawater samples. The developed method is an improvement on similar available methods and uses commercially available resin (IDA) as opposed to the one that requires synthesis in the laboratory. Furthermore, the method requires reduced reagent concentrations thereby providing better results in a cost-efficient and easy manner. The improvements resulted in better precision while eliminating the loss of resin through bleeding, a common problem when using 8-HQ resin as per prior methods. Method validation was performed using internationally calibrated reference material provided by GEOTRACES and the values obtained were within the error limits of certified range. An inter-laboratory calibration was also conducted as part of the verification of the system. Surface samples from the SANAE 51 cruise were analysed for dFe and TdFe. Subsequently, the method was implemented on the SANAE 53 voyage on board the SA Agulhas II, to assess trace metal sampling protocol for any contamination issues, as well as for the analyses of collected samples. Current results suggest some contamination during collection stages, but this is still to be verified by complementary data on macronutrients and chlorophyll. The method was successfully developed and implemented in a land based clean laboratory, as well as on board a vessel.

Opsomming

Yster is 'n noodsaaklike mikrovoedsel vir fitoplankton en word in seewater in pikomolêre konsentrasies gevind. Hierdie lae konsentrasies en potensiële besoedeling gedurende monsteropname vanaf 'n skip se platform maak akkurate Fe-analise moeilik. Vir die eerste keer in Suid-Afrika is 'n tegniek ontwikkel wat gebruik maak van 'n vloeï- inspuitinganaliseerder (VIA), met 'n geassosieerde chemiluminessensiereaksie, om die analise van Fe in seewatermonsters uit te voer. In teenstelling met soortgelyke bestaande metodes wat laboratorium-gesintetiseerde hars vereis, is die nuut-ontwikkelde metode 'n verbetering wat gebruik maak van 'n kommersieel-beskikbare hars (IDA). Verder vereis die metode verminderde reagenskonsentrasies wat sodoende beter resultate lewer op 'n koste-effektiewe en eenvoudiger wyse. Die verbeteringe het gelei tot verhoogde akkuraatheid en uitskakeling van die verlies van hars deur dreinerings – 'n algemene probleem wat ondervind is met die gebruik van 8-HQ hars in vorige metodes. Geldigheidsbepaling van die metode is met internasionaal-gekalibreerde verwysingsmateriaal, verskaf deur GEOTRACES, uitgevoer. Die waardes wat verkry is, was binne die foutgrense van die gesertifiseerde skaal. 'n Interlaboratorium-kalibrasie is ook uitgevoer as deel van die verifikasie van die stelsel. Daarna is die metode geïmplementeer gedurende die SANA 53 reis op die SA Agulhas II, om die spoormetaal-monsternemingprotokol vir enige besoedelingskwessies te evalueer, asook vir die ontleding van versamelde monsters. Huidige resultate dui op 'n mate van besoedeling tydens die versamelingstadiums, maar dit moet nog geverifieer word deur aanvullende data van die totale oplosbare Fe, makrovoedingstowwe en chlorofil.

Acknowledgements

I would like to say my thanks to CSIR and the SOCCO group for the facilities and equipment supplied by them during the cruises and development of the method. I would like to thank the NRF (SNA2006041200002) and Inkaba yeAfrica (Publication No. 114) for the funding of the project.

Thank you to the crew and captain of the SA Agulhas and SA Agulhas II for the assistants during the deployment of the equipment utilized during the sampling, as well as to the staff from Sea Technologies Services (STS) for running the CTD and to the passengers on of the SANAE 53 cruise who have assisted in carrying the Go-Flo bottles from the laboratory to the CTD rosette and back.

Great thanks go out to E. Bucciarelli for the visit to the LEMAR as well as to M. Lohan for accommodating us in their laboratory and assist in the development phase of the FIA.

A thank you also goes out to T. Kruger and M. le Roux for assisting in the translation of the abstract from English to Afrikaans.

Table of contents

Declaration.....	I
Abstract	II
Opsomming	III
Acknowledgements.....	IV
Table of contents	V
List of Figures	VIII
List of Tables	XI
Abbreviations	XII
Chapter 1: Introduction	1
1.1 The Role of Iron	1
1.2 Aims and objective	6
1.3 Structure of the thesis	6
Chapter 2: Historical development of analytical Methods used for the analysis of Fe.....	8
2.1 Historical overview of methods.....	8
2.2 Land versus ship based methods.....	10
2.2.1 Pure land based methods.....	11
2.2.1.1 Inductively coupled plasma mass spectrometry	11
2.2.1.2. Graphite furnace atomic absorption spectrometry	13
2.2.1.3. Electrochemical stripping procedures.....	14
2.2.2. Land and Ship based methods	15
2.2.2.1 Colorimetry.....	15
2.2.2.2. Flow Injection analysers	16
2.2.3. Other systems or methods.....	22
Chapter 3: Development of Flow Injection Analyser with Chemiluminescence	24
3.1. Analytical setup.....	24
3.1.1. The manifold.....	24
3.1.2. The Setup.....	25
3.1.3. Resins	27
3.1.4. Chemicals and reagents and preparation	28
3.1.5. Determination of Fe Concentration	29
3.1.5.1 Standard and Sample Preparation	29

3.1.5.2 The operating cycle	29
3.1.5.3. Blank determination	30
3.1.5.4. Calculating the Concentration of Fe	31
3.2. Development of the method	38
3.2.1 Length of the reaction coil.....	38
3.2.2 Reaction temperature	39
3.2.3 Luminol brands	40
3.2.4 Reagent concentrations.....	41
3.2.5 Chelating pH.....	42
3.2.6 Buffer.....	44
3.2.7 Accuracy.....	45
3.2.8 Precision.....	49
3.2.9 Internal Reference Material	49
3.3 Problems encountered during the development stage.....	50
3.3.1 Backpressure	50
3.3.2 Loss of resin	50
3.3.3 Contamination	51
Chapter 4: Application of the FIA-CL to measure iron in Southern Ocean Samples	53
4.1 Discovery samples.....	53
4.1.1 Sampling	54
4.1.2 Analytical method	54
4.1.3 Results and Discussion	54
4.2 SANAE 51 samples.....	57
4.2.1 Sampling	58
4.2.2 Analysis.....	59
4.2.3 Results	59
4.2.4 Discussion.....	61
4.3 Optimization of on-board sampling protocol: SANAE 53	63
4.3.1 Transportation of Go-Flo bottles	64
4.3.2 Sampling Procedure	65
4.3.3 Mega Station 2	67
Chapter 5: Conclusion	72
References	74

Appendices	80
Appendix 1	80
Appendix 2	82
Appendix 3	85
Appendix 4	86
Appendix 5	87
Appendix 6	88

List of Figures

Chapter 1: Introduction

Figure 1.1: Barnola et al., (2003) CO ₂ concentrations over the past 400 kyr BP	1
Figure 1.2: Displaying the oceanic physical and biological pump of the carbon (Chisholm 2000)..	2
Figure 1.3: Photosynthesis cycle (Briat et al., 2014). Iron is essential for the structure and function of the photosynthetic electron transfer chain. There are in total 22 Fe ions responsible for the function of photosynthesis.....	3
Figure 1.4: Iron Cycle, simplified from Nédélec (2006). Blue arrows indicate input of Fe, and red arrows indicate removal of Fe.....	4
Figure 1.5: Physical and Chemical speciation of Fe found in the Ocean, (Bruland and Rue (2001)).....	5

Chapter 2: Historical development of analytical Methods used for the analysis of Fe

Figure 2.1: The interface region of an ICP-MS (Ruth (2005)).	11
Figure 2.2: Representation of a GFAAS system. The cuvette revers to the graphite coated furnace (Thermal Elemental, 2001).....	13
Figure 2.3: Displays luminol and its products during the formation of the chemiluminescence reaction (Figure after Xiao <i>et al.</i> , 2000).....	21

Chapter 3: Development of Flow Injection Analyser with Chemiluminescence

Figure 3.1: Diagram showing the FIA setup.....	24
Figure 3.2: The photon tube multiplier used in the system	25
Figure 3.3: Diagram displaying the spiral used in front of the PMT.....	26
Figure 3.4: Indicating the positions during the load (a) and inject (b) phase.....	30
Figure 3.5: Blank determination for the Peak Height (PH) method.....	30
Figure 3.6: Blank determination for the Integral method.....	31
Figure 3.7: Graph displays how the PH method is calculated, by deducting the starting value (399 420) of the graph from the peak value (6 609 548).....	32
Figure 3.8: Indicates the calibration graph obtained when plotting the added standard concentration against the blank corrected peak height.....	33
Figure 3.9: Graph obtained after correcting for the baseline, removing the negative dip prior to the rise in the graph.....	35
Figure 3.10: Bringing the baseline to zero to allow for the area under the graph to be determined in the integral method.....	36
Figure 3.11: Calibration curve obtained in the integral method.....	37
Figure 3.12: Represents the mean integral value of the length used for the optimization of the reaction coil.....	39
Figure 3.13: Indicates the curve obtained when running the different brands of luminol tested. Sigma unpurified gave the highest peak height (PH) difference (mean PH 2 011 092 with a RSD% of 2.4%). The worst results came from the Fluka purified (mean PH 1 362 563 and a RSD% of 7.2%).....	41
Figure 3.14: Sensitivity improvements, (a) indicates a poor sensitivity as the gradient is very low, (b) indicates a better sensitivity with a steeper gradient	41

Figure 3.15: Indication of the peaks obtained by the various pH of the SAFe D1 sample used for the pH test.....	42
Figure 3.16: SAFe D1 concentrations obtained at various pH levels. pH 3.7 is the only pH at which the concentration is within the consensus value (0.687 ± 0.041 nM).....	44
Figure 3.17: Displays the relative values (normalized to the no purification) of the buffer test for 0x, 1x, 2x, 3x purifications.....	45
Figure 3.18: SAFe D2 reference material was used over several days during the development phase until a consistent result within the range of the certified value was achieved (only 2 were possible as the material ran out). The black dotted line indicates the mean SAFe value, the yellow and red dotted lines indicate the upper and lower limit of the SAFe value.....	46
Figure 3.19: SAFe D1 reference material was used over several days during the development phase until a consistent result within the range of the certified value was achieved. The black dotted line indicates the mean SAFe value, the yellow and red dotted lines indicate the upper and lower limit of the SAFe value.....	47
Figure 3.20: Shows the results for the SAFE D1 reference material run at the beginning and at the end of the day (15h later). Blue represents the PH method and green the Int method. The black dotted line indicates the mean SAFe value, the yellow and red dotted lines indicate the upper and lower limit of the SAFe value.....	48
Figure 3.21: Standards were run for ten cycles each, to assess the precision of the system.....	49
Chapter 4: Application of the FIA-CL to measure iron in Southern Ocean Samples	
Figure 4.1: Indicates sample location of D357 and Chever et al., (2010).....	53
Figure 4.2: Displays the values obtained from the D357 cruise at station 3 for both methods. The insert shows the upper 500m Data presented in Appendix 3.....	55
Figure 4.3: Comparison of the D357 data with that of Chever et al., 2010. The insert shows the upper 200m.....	56
Figure 4.4: Indication of the cruise track where the samples have been collected.....	57
Figure 4.5: The torpedo fish used for the sampling of the surface waters during the SANAE 51 cruise.....	58
Figure 4.6: Display of the dFe concentrations for surface water samples from the SANAE 51 cruise.....	60
Figure 4.7: Display of the TdFe concentrations for surface water samples from the SANAE 51 cruise.	61
Figure 4.8: SANAE 53 cruise track.....	64
Figure 4.9: Transfer of Go-Flo bottle from carrier to receiver, including the person responsible for the removal of the plastic sheath (Foto by N. Knox).....	65
Figure 4.10: Represents the concentration of the 24 Go-Flo bottles before cleaning and after the final cleaning and soaking step.....	66
Figure 4.11: Comparison between the LDPE bottles and the polycarbonate bottles, showing that there is not a great difference in the two results.....	67
Figure 4.12: Indication where Mega station 2 has been sampled compared to that of Klunder et al., (2011).....	68
Figure 4.13: Comparison of the LDPE and PC bottles on a profile, clearly indicating that the sampling in LDPE bottles leads to contamination.....	69

Figure 4.14: Comparison between our data and Klunder et al., (2011). Klunder et al (2011)
is in general lower than our data.....70

List of Tables

Table 2-1: List of a variety of methods used during the development of analysis for trace metal Fe concentrations	9
Table 3-1: Indicates the level of confidence from the lengths of the reaction coil	39
Table 3-2: Shows the variety of concentration of the reagents used by different authors	41
Table 3-3: Indicates the pH values, the RSD%, concentration of Fe obtained as well as the standard deviation (STD)	43
Table 3-4: Indicating the mean peak heights observed as well as the RSD% value	49

Abbreviations

8-HQ – 8-hydroxyquinoline

ACSV – Adoptive cathodic stripping voltammetry

CCSV – Cathodic stripping voltammetry

CLE- – Competitive ligand exchange-adsorptive cathodic stripping voltammetric

conc. – concentration

dFe – Dissolvable iron

FIA-CL – Flow injection analysis with chemiluminescence

FIA-S – Flow injection analysis spectrophotometric

GFAAS – Graphite furnace atomic absorption spectrometers

HR-ICP-MS – High-resolution inductively coupled plasma mass-spectrometry

ICP-MS – Inductively coupled plasma mass spectrometry

ICP-SFMS – Inductively coupled plasma-sector field mass spectrometry

ID – Internal diameter

IDA – Iminodiacetic acid

Int – Integral method

LWCFC – Long liquid waveguide capillary flow cell

PFe – Particulate iron

PH – Peak Height method

PMT – Photomultiplier tube

SANAE – South African National Antarctic Expedition

SCP – Adsorptive stripping chronopotentiometry

sFe – Soluble iron

sp. – suprapur

TdFe – Total dissolvable iron

up. – ultrapur

Chapter 1: Introduction

1.1 The Role of Iron

Over the past decade, the concern for climate change and global warming has been playing a vital role in our societies and much research has been developed in the scientific community to better understand the climate system. During the last glacial maximum the atmospheric CO₂ concentrations were as low as 200 ppm and higher prior to that (Barnola *et al.*, 1987; Petit *et al.*, 1999 and Barnola *et al.*, 2003). From the last glacial maximum till the start of the industrial revolution the concentrations were at 280 ppm (Barnola *et al.*, 1987) (Figure 1.1).

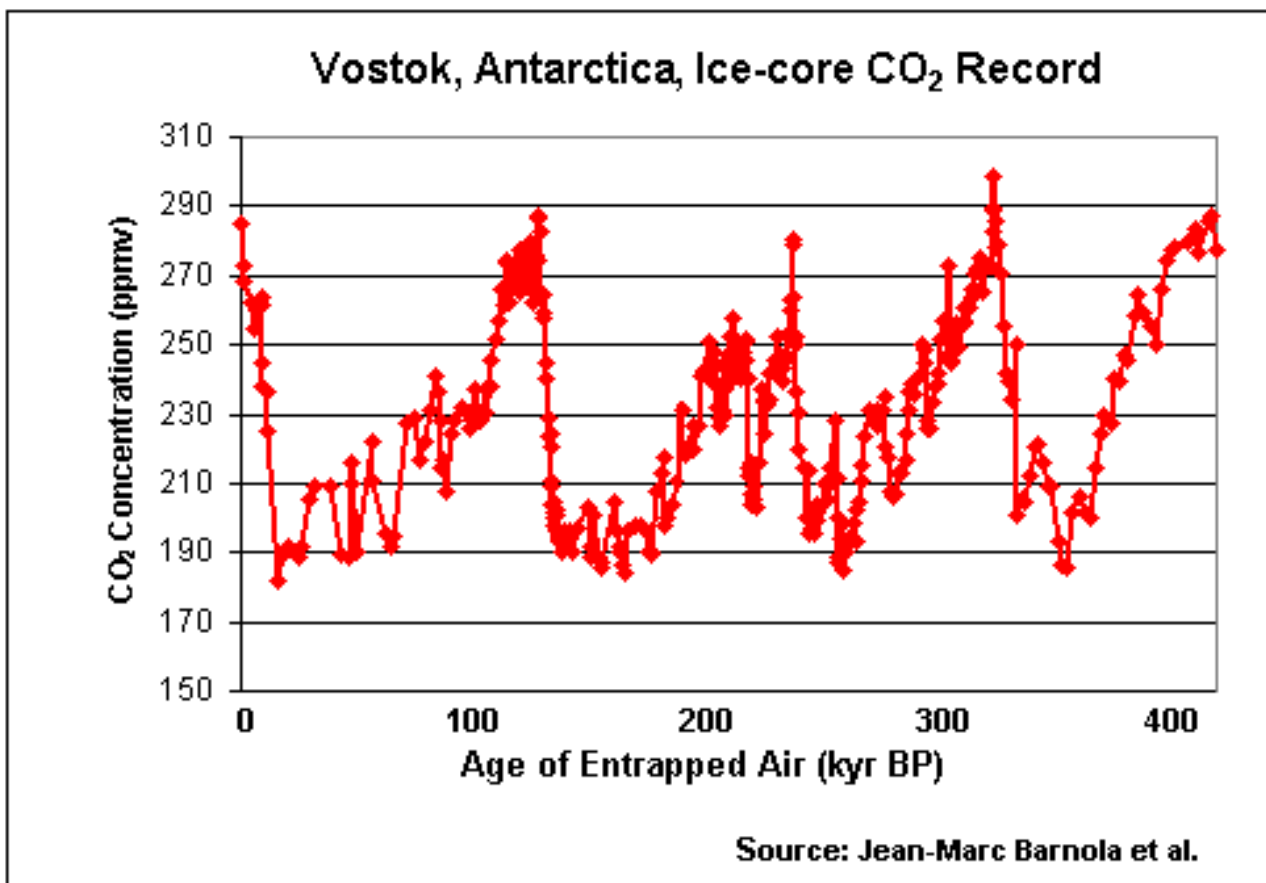


Figure 1.1: Barnola et al., (2003) CO₂ concentrations over the past 400 kyr BP

Recent measurements indicate concentrations close to 400ppm at Mauna Loa, Hawaii (www.esrl.noaa.gov). Carbon dioxide concentrations almost doubled in the last 150 years compared to the last 18000 years. Increased carbon dioxide concentration in the atmosphere due to anthropogenic activities is considered as one of the main causes for global warming (Pachauri and Reisinger, 2007). This has major implications for environmental changes, for example increase in frequency and intensity of droughts and floods, the melting of glaciers and the ice caps (Pachauri and Reisinger, 2007). The rate of change in atmospheric CO₂, depends, however, not

only on human activities but also on oceanic processes (Falkowski *et al.*, 2000). Two oceanic processes control the oceanic C cycle (Figure 1.2).

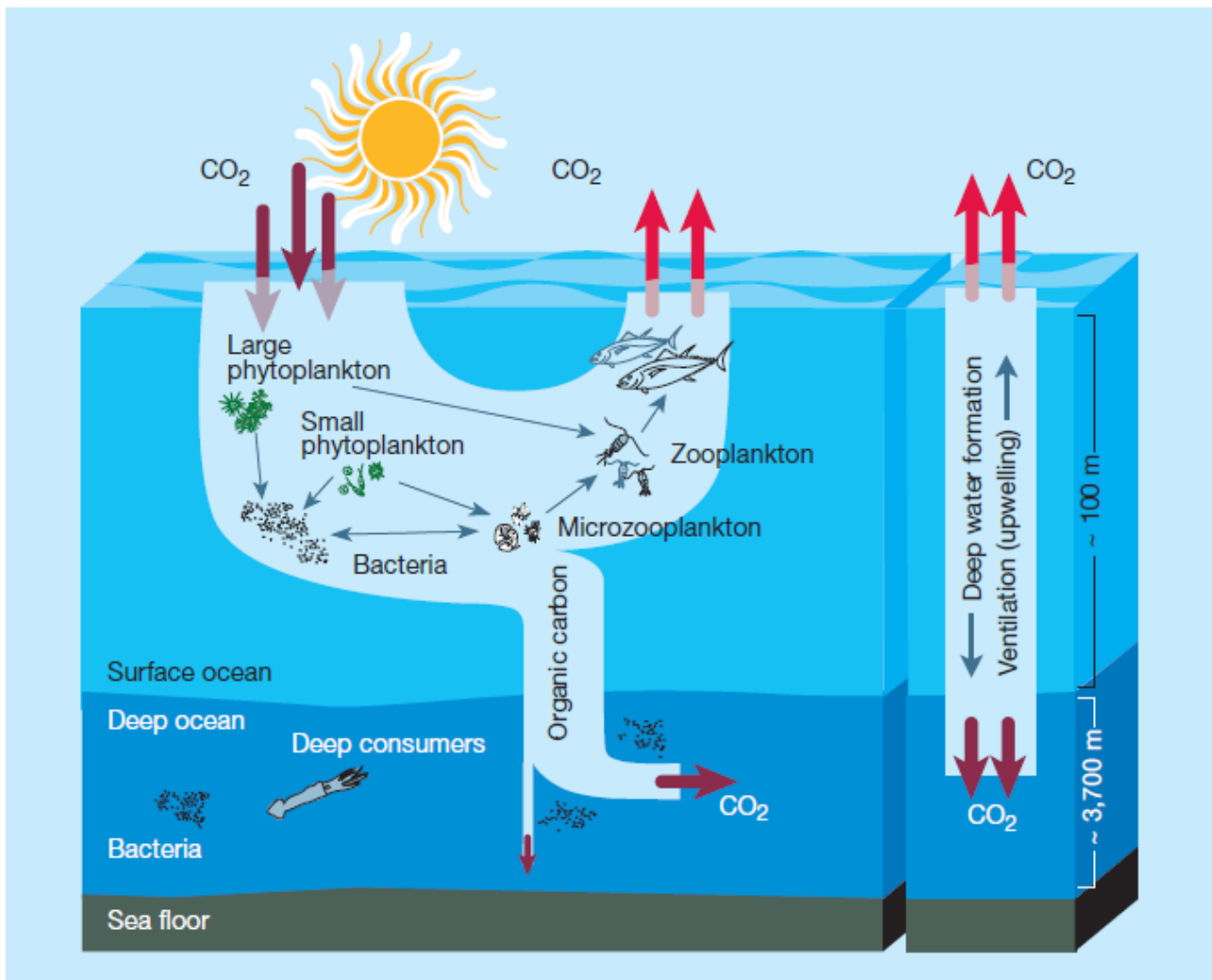


Figure 1.2: Displaying the oceanic physical and biological pump of the carbon (Chisholm, 2000)

The physical pump refers to CO₂ exchanges with the ocean surface, CO₂ being dissolved into the water or released from the water back into the atmosphere. The biological pump is the removal of CO₂ by the uptake of phytoplankton through photosynthesis and the sinking of these organisms to the seafloor (Broecker, 1982a; Broecker, 1982b and Chisholm, 2000). Without phytoplankton in the ocean, the atmospheric CO₂ concentrations would increase by 150-200 ppmv, a considerable fraction on top of to the present ~380 ppmv (Falkowski *et al.*, (2000)).

The question came about how the CO₂ concentration decreased prior to the last glacial maximum, leading to the iron hypothesis of Martin (1990). This hypothesis states that iron is a limiting nutrient in the production of phytoplankton and would assist in the biological pump.

Many areas in the oceans show little primary productivity as observed from remotely sensed chlorophyll data. In particular, vast areas of the open ocean have low chlorophyll concentrations whereas nutrients such as nitrate, that phytoplankton need for growing, are

plentiful. This is the case for the following regions: the eastern equatorial Pacific, the Sub-arctic Pacific and the Southern Ocean (Achterberg *et al.*, 2001; de Baar *et al.*, 2005 and Boyd and Ellwood, 2010). These regions are known as High Nutrient Low Chlorophyll Regions (HNLC) and represent about 40% of the world's oceans (Watson, 2001). Martin (1990) postulated that the trace metal iron was the limiting factor for phytoplankton growth (and as a result for CO₂ uptake) in these regions. Iron indeed plays a vital role in plants metabolism where it is essential for photosynthetic and respiratory electron transport, nitrate reduction, chlorophyll synthesis and detoxification of reactive oxygen species and is used in a variety of enzymes (Sunda, 2001; Moral and Price, 2003). During photosynthesis 22 Fe atoms are required for the electron transfer during the photosynthetic reaction (Briat *et al.*, 2014) (Figure 1.3), therefore an iron-limitation inefficient functioning of the electron transport system which reduces the photosynthetic yield per unit of chlorophyll (Behrenfeld *et al.* 1996). As such, substantial research has been conducted in the last 30 years to test this hypothesis, and demonstrated that Fe indeed limits phytoplankton growth and impacts the biogeochemical cycle of carbon in these vast areas (see review by de Baar *et al.*, 2005; Boyd and Ellwood, 2010). However, the links between iron and the global carbon cycle are still poorly understood.

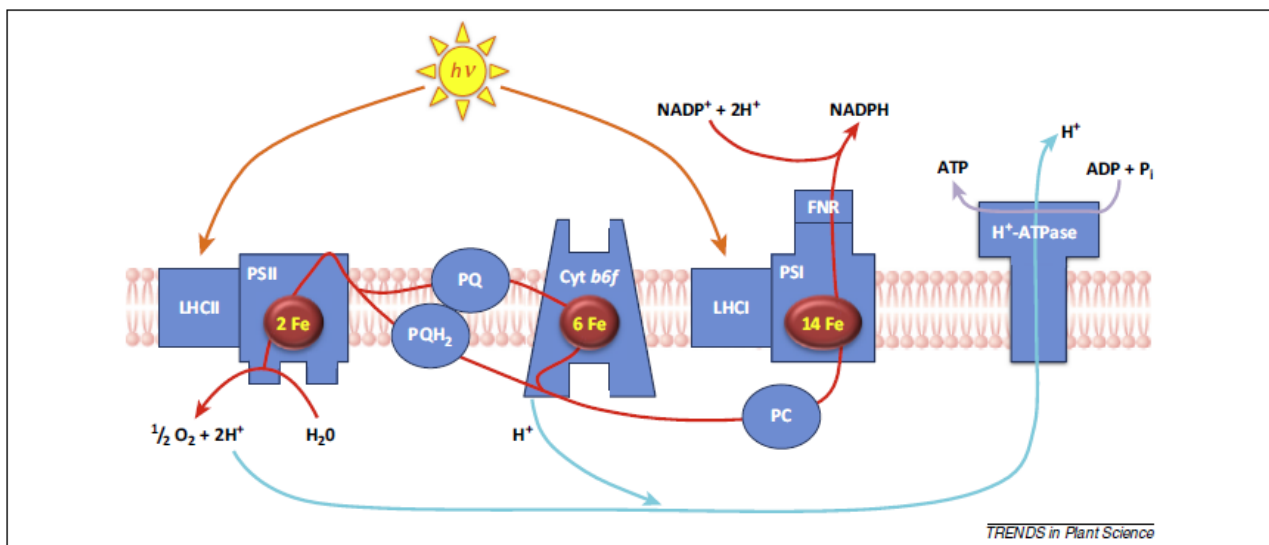


Figure 1.3: Photosynthesis cycle (Briat *et al.*, 2014). Iron is essential for the structure and function of the photosynthetic electron transfer chain. There are in total 22 Fe ions responsible for the function of photosynthesis.

Figure 1.4 after Nédélec (2006) depicts a summary of the biogeochemical cycle of iron. The external sources of Fe to the ocean include rivers, dust deposition, seasonal ice melt (icebergs), continental margins weathering (and lateral advection), hydrothermal vents and black smokers and horizontal advection (e.g. upwelling) (Boyd and Ellwood, 2010). The chemical side is the reaction of Fe reduction and oxidation. Iron is removed from the system through the uptake by primary production and by the adsorption to particles, and the sinking of particles (Nédélec, 2006).

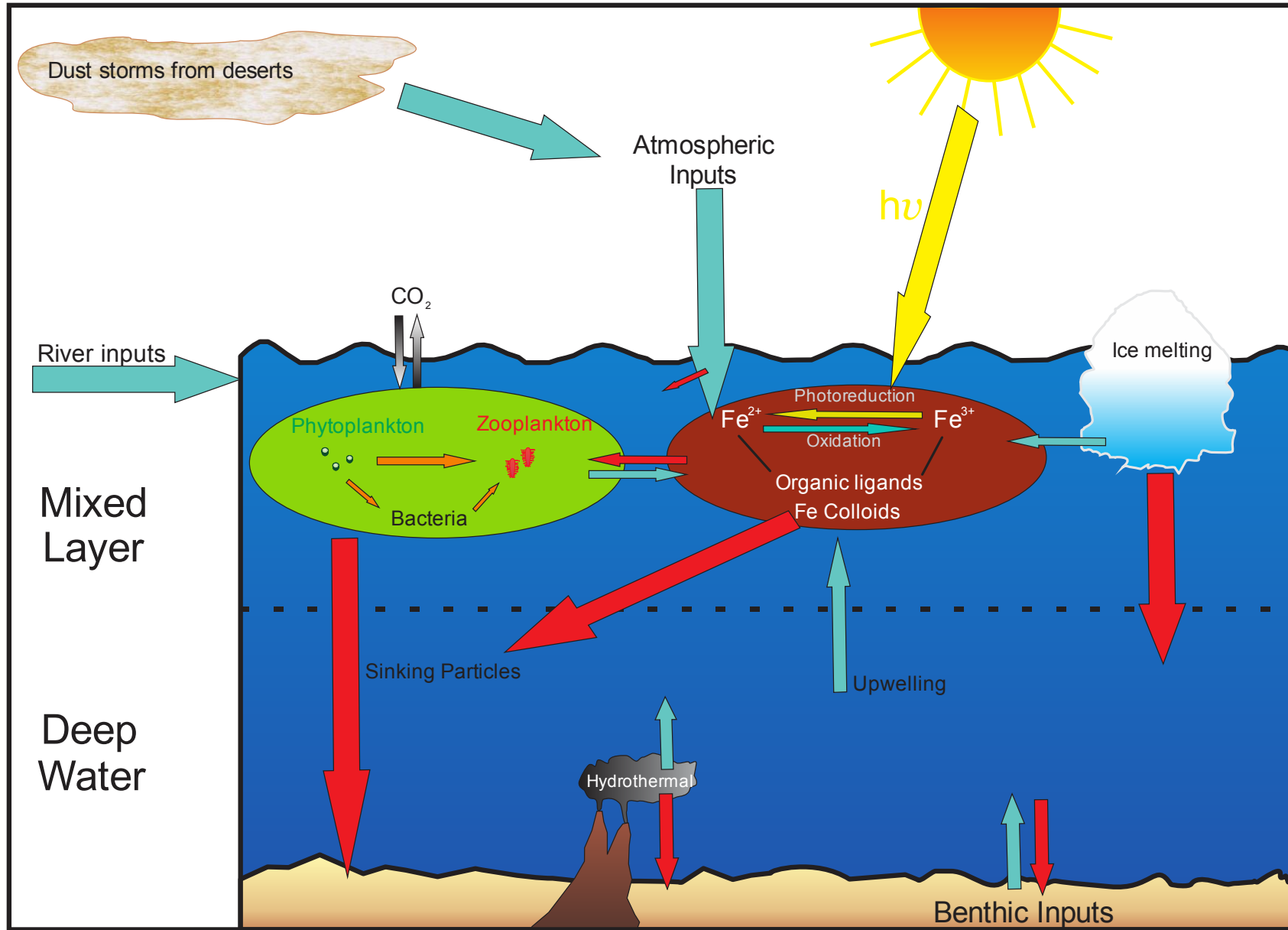


Figure 1.4: Iron Cycle, simplified from Nédélec (2006). Blue arrows indicate input of Fe, and red arrows indicate removal of Fe.

One of the main unanswered questions is what fraction of iron is bioavailable, i.e. what physical or chemical species of iron can be used by phytoplankton. Although Fe is the fourth most abundant element on the earth's crust, it is only present at very low concentrations in oxygenated water column of the oceans (de Baar and de Jong, 2001). Deep waters have $\sim 0.7 \text{ nmol l}^{-1}$ (Boyd and Ellwood, 2010) and generally lower concentrations ($< 0.1 \text{ nmol l}^{-1}$ (Boyd and Ellwood, 2010)) in surface waters of HNLC regions. Different physical fractions of Fe exist (Figure 1.5): soluble Fe ($< 0.02 \mu\text{m}$), colloidal Fe (between 0.02 and $0.2 \mu\text{m}$) and particulate Fe ($> 0.2 \mu\text{m}$) (Bruland and Rue, 2001).

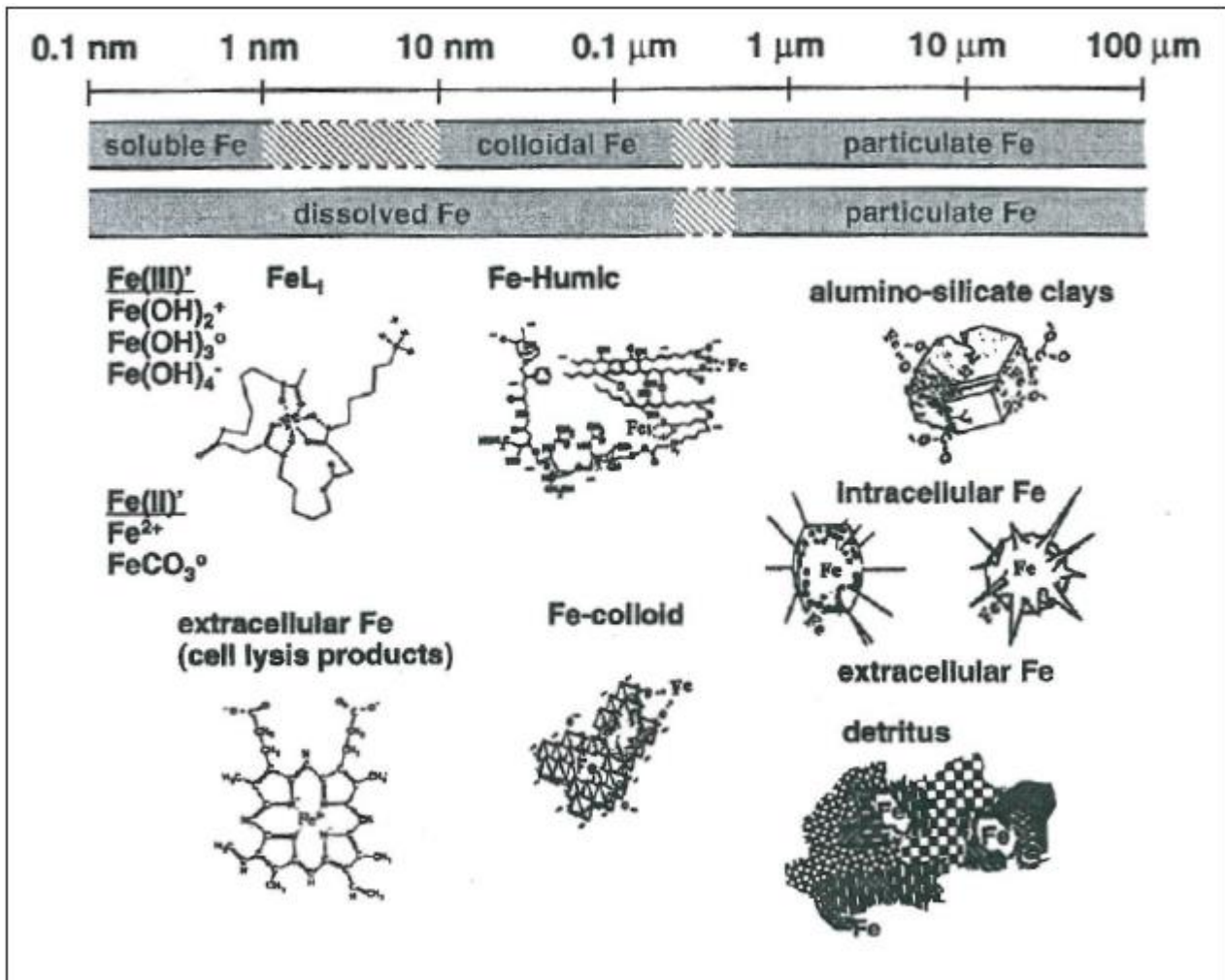


Figure 1.5: Physical and Chemical speciation of Fe found in the Ocean, (Bruland and Rue, 2001)

More than 90% of dissolved Fe (i.e. soluble + colloidal) is bound by organic molecules called ligands, which avoid Fe precipitation. These ligands, most probably released by bacteria and phytoplankton, are believed to increase the level of dissolved iron in the oxygenated water column (de Baar and de Jong, 2001). However, the role of these organic ligands in the dissolution of particulate iron or stabilization of dissolved iron is still poorly understood.

South Africa's interest in climate change triggered the need to better constrain the carbon cycle, and consequently to study the oceanic biogeochemical cycle of iron. South Africa is a gateway to the Southern Ocean, the biggest HNLC region of the ocean. The annual relief voyages

to Marion Island, Gough Island and Antarctica, thus provides perfect opportunities for oceanographic research in the Southern Ocean to understand the coupling of Fe-C cycles.

To gain an understanding of Fe cycle, a first, crucial step was to set up an analytical method which would allow for picomolar concentrations of iron to be analysed. A variety of methods do exist (which are described in chapter 2 in detail), which include ICP-MS, GFAAS, CSV and FIA's. We are focusing in this work at the development of a flow injection analysis with chemiluminescence for the analysis of Fe(III) as dissolvable and total dissolvable iron in the picomolar range.

1.2 Aims and objective

The overall aim of this project was to optimize an analytical method to analyse seawater samples for the determination of dissolved Fe concentrations at the picomolar level. Other considerations include:

- The analytical method had to be mobile and easy to be setup.
- The analytical method should be developed in such a way that it can easily be used in a land based laboratory as well as a ship based laboratory
- Validate the method by measuring reference material
- Applying the method for measurement of seawater samples and validate sampling protocol for sample collection aboard a ship

1.3 Structure of the thesis

- Chapter 1 Introduction to the thesis including aims and objectives
- Chapter 2 describes the various existing methods to analyse Fe concentrations in the water column and the system which was selected for this project.
 - This section looks into detail which methods have been used and how the development history of these has come along till to date.
- Chapter 3 describes the development phase of the system.
 - This section looks in detail how our system was developed which includes optimization, accuracy and precision tests.
 - It also explains about a variety of problems which had been encountered
- Chapter 4 describes the field implementation and results.
 - This section represents results from the D357 cruise, the SANAE 51 and SANAE 53 results.

- This section also describes practical implementation of the system on board a vessel, where it was used to validate the sampling method.
- Chapter 5 concludes the thesis.

Chapter 2: Historical development of analytical Methods used for the analysis of Fe

2.1 Historical overview of methods

Since the early 1930's analytical methods for the determination of iron in seawater have been set up using first colorimetry (Thompson *et al.*, 1932; Rakestraw *et al.*, 1936), and then later on in the 1970 Graphite furnace atomic absorption spectrometers (GFAAS) (Spencer *et al.*, 1970). Original concentrations measured were over 40 nM Fe. The GFAAS method has been optimized in the 1980's, which brought down the measured concentration to 0.01-1.55nM (Gordon *et al.*, 1982; Martin *et al.*, 1990). A flow injection analysis with chemiluminescence detection (FIA-CL) emerged in the mid 1980's (Alwarthan and Townshend, 1986), but was only properly perfected in the 1990's to allow for the analysis of Fe (II) and Fe (III) (Elrod *et al.*, 1991; Obata *et al.*, 1993). Stringent anti-contamination techniques by Martin *et al.*, (1976) and Bruland *et al.*, (1979) made it possible for even lower concentrations to be measured. The FIA method allowed concentration measurement as low as 0.05 nM Fe (de Jong *et al.*, 1998). However, FIA can also give access to the physical speciation of iron particulate, dissolved and soluble fractions. Cathodic stripping voltammetry (CSV) was developed to measure the organic Fe concentrations (Rue and Bruland, 1994; Gledhill and van den Berg, 1994; Wu and Luther III, 1994; Witter and Luther III, 1998). This method can also be used for the determination of Fe (II) and Fe (III), (Gledhill and van den Berg, 1995; Aldrich and van den Berg, 1998; Segura *et al.*, 2008). Over the last two decades a variety of other different methods have been developed, which include FIA spectrophotometric (FIA-S) (Measures *et al.*, 1995; Weeks and Bruland, 2002; Bowie *et al.*, 2004; Laës *et al.*, 2005; Feng *et al.*, 2005; Páscoa *et al.*, 2009), Inductively coupled plasma mass spectrometry (ICP-MS) (Lohan *et al.*, 2005; Saito and Schneider, 2006; Wu, 2007; Milne *et al.*, 2010), adsorptive stripping chronopotentiometry (SCP) (Riso *et al.*, 2007) and Photothermal deflection spectroscopy (Ferrizine) (Khrycheva *et al.*, 2008). Refer to Table 2.1 for a complete list of all different types of methods.

Table 2-1: List of a variety of methods used during the development of analysis for trace metal Fe concentrations (Total dissolvable iron (TdFe); dissolveble iron (dFe); particulate iron (PFe))

Location	Method	Fe Speciation	Year	Reference
North Pacific	Colorimetry (thiocyanate)	TdFe	1932	Thompson <i>et al.</i> , (1932)
North-west Atlantic	Colorimetry (thiocyanate)	dFe	1936	Rakestraw <i>et al.</i> , (1936)
North East Pacific	GFAAS (APDC/DDDC extraction)	dFe + PFe	1987	Landing and Bruland (1987)
North Atlantic	Spectrophotometric (Colorimetry) (Ferrizine)+ GFAAS	Fe(II)+ TdFe	1991	King <i>et al.</i> , (1991)
Not known	FIA-CL	TdFe + Fe(II)	1991	Elrod <i>et al.</i> , (1991)
Pacific	FIA-CL	Fe	1993	Obata <i>et al.</i> , (1993)
Menai Straits	CCSV	Fe-ligands	1994	Gledhill and van den Berg (1994)
North Pacific	CLE-ACSV GFAAS (APDC/DDDC)	Fe-ligands TdFe	1995	Rue and Bruland (1995)
North Sea	CCSV	Fe (II) + Fe(III)	1995	Gledhill and van den Berg (1995)
Not known	FIA-CL	Fe(II)	1995	King <i>et al.</i> , (1995)
North Pacific, Sargasso Sea and Narragansett Bay	FIA-CL	Fe (II) + reducible Fe(III)	1995	O'Sullivan <i>et al.</i> , (1995)
Equatorial Pacific, Northern Atlantic and Central Pacific	FIA-S	Fe	1995	Measures <i>et al.</i> , (1995)
Not known	Spectrophotometric	Fe(II) + Fe(III)	1995	Blain and Tréguer (1995)
Sothern Indian Ocean and East China Sea	FIA-CL	TdFe + Fe-ligands	1997	Obata <i>et al.</i> , (1997)
Atlantic	FIA-CL	dFe (Fe(II))	1998	Bowie <i>et al.</i> , (1998)
North Atlantic	CCSV	Fe (II) + Fe (III), TdFe	1998	Aldrich and van den Berg (1998)
Southern Ocean (Atlantic)	FIA-CL	dFe	1998	de Jong <i>et al.</i> , (1998)
Coastal, Rain and Tap water	FIA-CL	Fe (II)	1999	Hirata <i>et al.</i> , (1999)
North Atlantic	ICP-MS (Mg(OH) ₂ Preconcentration)	TdFe	1998	Wu and Boyle (1998)
South Atlantic	FIA-CL	Fe	2000	Vink <i>et al.</i> , (2000)
Not known	Colorimetric (Gas segmented continues flow)	Fe(II) + TdFe	2001	Zhang <i>et al.</i> , (2001)
Ross sea	FIA-S	dFe + TdFe	2000	Sedwick <i>et al.</i> , (2000)
Coastal (Swedish west coast)	CLE-ACSV (TAC)	Fe labile	1999	Croot and Johansson (1999)
North Atlantic Ocean	CSV (DHN)	Fe (III)	2001	Obata and v. d. Berg (2001)

Location	Method	Fe Speciation	Year	Reference
Coastal (California)	FIA-S	dFe	2002	Weeks and Bruland (2002)
Southern Ocean (Atlantic)	FIA-CL	Fe (II)	2002	Croot and Laan (2002)
Southern Ocean (South of Australia)	FIA-CL	dFe (Fe(II))	2005	Bowie <i>et al.</i> , (2005)
Open Ocean	ICP-SFMS	TdFe	2005	Lohan <i>et al.</i> , (2005)
Southern Atlantic	FIA-S	dFe	2005	Laës <i>et al.</i> , (2005)
Southern Ocean (Ice)	FIA-CL	TdFe + dFe	2005	Lannuzel <i>et al.</i> , (2005)
River water	FIA-S	TdFe	2005	Feng <i>et al.</i> , (2005)
Equatorial Pacific	ICP-MS (Mg(OH) ₂ Preconcentration)	TdFe	2006	Saito and Schneider (2006)
Equatorial Pacific	HR-ICP-MS (Mg(OH) ₂)	TdFe	2007	Wu (2007)
Aulne estuary	SCP	dFe	2007	Riso <i>et al.</i> , (2007)
Not known	Photothermal deflection spectroscopy (Ferrizine)	Fe (II)	2008	Khrycheva <i>et al.</i> , (2008)
Not Know	ACSV (BiFE)	Fe (III)	2008	Segura <i>et al.</i> , (2008)
Coastal (English Channel), North Atlantic* and Pacific*	FIA-CL	Fe (II) + Fe (III)	2009	Ussher <i>et al.</i> , (2009)
Reference material	LWCC MSFIA spectrophotometric	Fe (II) + Fe (III)	2009	Páscoa <i>et al.</i> , (2009)
North Atlantic	HR-ICP-MS	TdFe	2010	Milne <i>et al.</i> , (2010)

2.2 Land versus ship based methods

All methods mentioned above are land based, but some of them can be used for ship based analysis as well. These are Colorimetry and the Flow injection analysers. The reason for this is that they are small and compact and can be carried on board a ship. The other systems are often too big to be installed on a ship e.g. ICP-MS, or they are influenced by the vibrations of the ship e.g. CSV (Achterberg *et al.*, 2001).

The following section is divided into pure land based systems and land and sea based systems.

al., 2010). With this setup very low detection limit for Fe (21 pM) have been reported (Milne *et al.*, 2010), but this can only be achieved by introducing a pre-concentration step.

There are two widely used preconcentration methods for the analysis on ICP-MS which are not extensively time consuming. The one method makes use of resins which have a high affinity for metals (Lohan *et al.*, 2005 and Milne *et al.*, 2010) with minimum sample handling and pre-treatment (Achterberg *et al.*, 2001) and the other is using $\text{Mg}(\text{OH})_2$ precipitation (Wu and Boyle, 1998, Saito and Schneider, 2006, Wu, 2007 and Wu *et al.*, 2011)

Nitriloacetic acid (NTA) Superflow is a commercially available resin which allows for the preconcentration of Fe at pH1.7 (Lohan *et al.*, 2005), which has the potential to release Fe from the strong ligands (Boukhalfa and Crumbliss, 2001), and therefore preventing re-complexion with natural organic ligands (Lohan *et al.*, 2005). This resin first has to be condition with acetic acid/ammonium buffer prior to loading of the sample. More recently Milne *et al.* (2010) made use of Toyopearl AF-Chelate-650M resin which has an iminodiacetate (IDA)-type functional group and was previously used for other metals (Pb, Cu, Cd, Mn, Zn and Ni) (Warnken *et al.*, 2000; Beck *et al.*, 2002). This resin does not need to be pre-conditioned and has an affinity for Fe at low pH (De Baar *et al.*, 2008). This new method makes use of a low volume of sample, saving reagents and time to analyse for a variety of elements including Fe simultaneously. Both resins also have the advantage to work at pH1.7, which is the pH value recommended to store Fe samples (www.geotraces.org)

The Mg precipitation preconcentration technique requires more sophisticated preparations prior to analysis and is more time consuming than the in-line preconcentration method. This method makes use of an isotropic spike (^{57}Fe) to a known volume of seawater for the quantification of trace metals. A base (NH_4OH) is added for the precipitation of $\text{Mg}(\text{OH})_2$ followed by discarding the supernatant by centrifugation. $\text{Mg}(\text{OH})_2$ is then re-dissolved with a small volume of diluted nitric acid, followed by ICP-MS analysis (Wu and Boyle, 1998; Saito and Schneider, 2006). A slight variation to the method, known as double $\text{Mg}(\text{OH})_2$ precipitation, is that the preconcentration step is repeated by addition of the same volume of seawater and base to the re-dissolved $\text{Mg}(\text{OH})_2$ (Wu (2007)).

The greatest advantage of making use of the ICP-MS is the high sensitivity for the detection of Fe as well as a whole range of other trace elements that can be detected at the same time, in the same sample (Saito and Schneider, 2006; Milne *et al.*, 2010). Inductively coupled plasma mass spectrometry allows for the determination of isotope speciation. Hence, Fe isotopes are used to determine the absorbance of Fe to organic ligands (Wu, 2007).

The ICP-MS is an expensive apparatus, which are bulky in size and fragile (Achterberg *et al.*, 2001). A preconcentration step is required for the analysis of trace metals (Wu, 2007). It does

not allow for the measurement of organically complexed iron or redox state (Achterberg *et al.*, 2001).

2.2.1.2. Graphite furnace atomic absorption spectrometry

The GFAAS was a strong competitor in the 1980's versus the ICP-MS for trace metal analysis. The GFAAS allows samples to be vaporized in a graphite coated furnace. This vapour is then radiated by light in which the atoms absorb at specific wavelengths. The absorbed wavelengths are measured for the determination of the concentrations of the elements (Figure 2.2).

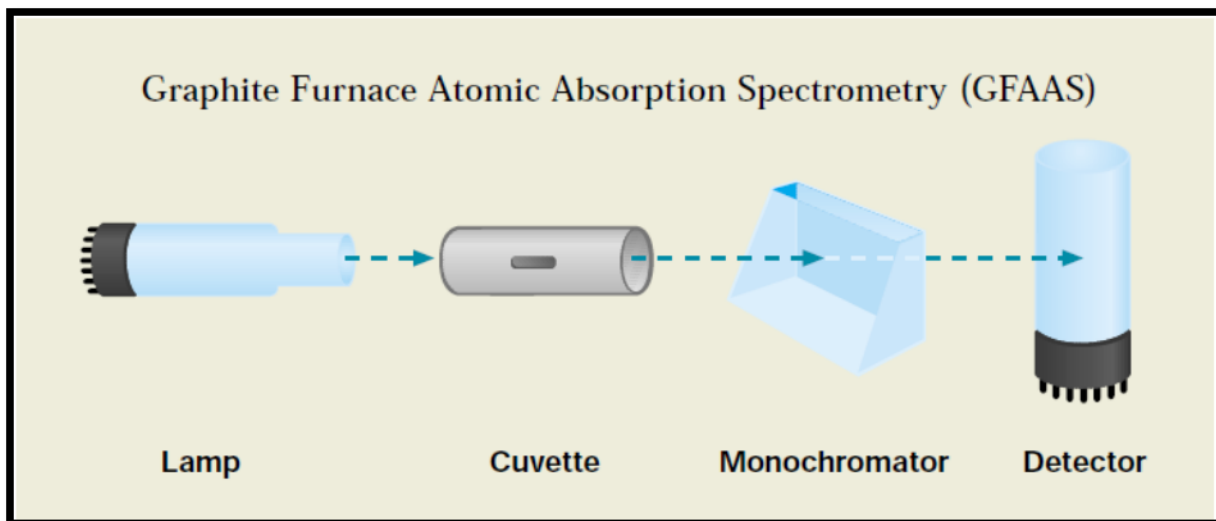


Figure 2.2: Representation of a GFAAS system. The cuvette refers to the graphite coated furnace (Thermal Elemental (2001)).

A solvent extraction is used as a pre-concentration step, either with ammonium 1-pyrrolidinedithiocarbamate (APDC) and diethylammonium diethyldithiocarbamate (DDDC) into chloroform, dried and then back extracted into nitric acid (Landing and Bruland, 1987; Martin and Gordon, 1988; Martin *et al.*, 1988; Martin *et al.*, 1990; Löscher *et al.*, 1997) or with DDDC complexes into Freon113 and back extracted into acidic solution (Danielsson *et al.*, 1985). Saager *et al.*, (1989) used a Chelex-100 resin column for the extraction of Fe with a detection limit of 0.15 nM. The Zeeman background correction needs to be applied in all results obtained. The Zeeman background correction requires the splitting of the atomic spectral lines in the presence of a magnetic field into the π component and two σ components. A polarizer is used to remove the π component, which allows for the background absorption. Total absorption is measured without the magnetic field. The Zeeman correction is the subtraction of the background absorbance from the total absorbance (Flajnik and Delles, 2010).

The most recent results by Löscher *et al.*, (1997) gave a detection limit between 0.03-0.31 nM over six days. This large variation makes the method redundant as surface waters have concentrations below the 0.31 nM detection limit (Achterberg *et al.*, 2001) and can therefore not be

analysed. Sarthou and Jeandel (2001) reported a detection limit of 0.16 nM, which is still above the low values of surface waters. Therefore this method is not suitable for surface waters due to the high and variable detection limit.

2.2.1.3. Electrochemical stripping procedures

There are two electrochemical stripping procedures used presently for the analysis of Fe, namely cathodic stripping voltammetry (CSV) and adsorptive stripping chronopotentiometry (SCP).

(i) Cathodic stripping voltammetry

Cathodic stripping voltammetry has the greatest advantage of allowing for analysis of both physical and chemical iron speciation (Gledhill and van den Berg, 1994; Gledhill and van den Berg, 1995; Rue and Bruland, 1995; Aldrich and van den Berg, 1998; Witter and Luther III, 1998; Croot and Johansson, 2000 and Segura *et al.*, 2008). However, great care needs to be taken in the determination of subnanomolar Fe due to the interfering background peaks caused by the impurities in the artificial ligand used, leading to an overestimation in the results (Obata and van den Berg, 2001). Total time for one sample analysis is between 100s-340s, with a longer absorption time allowing for a lower detection limit (Obata and van den Berg, 2001).

This technique does not require matrix removal but utilises a pre-concentration step. First, iron is complexed as Fe(III) by adding an artificial ligand competing with the natural ligands in seawater: 1-nitroso-2-naphthol (NN) at pH 6.9 (Gledhill and van den Berg, 1994; Gledhill and van den Berg, 1995; Aldrich and van den Berg, 1998 and Witter and Luther III, 1998), salicylaldoxime at pH 8 (Rue and Bruland, 1995), 2-(2-thiazolylazo)-p-cresol (TAC) at pH 8 (Croot and Johansson, 2000), 2,3-dihydroxynaphthalene (DHN) at pH 8 (Obata and van den Berg (2001)) or 1-(2-pyridylazo)-2-naphthol (PAN) at pH 4 (Segura *et al.*, 2008). A mercury drop electrode (HMDE) (Gledhill and van den Berg, 1994; Gledhill and van den Berg, 1995; Rue and Bruland, 1995; Aldrich and van den Berg, 1998; Witter and Luther III, 1998 and Croot and Johansson, 2000) or a bismuth-coated glassy carbon electrode (BiFE) (Segura *et al.*, 2008) pre-concentrates Fe complexed to the artificial ligand. The addition of bromate and N-2-2-hydroxyethylpiperazine-N'-3-propanesulphonic acid (HEPPS) buffer to NN (Aldrich and van den Berg, 1998) or DHN (Obata and V. d. Berg, 2001) allows for the determination of measurements at pH 8. This complex is electro active and a voltammetric scan at a specific potential allows determining the Fe adsorbed to the electrode, by reducing the Fe(III)-complex to an Fe(II)-complex..

The addition of an oxidant such as H₂O₂ (Gledhill and van den Berg, 1995) or KBrO₃ (Aldrich and van den Berg, 1998) increases the sensitivity as these chemicals reoxidized the Fe(II)-complex back to Fe(III)-complex, repeatedly adding to the peak current (Aldrich and van den Berg, 1998). The addition of 2,2-bipyridyl masks the Fe(II) speciation, which allows for an indirect determination of the Fe(II) speciation (Gledhill and van den Berg, 1995). Aldrich and van den Berg

(1998) have reported detection limits of 0.08 nM Fe by making use of the NN ligand and Croot and Johansson (2000) have reported a detection limit of 0.1 nM Fe by using the TAC ligand Obata and van den Berg (2001) reported a detection limit of 0.013 nM Fe. They all report that an increase in adsorption time will further decrease the detection limit. This allows for the method to be suitable for the analysis of surface waters. For the analysis of total Fe the samples have to be UV digested at pH2 to break down the natural organic complexes (Aldrich and van den Berg, 1998 and Croot and Johansson, 2000).

This method would be suitable for the use on board a ship due to its low costs, compact and portability of the instrument and its high sensitivity. However, the ships vibrations may obscure results due to the slow scan speeds of the waveforms and the long deposition times (Achterberg *et al.*, 2001), therefore this method should be used on land.

(ii) Adsorptive stripping chronopotentiometry

Adsorptive stripping chronopotentiometry makes use of the basic principle used in CSV, with the addition of a ligand (NN) and a mercury film electrode. The main difference is that it uses low constant current instead of a sweeping potential during the stripping process. Adsorptive stripping chronopotentiometry takes a measurement as a function of time and not as a change in current. Adsorbed organic matter has a lower effect on SCP than on CSV (Riso *et al.*, 2007). Riso *et al.*, (2007) reported a detection limit of 0.09 nM for Fe.

The advantage of SCP versus CSV is that it does not require a catalyst for an increased sensitivity (Riso *et al.*, 2007). This method can easily be adopted for on board analysis but no successful systems had been reported yet.

2.2.2. Land and Ship based methods

The biggest advantages of all following methods are that they can be used both on land and ship due to their easy setup and mobility.

2.2.2.1 Colorimetry

The first method described for the measurement of iron was by Thompson *et al.*, (1932). They used a sulphuric acid evaporation procedure to remove the chlorides, fluorides, nitrates, nitrites from the seawater matrix and to break down organic matter. The addition of bromide and thiocyanate, forms the red complex $\text{Fe}(\text{CNS})_6^{3-}$, which is quantified by colorimetry. Rakestraw *et al.*, (1936) improved the method of Thompson *et al.*, (1932) using a co-precipitation of magnesium rather than the sulphuric acid evaporation procedure.

Thompson *et al.*, (1932) reported that there is a loss in the intensity of the colour over time and that it is crucial to work within a short time period. They reported that 20 samples could be compared per set of standards before the standards lost their intensity in colour. Rakestraw *et al.*,

(1936) added small amounts of ethylene glycol monobutyl ether to stabilize the colour for a longer time period.

This colorimetric method has a detection limit in the milligram range (Thompson *et al.*, 1932; Rakestraw *et al.*, 1936), which is not suitable for trace metal study. King *et al.*, (1991) improved the sensitivity of that method by using a spectrophotometer and ferrozine bound to a Sep-Pak (Sep-Pak FZ) and methanol for the colorimetric reaction. O'Sullivan *et al.*, (1991) further optimized the method of King *et al.*, (1991) by decreasing the methanol volume and increased the NaCl concentration during the optimisation of the Sep-Pak. A constant volume of 400ml of seawater was allowed to pass through the Sep-Pak FZ, resulting in better detection limits. Blain and Tréguer (1995) modified the method of King *et al.*, (1991) by introducing a constant flow system with an online column for the extraction of Fe(II) reducing sample handling, resulting in a detection limit similar to O'Sullivan *et al.*, (1991). This new method of colorimetry resulted in low detection limits (0.6 nM (King *et al.*, 1991); 0.12 nM (O'Sullivan *et al.*, 1991) and 0.1 nM for Fe(II) and 0.3 nM for Fe(III) (Blain and Tréguer, 1995)), which are for trace metal work in certain environments (e.g. Fe-enriched coastal seawater).

A recent development of these colorimetric methods is described below, in the paragraph entitled "Flow injection analyser –catalytic spectrophotometry".

2.2.2.2. Flow Injection analysers

Flow injection analysers (FIA) with in-line preconcentration is by far the most used method at present (Elrod *et al.*, 1991; Obata *et al.*, 1993; Measures *et al.*, 1995; Obata *et al.*, 1997; Gordon *et al.*, 1996; Bowie *et al.*, 1998; de Jong *et al.*, 1998; Hirata *et al.*, 1999; Vink *et al.*, 1999; Sedwick *et al.*, 2000; Weeks and Bruland, 2002; Croot and Laan, 2002; Bowie *et al.*, 2004; Laës *et al.*, 2005; Bowie *et al.*, 2005; Lannuzel *et al.*, 2005; Feng *et al.*, 2005; Ussher *et al.*, 2005; Nédélec *et al.*, 2007 and Ussher *et al.*, 2009). It allows for rapid and efficient separation of iron from the saline matrix, hence resulting in low detection limits (Landing *et al.*, 1986; de Jong *et al.*, 1998). FIA's allow for low reagent consumption, simplified sample handling, reduced contamination risks, an increased sample throughput, multiple analysis of same sample with small volumes of sample and a low detection limit with good precision (Powell *et al.*, 1995; Nédélec, 2006). The drawback is that they can only analyse for one element at a time (Powell *et al.*, 1995) and one redox species (Achterberg *et al.*, 2001).

There are two types of FIA's: catalytic spectrophotometric FIA (FIA-S) and chemiluminescent FIA (FIA-CL).

(i) Flow injection analyser - Catalytic Spectrophotometry

Measures *et al.*, (1995) described the basic FIA-S system of which many other systems followed (Sedwick *et al.*, 2000; Vink *et al.*, 2000; Weeks and Bruland, 2002; Bowie *et al.*, 2004; and Laës *et al.*, 2005). This system consists of (1) a peristaltic pump, which allows for the

transportation of the reagents as well as for the sample, (2) a resin column (8-HQ) for the preconcentration of Fe, (3) a reducing agent (N,N-dimethyl-p-phenylenediamine (DPD)) and the oxidant hydrogen peroxide.

Fe(III) is reduced by DPD to Fe(II). The H₂O₂ then re-oxidizes Fe(II) back to Fe(III) which is then available for reduction by DPD again. This is enhancing the catalytic effect and gives rise to a stronger signal output, which is measured by a variable wavelength spectrophotometer at 540nm. The optimum pH for this reaction is pH 5.5-6.1 (Weeks and Bruland, 2002 and Laës *et al.*, 2005). Vink *et al.*, (2000) combined a FIA system for the analysis of Fe and Al as the required pH for Al is the same as that of Fe(II). Detection limits of less than 25 pM Fe have been reported (Measures *et al.*, 1995; Weeks and Bruland, 2002 and Bowie *et al.*, 2004).

The short fall of this method is that it does not allow for redox speciation measurements (Achterberg *et al.*, 2001).

(ii) Flow injection analyser – Chemiluminescences

The greatest advantage of the FIA-CL over the FIA-S is that it allows for the analysis of redox speciation. For that, two different systems have to be setup, one for Fe(II) and one for Fe(III).

(a) The iron (II) system

Iron (II) is easily oxidized to Fe(III), and therefore samples need to be treated rapidly to prevent the oxidation of Fe(II) (Achterberg *et al.*, 2001). Reduction of the seawater pH with a buffer will slow the oxidation of Fe(II), or the addition of a reducing agent (Fe(II) chelator or organic ligands) stabilise Fe(II) in seawater (O'Sullivan *et al.*, 1995; Croot and Laan, 2002).

The first preconcentration micro column system for the analysis of Fe(II) and dissolved Fe (dFe) was described by Elrod *et al.*, (1991). This system preconcentrates Fe(II) onto 8-HQ at pH 5 to pH 6, which then is eluted and mixed with brilliant sulfoflavin (BSF; sodium 4-amino-N-(p-tolyl)-naphthalimide-3-sulfonate) and H₂O₂ for the chemiluminescences reaction to take place. This chemiluminescent reaction, which requires a pH of 8.3, is catalysed by iron and emits photons, which are detected by a photomultiplier tube (PMT). Hirata *et al.*, (1999) modified the system by changing the resin column to Amberlite XAD-4 and made use of the deferoxamine B, which chelates Fe(III) to allow successful analysis of Fe(II). Detection limits 0.45nM (Elrod *et al.*, 1991) and 0.8 nM (Hirata *et al.*, 1999) were reported. These are not low enough for surface water analysis, leading to an alternative method of analysis.

Obata *et al.*, (1993) developed a method for the analysis of Fe(III) using luminol (5-Amino-2,3-dihydro-1,4-phthalazinedione) for the chemiluminescent reaction with hydrogen peroxide at basic pH, catalysed by Fe(III), and reporting a detection limit of 50 pM. The first FIA-CL systems for the analysis of Fe(II) made use of direct injection of the sample in the presence of oxygen and not H₂O₂ for the chemiluminescences reaction (King *et al.*, 1995; O'Sullivan *et al.*, 1995). This

eliminates any kind of pre-treatment of the samples preventing contamination. Croot and Laan, (2002) modified the system from King *et al.*, (1995) to allow for continued underway analysis of Fe(II) in surface waters. There is a short fall of this method: obtaining a reliable blank signal and a reliable load of detection, decreasing the accuracy of the Fe(II) concentration (Ussher *et al.*, 2005). Ussher *et al.*, (2005) investigated the direct injection method with the preconcentration method and found that organic compounds could interfere with the reaction, affecting the accuracy of Fe(II) determination. They used a resin column to remove the Fe(II) from the matrix, allowing for the analysis of Fe(II) only. Other advantage of a preconcentration column is the enrichment factor allowing for a lower detection limit and at the same time the removal of other interfering metals in the chemiluminescence reaction (Obata *et al.*, 1993 and Nédélec, 2006).

Powell *et al.*, (1995) introduced a 8-HQ resin column into King *et al.*, (1995) system, which has an affinity for Fe(II) at pH 5.5 - 6 (Obata *et al.*, 1993). Samples had to be buffered to that pH using a ammonium acetate buffer. Care should be taken that the samples are not too alkaline as Fe(III) formation is encouraged (Nédélec, 2006). This method gave rise to a higher detection limit then that of O'Sullivan *et al.*, (1995), 0.1 nM Fe(II) compared to 0.06 nM. Bowie and co-workers (1998) improved the system of Powell and co-workers (1995) by using a three pump system: 1) Wash pump; 2) Sample pump; 3) Reagents pump. Their resin column is being washed after elution by a HCl/HNO₃ acid wash to remove any iron residual which may not have been removed by the elution. They also prepared their luminol in a carbonate buffer rather than a borate buffer. This led to a detection limit of 0.04 nM Fe(II). This method has widely been adopted in literature (Bowie *et al.*, 2004 and Ussher *et al.*, 2005). With some modification the system was able to be implemented on board for continuous underway analysis of Fe(II) in surface waters with a detection limit of 0.08-0.012 nM Fe(II) (Bowie *et al.*, 2002b) as well as automated FIA-CL system with a detection limit of 0.021 nM (Bowie *et al.*, 2005).

The FIA-CL system for the analysis of Fe(II) has been well developed over the past two decades. The optimal system uses luminol without an oxidation reagent at pH10.4 (Bowie *et al.*, 1998). The system can analyse for either dFe by reducing Fe(III) or for the Fe(II) speciation. The system has a very low detection limit which gives rise to more accurate results for the measurement of trace concentrations of metals.

(b) The iron (III) system

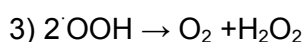
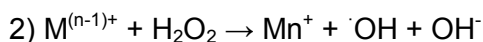
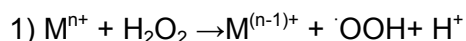
The first system was described by Obata *et al.*, (1993) and was modified by de Jong *et al.*, (1998) and Sarthou *et al.*, (2007). This system is very similar to that of the Fe(II) system, the major difference is that an extra reagent (H₂O₂) is added to the chemiluminescence reaction and a water bath is introduced prior to the PMT to increase the sensitivity of the chemiluminescences reaction. The ammonium concentration is also slightly changed to allow for a final reaction pH 9.5 compared to the Fe(II) system where the pH is 10.5.

For the analysis of Fe(III) all samples are acidified to pH < 2.0. This prevents precipitation of Fe from the water. An oxidant (H₂O₂ solution) is added to the samples prior to analysis to allow for all the dissolved Fe to be in the Fe(III) state.

Since the beginning of the 1990's chemiluminescence reactions have been used for the analysis of Fe in seawater, by FIA. This led to experiments revolving around the chemiluminescence reaction and what the role of iron is in this reaction. Luminol is the preferred reagent due to its higher sensitivity for trace metal detection (Nédélec, 2006). The luminol reaction is discussed in more detail below.

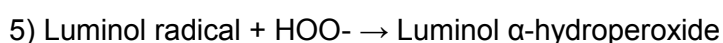
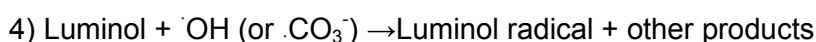
The luminol reaction in the presence of Fe(II) requires no H₂O₂ additions and has the best sensitivity at pH ~10.5 (King *et al.*, 1995; Bowie *et al.*, 1998 and Rose and Waite 2001). On the other hand in the presence of Fe(III) it requires H₂O₂ to improve the sensitivity and the optimal pH is pH ~9.5 (Obata *et al.*, 1993). A complete description of the luminol chemiluminescence reaction has been published by Xiao *et al.*, (2000) and Rose and Waite (2001). Here is a summary of their findings describing the luminol chemiluminescence reaction for the system developed in this work.

For the chemiluminescence reaction to produce a signal, a transition metal (M) with more than one oxidation state is required. The first mechanism is the production of oxygen by the decomposition of H₂O₂ and the production of a hydroxyl radical which oxidizes organic compounds. This is required for the chemiluminescence reaction to take place. This is achieved by the following reaction:

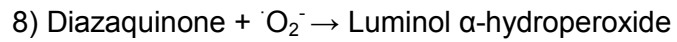
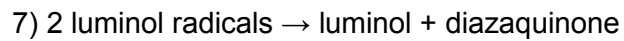


(M-stands for any transition metal with more than one oxidation state)

The second mechanism is a two-electron decomposition or oxidation. This leads to the formation of a M-H₂O₂ complex which reacts with luminol or breaks down to its basic state M and O₂ (reaction 3). The reaction between the intermediate M-H₂O₂ complex and luminol forms a luminol radical (Figure 2.3), which is the product of the hydroxyl radical. Often a carbonate radical enhances the luminol radical formation (Xiao *et al.*, 2002). The luminol radical reacts with H₂O₂ under basic conditions to form luminol α-hydroperoxide. The decomposition of the luminol α-hydroperoxide results in the emission of blue light (425nm).



A second reaction is taking place simultaneously forming the luminol α -hydroperoxide. This is obtained by the formation of diazaquinone from two luminol radicals. Diazaquinone reacts with a superoxide radical leading to the formation of luminol α -hydroperoxide,



followed by reaction 6.

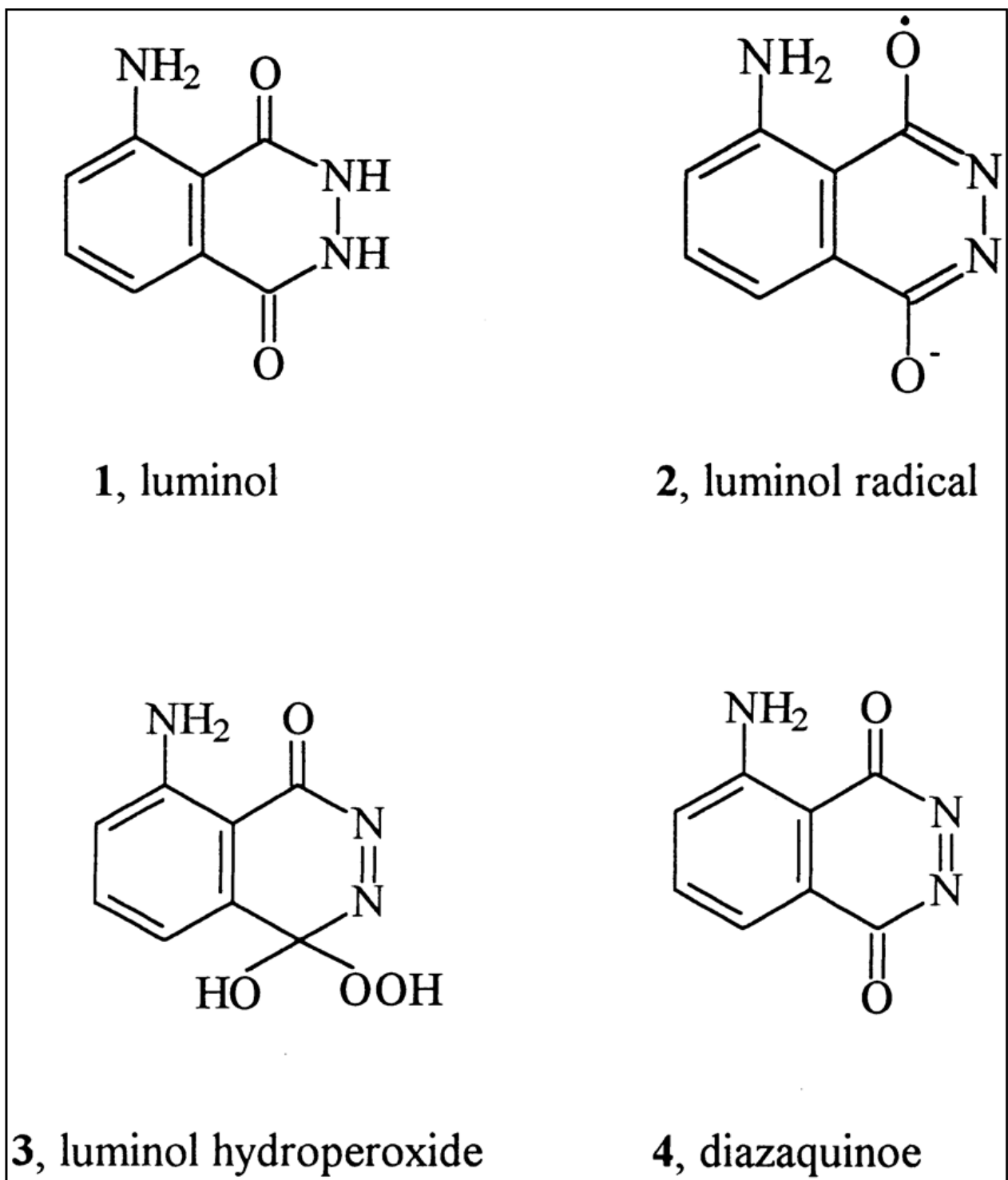


Figure 2.3: Displays luminol and its products during the formation of the chemiluminescence reaction (Figure after Xiao *et al.*, 2000)

The rate limiting step in the system is the decomposition of H_2O_2 . This can be improved in various ways.

- The addition of triethylenetetramine (TETA) (Obata *et al.*, 1993)
- An increased reaction temperature (30°C) (Xiao *et al.*, 2000)
- Optimisation of the reaction coil length. (Xiao *et al.*, 2000)

If H_2O_2 is kept under light conditions it produces hydroxyl radicals, which would enhance the baseline of the system (Xiao *et al.*, 2002), therefore exposure to light should be minimised. Luminol is also photo sensitive; producing luminol radicals, resulting in a lower chemiluminescence response (Rose and Waite, 2001). Therefore it is advised that luminol stock solution is kept in the dark and that a new luminol solution is made every 2-3 days.

Obata *et al.*, (1993) showed that Fe(III) chelates to the 8-HQ resin at pH 4.5, therefore all samples are buffered to that pH. The most common buffer used is ammonium acetate (de Jong *et al.*, 1998; Bucciarelli *et al.*, 2001; Laës *et al.*, 2003; Sarthou *et al.*, 2003; Sarthou *et al.*, 2007; Ussher *et al.*, 2009 and Chever *et al.*, 2010). de Baar *et al.*, (2008) modified the system by replacing the 8-HQ by iminodiacetic acid (IDA) which due to its wider pH tolerance removes the need for the buffer, hence samples can be analysed at pH 1.8.

Besides analysing for Fe in seawater the FIA-CL system has also been used for the analysis of Fe in river water and estuaries (Al-Gailani *et al.*, 2007) and sea ice (Lannuzel *et al.*, 2006). Qin *et al.*, (1998) even developed a FIA-CL system for the analysis of Fe in blood. This shows that the FIA-CL system has a wide variety of media which can be analysed for Fe.

2.2.3. Other systems or methods

The main methods and most developed methods for the analysis of Fe in seawater have been described above. Here are a few methods which have been lesser developed nature: Photothermal deflection spectroscopy (Khrycheva *et al.*, (2008)), Gas-segmented continuous flow analysis (Zhang *et al.*, 2001) and multi-syringe flow injection system (Páscoa *et al.*, 2009).

Khrycheva *et al.*, (2008) describe the Photothermal deflection spectroscopy method, reporting a detection limit of 8 fmol. This method chelates the sample to ferrozine before it applies the sample to a Silufol plate, which is dried before a laser probe beam zaps the sample, forming a gas which is then evaluated for its Fe concentration. Disadvantage of this system is that it cannot be utilized on board a vessel.

Zhang *et al.*, (2001) describe the gas-segmented continuous flow analysis method, using a long liquid waveguide capillary flow cell (LWCFC), connected to a fibre optic cable, which transmits light from a light source via the LWCFC to a photodiode for the detection of Fe. The photodiode measures the 562nm light emission which is formed from the Fe(II)-ferrozine complex. This system can be utilized for the analysis of Fe(II) and dFe. Fe(III) can be determined by the deduction of Fe(II) from dFe, with a detection limit of 0.1nM. The greatest advantage of the system is the high precision, small sample volume and automation. It can be implemented on board ships.

Páscoa *et al.*, (2009) described the multi-syringe flow injection system with spectrophotometric determination, reporting a detection limit of 0.89 nM. This method makes use

of a multi-syringe flow injection coupled to a preconcentration column (NTA resin). The Fe is then eluted and mixed with a colour reagent (ferrozine or ammonium thiocyanate). This colour complex is then analysed by a LWCFC spectrophotometrically at 480nm for Fe- ammonium thiocyanate or at 562nm for Fe-ferrozine complexes. The problem with this system is that it cannot be utilized for the analysis of Fe at trace metal concentrations.

Chapter 3: Development of Flow Injection Analyser with Chemiluminescence

A flow injection analyser with chemiluminescence detection was developed according to Obata *et al.*, (1993), with some modifications from de Baar *et al.*, (2008) for the analysis of Fe(III) speciation. This is not a commercially available method, but has to be custom built for each independent laboratory environment. This section will describe the development procedures, including the manifold, reagents, calculations, precision and accuracy tests and problems which occurred during the development phase.

3.1. Analytical setup

3.1.1. The manifold

The flow injection analyser is custom built, consisting of the following parts (Figure 3.1):

- a six channel valve (IDEX Health and Science),
- a peristaltic pump with a eight line pump head (Gilson Minipuls 3),
- a six port rotary inject valve (Scivex), with preconcentration resin
- temperature controlled water bath (PolyScience),
- photomultiplier tube (Hamamatsu Photonics K.K, H9319-01) (PMT) (Figure 3.2), powered by a programmable DC power supply (Manson NDP 4601)
- Laptop (Dell) with Windows XP

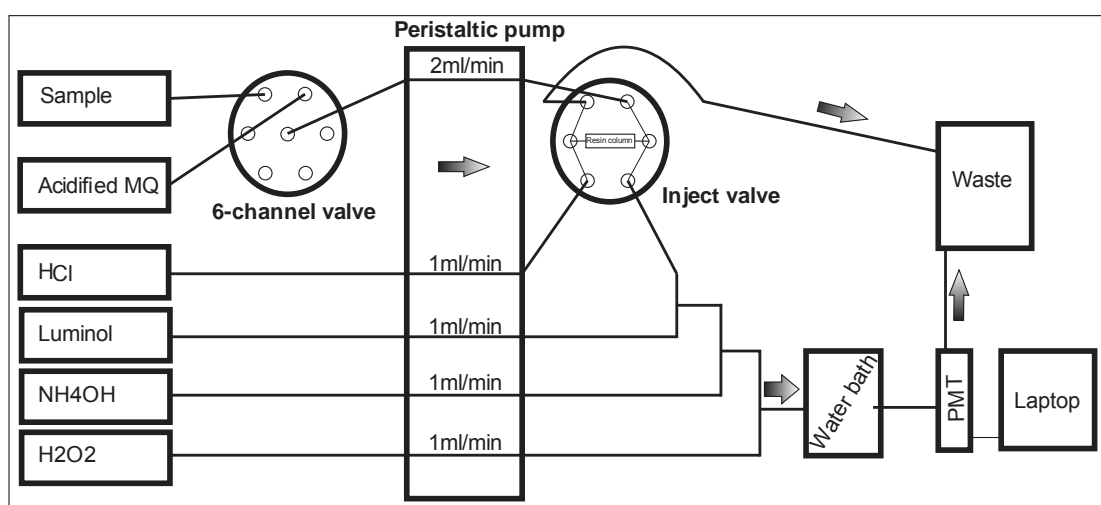


Figure 3.1: Diagram showing the FIA setup at Stellenbosch University.



Figure 3.2: The photon tube multiplier used in the system.

A pH meter (WTW Multi 350i) is used separately from the manifold to determine the reaction pH and sample pH.

All tubing is 1/16" ID FEP tubing (Cole Parmer) and all 2-stop pump tubing is tygon tubing (Precision Glassblowing). For each of the reagents (HCl, luminol, NH_4OH and H_2O_2) 1.3 mm ID 2-stop pump tygon tubing and for sample/MQ 1.85 mm ID 2-stop pump tygon tubing was used on the pump. The resin preconcentration column was made from a two centimetre piece of the 2.04 mm ID 2-stop pump tygon tubing.

All T-connectors were from polyetheretherketone (PEEK) material (Cole Parmer)

30 μm , 2.4 mm Polytetrafluoroethylene (PTFE) frits (Savillex) was used for the preparation of the columns.

3.1.2. The Setup

All reagent bottles, sample and acidified MQ were placed within a laminar flow hood (Pico Trace). The peristaltic pump was set to allow for a flow rate of 1ml per minute for reagents and at 2ml per minute for sample/MQ (the setting on the pump was at 8rpm). FEP tubing connects the reagents and the pump tubing. Ten centimetres FEP tubing connects the front (outlet) of the six channel valve with the tygon pump tubing. Position 1 on the six channel valve is connected via FEP tubing to the sample bottle, and position 2 is connected via FEP tubing to the acidified MQ bottle (Figure 3.1).

A 10 cm tubing connects the sample/MQ tygon tubing and the HCl tygon tubing with the six port rotary inject valve, with the sample line entering on the load position and the HCl line entering the inject position. A 4 cm column filled with IDA resin is placed over the middle two valves. The sample/MQ line leaves the outlet valve directly into waste via a short piece of FEP tubing and the rest of the line is grey-grey pump tubing. The HCl line leaves the outlet valve into the carrier line with 5 cm tubing connecting to the first T-connector.

All other reagents have 10 cm tubing connected to the tygon tubing on the outlet side. Luminol connects to the first T-connector where the HCl line comes in. Five centimetre tubing connects the first T-connector with the second T-connector. There is a knot in the tubing to assist in the mixing of the reagents. The NH_4OH line connects with the second T-connector, where five centimetres knotted tubing connects the second T-connector with the third T-connector. The H_2O_2 line connects to the third T-connector. A 23 cm piece of FEP tubing connects the 1.9 m long reaction coil with the third T-connector. The Reaction coil is placed into a water bath set at 30°C . A 17 cm piece of FEP tubing connects the reaction coil and the spiral cell. A small piece of 1.3 mm ID pump tubing is used as a connector between two FEP tubes. The spiral cell connects to the waste line which is 1.3 mm ID pump tubing.

The spiral cell is a 35 mm piece of FEP tubing coiled up as a snake into a cap (Figure 3.3). This cap is then placed over the PMT and taped to the PMT with black electric tape. The PMT is placed into a box for protection. The water bath and the PMT box are completely blacked out, to prevent any external light to influence any measurements. Half of the tubing going to waste and the tubing between the water bath and the PMT are also blacked out. The PMT is connected to a Laptop (Dell).

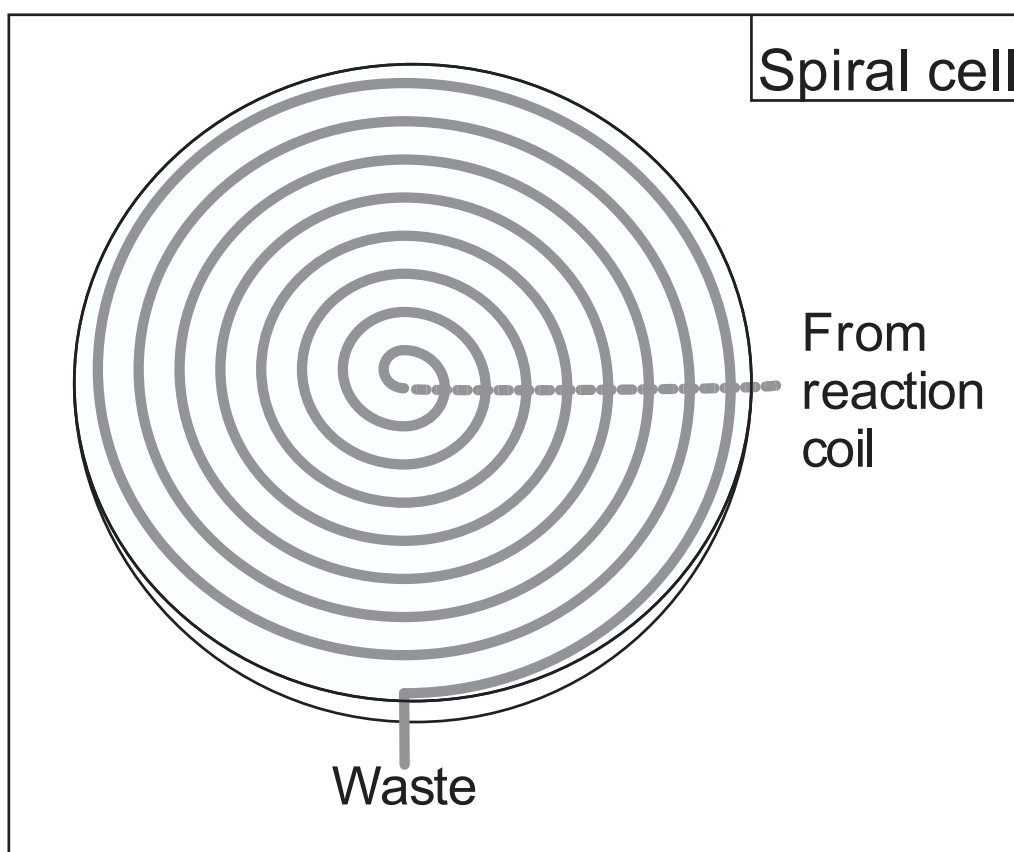


Figure 3.3: Diagram displaying the spiral used in front of the PMT.

The laptop with Windows XP was used to run the software (any windows program younger than XP will not run the program). The software was written at LEMAR laboratory (Brest, France) in QBASIC programming language. The software is set up to control the 6 channel valve and the

Load/Inject valve by allowing a determined time to pass before switching to the next position. It reads the number of counts the PMT is giving off and records this as a .DAT file which can be opened as a text document or imported into excel.

3.1.3. Resins

According to Bruland and Rue (2001) not enough research is put into resins used for concentration column on the FI-CL. There are a variety of commercial resins on the market which include Chelex 100, Amberlite XAD-4 and XAD-7, DDQ-resin. These have been tested by Obata *et al.*, (1993), who came to the conclusion that these cannot give the appropriate concentration, cannot work efficiently at the required pH; swell and contract as well as contaminate the results. Therefore Obata *et al.*, (1993) opted for the 8-hydroxyquinoline (8-HQ) resin. The 8-HQ resin tends to bleed, which is masking the low Fe concentrations. Therefore Obata *et al.*, (1993) synthesized – HQ on silica gel. The silica gel is diazo-coupled to the 8-quinolinol. The Fractogel TSK based resin from Landing *et al.*, (1986) is widely used. However the ester link to 5-amino-8-hydroxyquinoline · 2HCl used in Fractogel TSK is not stable to acid or base hydrolysis. The 8-HQ chelating resin has a long and complex synthesis and sometimes fails (Dierssen *et al.*, 2001). Therefore Dierssen *et al.*, (2001) developed a new production method and changed from the Fractogel TSK to an epoxy (Toyopearl TSK-Gel HW-65C). The Toyopearl TSK-Gel HW-65C binds to 5-amino-8-hydroxyquinoline · 2HCl via an amino link which is more stable. Weeks and Bruland (2002) compared the efficiency of the three different 8-HQ resins prepared. They showed that the silica gel based 8-HQ resin had the highest retention capacity and steepest elution profile. Appendix 1 shows the method used for the preparation of the 8-HQ resin used in this work.

One disadvantage of the use of 8-HQ is that it does not chelate Fe at pH < 3 and becomes unstable at a pH > 9 (Nédélec, 2006). Optimal conditions for this resin are between pH 3 and pH 6 (Measures *et al.*, 1995). Lohan *et al.*, (2005) looked for an alternative chelating resin which would be able to obtain results at a pH 1.7. This is the pH to which all samples are acidified, to keep the iron in its dissolved phase, or to dissolve any particulate iron. Nitriloacetic Acid (NTA) Superflow is a commercially available chelating resin which can chelate iron at a low pH (pH < 3) and at low concentrations (pM). The advantage of the NTA resin is that the acidified samples do not need to be buffered before analysis compared to the 8-HQ (Lohan *et al.*, 2005), which could induce contamination. The disadvantage is that the resin has to be conditioned with acetic acid/ammonium buffer, the same buffer used to bring the pH of 1.7 up to above 3 for 8-HQ to be effective.

De Baar *et al.*, (2008) looked at Toyopearl AF-Chelate-650M Iminodiacetic acid (IDA) which has a wide pH affinity for Fe(III), therefore samples could be analysed at pH 1.8 without the need

for a buffer. The advantage of the IDA resin is that it does not need a long time (120s) to be conditioned to seawater.

The amount of observations based on the 8-HQ resin proved to be inconsistent with each analysis. The NTA and IDA resin allow for analysis at pH 1.7, as an extra addition of buffer was no longer required. The difficulties in pre-conditioning the NTA resin, led to IDA as being a more superior resin. The IDA resin gave a consistent amount of observation for each run, without any variability in the values obtained.

3.1.4. Chemicals and reagents and preparation

All chemicals were prepared by using trace clean MilliQ (MQ) (Q-POD Element, Millipore) with resistance $\geq 18.2 \text{ M}\Omega$.

- Hydrochloric acid (0.25M)
 - 25ml of HCl (Merck, suprapur) in one litre MQ.
- Hydrogen peroxide (0.3M)
 - 30ml of H_2O_2 (Merck, suprapur) in one litre MQ.
- Ammonium (0.51M)
 - 40ml of NH_4OH (Merck, suprapur) in one litre MQ.
- Luminol stock (0.05M)
 - Diluting 530mg of luminol ($\geq 97\%$ (HPLC) 3-aminophthalhydrazide, Sigma Aldrich) and 620mg potassium carbonate (Merck, suprapur) in 60ml MQ.
- Luminal working solution (0.25mM)
 - 5ml of the luminol stock solution and 70 μl of TETA (triethylenetetramine, Merck) in one litre MQ.
- Buffer (ammonium acetate)
 - Mixing 100ml NH_4OH (Merck, suprapur) and 30ml acetic acid (Merck, suprapur) with 120ml MQ.
 - The buffer solution was three times purified through a 12cm long 8-HQ resin column.
- Fe stock solution (100 μM)
 - 279 μl of Iron atomic spectroscopy standard concentrate (Fluka) (which was prepared in one litre MQ) in 50ml MQ
- Fe working solution (300nM) (for the preparation of standards)

- 150µl of the Fe stock solution in 50ml MQ

Verbal communication with M. Lohan suggested to make use of slightly acidified MQ (pH 3) (100µl HCl (Merck, ultrapur) in one litre MQ) as rinsing solution to remove artefacts and salts from the column. A 10 mM H₂O₂ solution is prepared in 30 mL MQ.

3.1.5. Determination of Fe Concentration

3.1.5.1 Standard and Sample Preparation

Standards were prepared in 0.2µm filtered low Fe seawater, which was used to obtain the calibration curve. Twenty litres of 0.2µm filtered low Fe seawater was collected in an acid cleaned carboy of which one litre of the seawater was acidified with 2ml/L HCl ultrapur for a final pH ~1.7 (for standard preparation)). An acidified stock solution of 300nM FeCl₃ was added to 30ml acidified seawater (+0 nM: no addition, named Zero standard the Blank; +0.2nM; +0.4nM; +0.6nM; +0.8nM; +1.0nM) makes up the standards. 30µl of 10mM H₂O₂ solution is added to the standards one hour prior to the analysis for the oxidation of all Fe species (Johnson *et al.*, 2007). The ammonium acetate buffer is added immediately prior to analysis. Volume of addition is determined on a weekly basis, as the acetate portion of the buffer is more volatile than that of the ammonium and therefore loses its potential to buffer the standards/samples with the same volume weekly. Additions ranged between 110-120µl, to obtain a pH between 3.5- 3.7.

Samples are treated in the same manner as the standards.

3.1.5.2 The operating cycle

The standards/samples are loaded onto the resin for 120 seconds during the loading phase, when the inject valve is on the load position (Figure 3.4a). After, 60 seconds, acidified MQ rinse follows. The inject valve switches over to the inject position (Figure 3.4b), which is the start of the elution phase. The elution takes place for 120 seconds, removing the Fe from the resin. The eluting solution which contains the Fe mixes first with the luminol solution, then with the ammonium solution and finally with the hydrogen peroxide solution, before it reaches the reaction coil. The solution moves from the reaction coil through the spiral cell, where the photons from the chemical reaction are measured. The measured photons are output as a text file (Appendix 2), which is the data obtained.

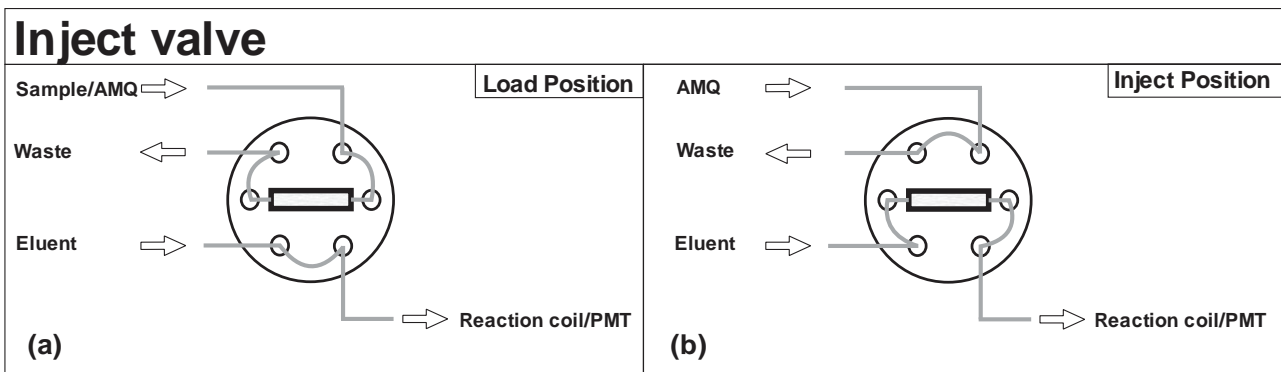


Figure 3.4: Indicating the positions during the load (a) and inject (b) phase.

3.1.5.3. Blank determination

The calibration curve is obtained by firstly determining the blank. This is done by pre-concentrating the Zero standard onto the resin for 10 seconds, 60 seconds or 120 seconds, and then eluting the resin for 120 seconds by HCl solution. By plotting these results and obtaining the y-intercept the blank value is obtained (Figure 3.5 & 3.6). The blank value represents the contribution by the reagents.

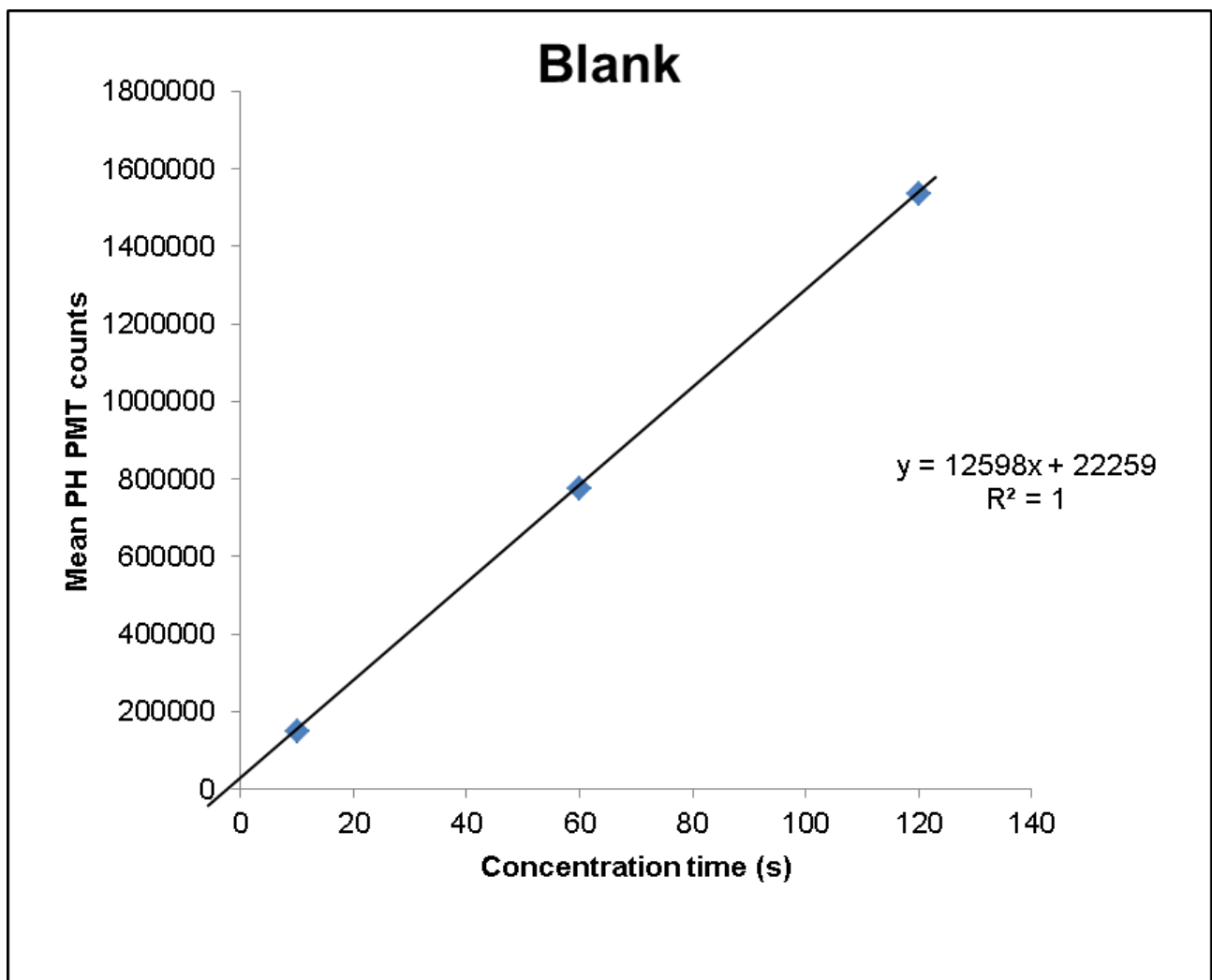


Figure 3.5: Blank determination for the Peak Height (PH) method

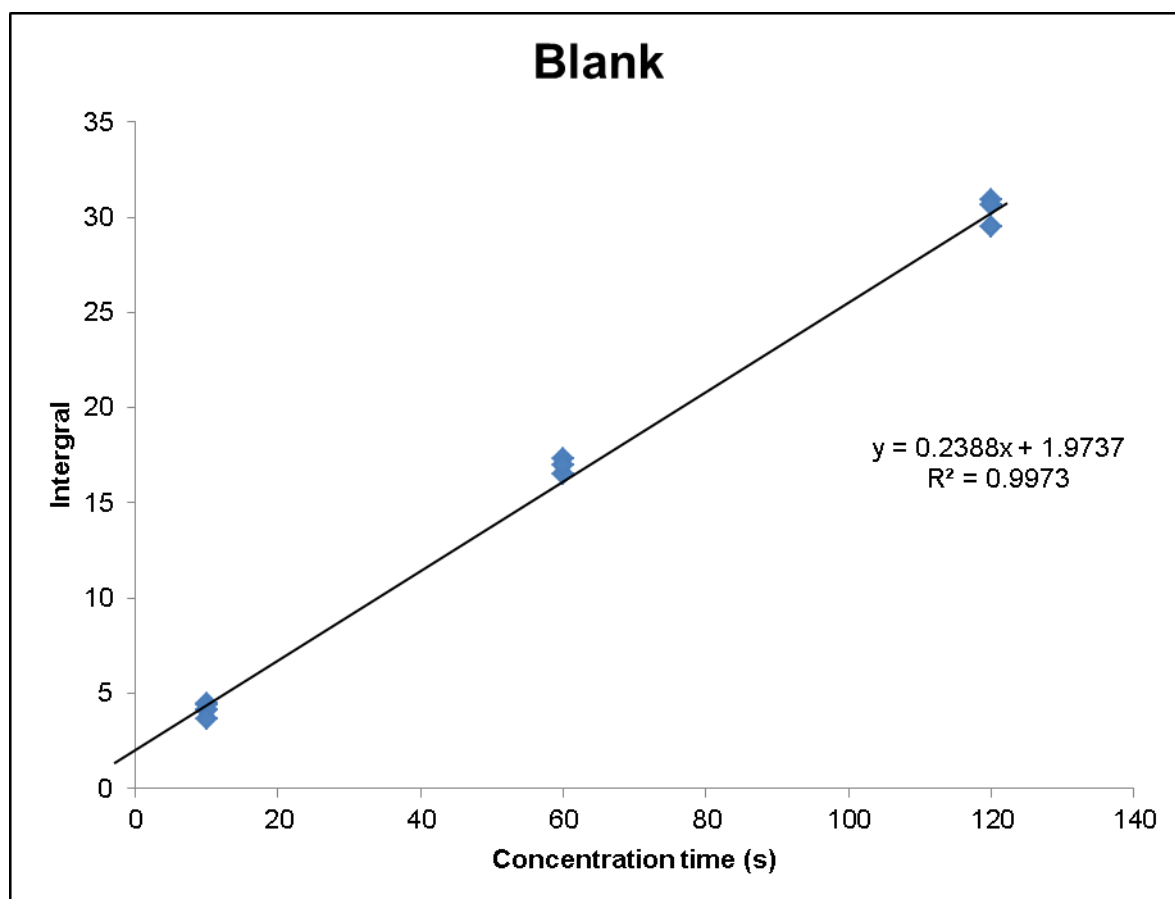


Figure 3.6: Blank determination for the Integral method

The calibration curve is obtained by pre-concentrating each standard onto the resin for 120 seconds, rinsed by acidified MQ for 60 seconds to remove the salts from the matrix, and then eluted for 120 seconds by HCl. This is repeated three times for each standard before moving on to the next one (n=3). These results are plotted to obtain the calibration curve. There are two methods for calculating the concentrations of iron, including the determination of the calibration curve. This will be discussed in the next section.

3.1.5.4. Calculating the Concentration of Fe

Two different mathematical methods were used to process the raw data (i.e. the signal from the PMT) and to calculate the concentration of iron in seawater. The first method uses the difference between the baseline and the peak height of the curve and will be referred to as the peak height (PH) method. The second method makes use of the area under the graph by taking the integral and will be referred to as the integral (Int) method.

(i) Peak height method

The peak height method subtracts the first value of the baseline from the maximum value of the graph also referred to as the peak of the graph (Figure 3.7). This is done for three consecutive runs. The mean and standard deviation is taken for those three runs.

The blank value is deducted from the mean to obtain the blank correction for the peak height method. The blank corrected value is then divided by the calibration slope to obtain the concentration. The calibration slope is determined by plotting the blank corrected values against the standard addition concentrations (Figure 3.8). The concentrations are derived by dividing the first standard deviation by the calibration slope.

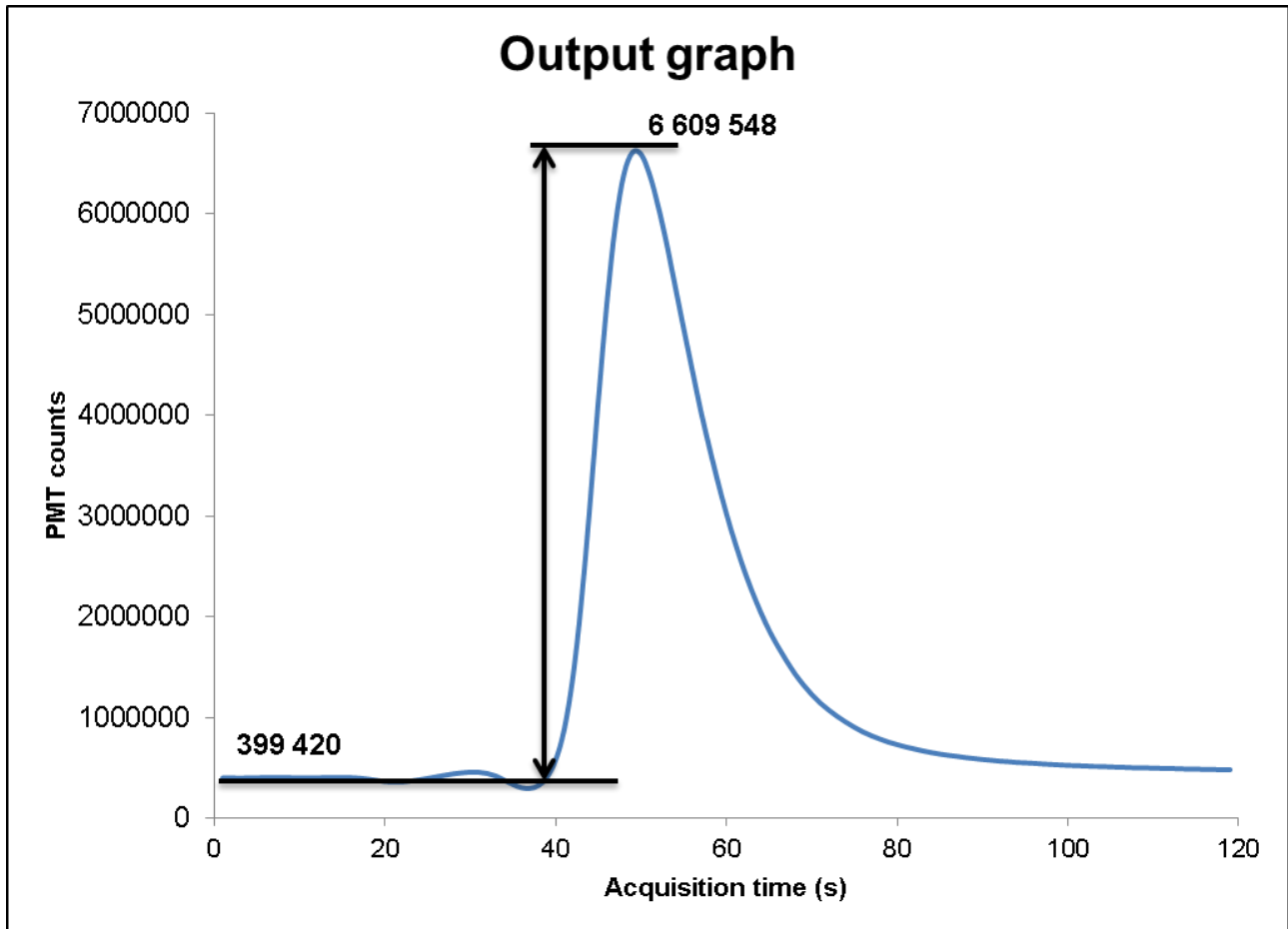


Figure 3.7: Graph displays how the PH method is calculated, by deducting the starting value (399 420) of the graph from the peak value (6 609 548)

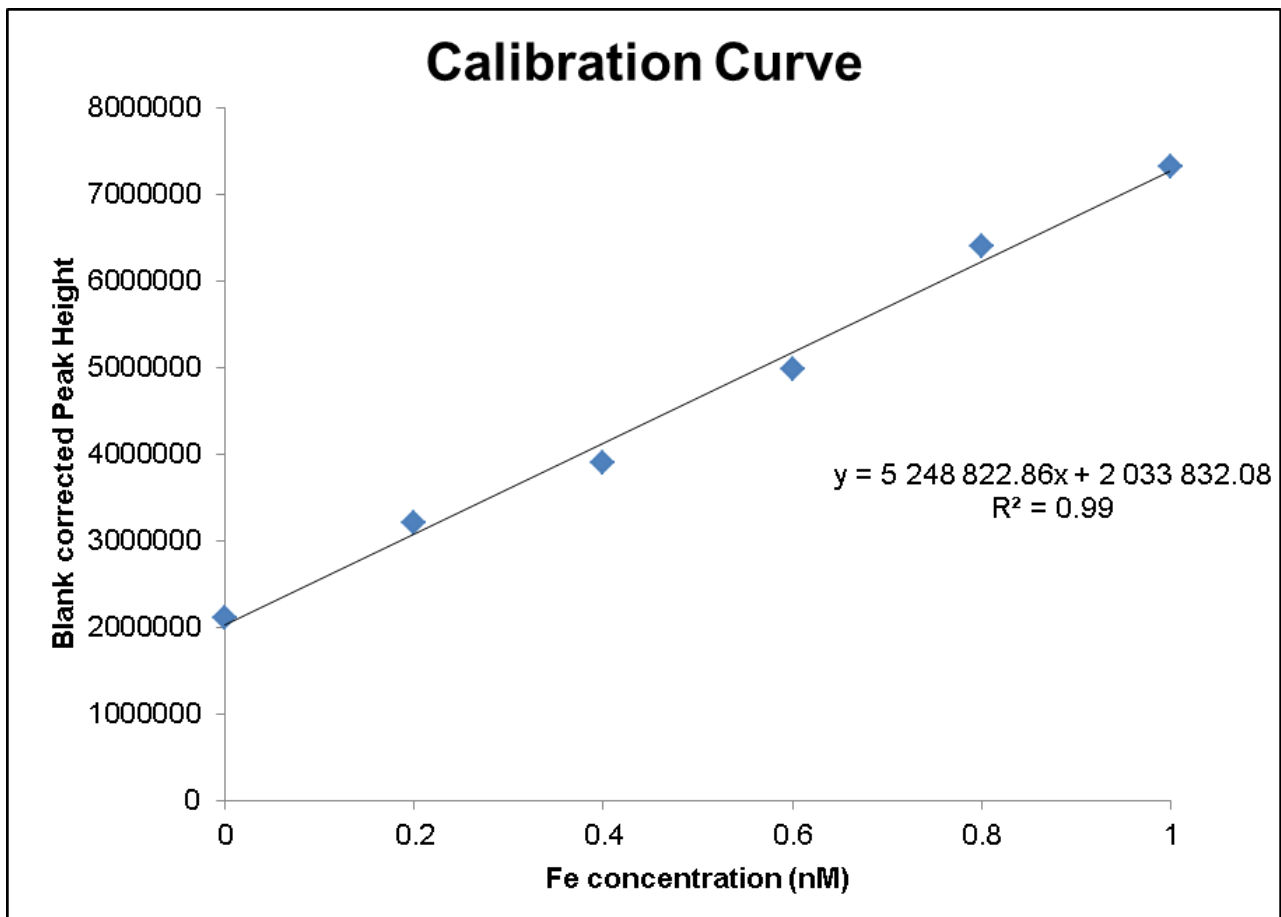


Figure 3.8: Indicates the calibration graph obtained when plotting the added standard concentration against the blank corrected peak height.

This method requires a correction for the final concentration to take the drift of the baseline over time into account. This is done by regularly running a known internal standard. The difference between the first standard and the next standard is used to correct all the values measured in between the two standards by taking into account the number of standards run in between.

$$\frac{x}{Slope + \frac{Slope * (Std_1 - Std_0)}{\frac{Std_0}{n_x}}}$$

x is the sample

Std is the standard

n_x no. of samples between the standards

(ii) Integral method

The Int calculates the area under the graph to determine the concentrations. This is done as a set of three for each individual sample or standard. The final concentration of each sample is the mean of the total set.

Each elution of 120 seconds has 119 acquisitions (observations) (Appendix 2) which can be plotted to obtain a graph as seen in the peak height method. The integral method uses these 119 counts to perform the following calculation.

Integral calculation

Step 1: The average baseline is obtained by taking the mean of the first eleven counts of every peak.

Step 2: Each individual count is divided by the average baseline.

Step 3: The initial (mean of the first eleven values, equal to 1 after Step2) and final average of the values (mean of the last eleven values, from the 86 to 96 acquisitions) obtained in step 2, are used to calculate the baseline slope. The baseline slope is calculated by dividing the difference between final and initial average by the number of counts between the initial and final values. This series of calculations results in the following Figure 3.9 below:

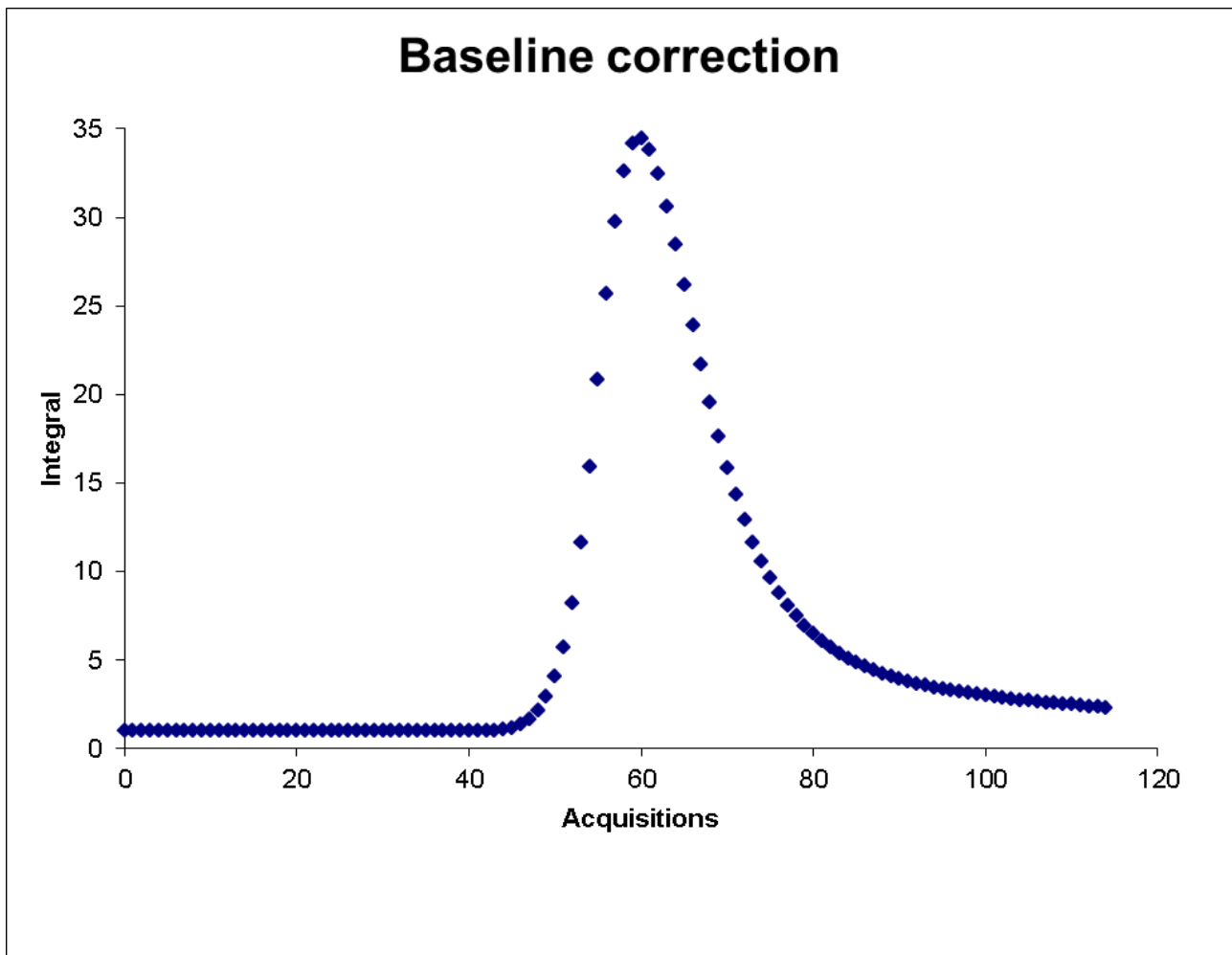


Figure 3.9: Graph obtained after correcting for the baseline, removing the negative dip prior to the rise in the graph.

Step 4: The first integral is obtained by summing all but the first seven values obtained in step 2. These first seven values are excluded as there is no difference due to the baseline being constant. Hence from here all values will only start from the 8th acquisition obtained originally.

Step 5: The original number of observations is thus reduced by eight (this is to make the new value on position zero). This number is then multiplied by the baseline slope value and then added to the initial average value. The value obtained is then subtracted from the value obtained in step 2 (Figure 3.10).

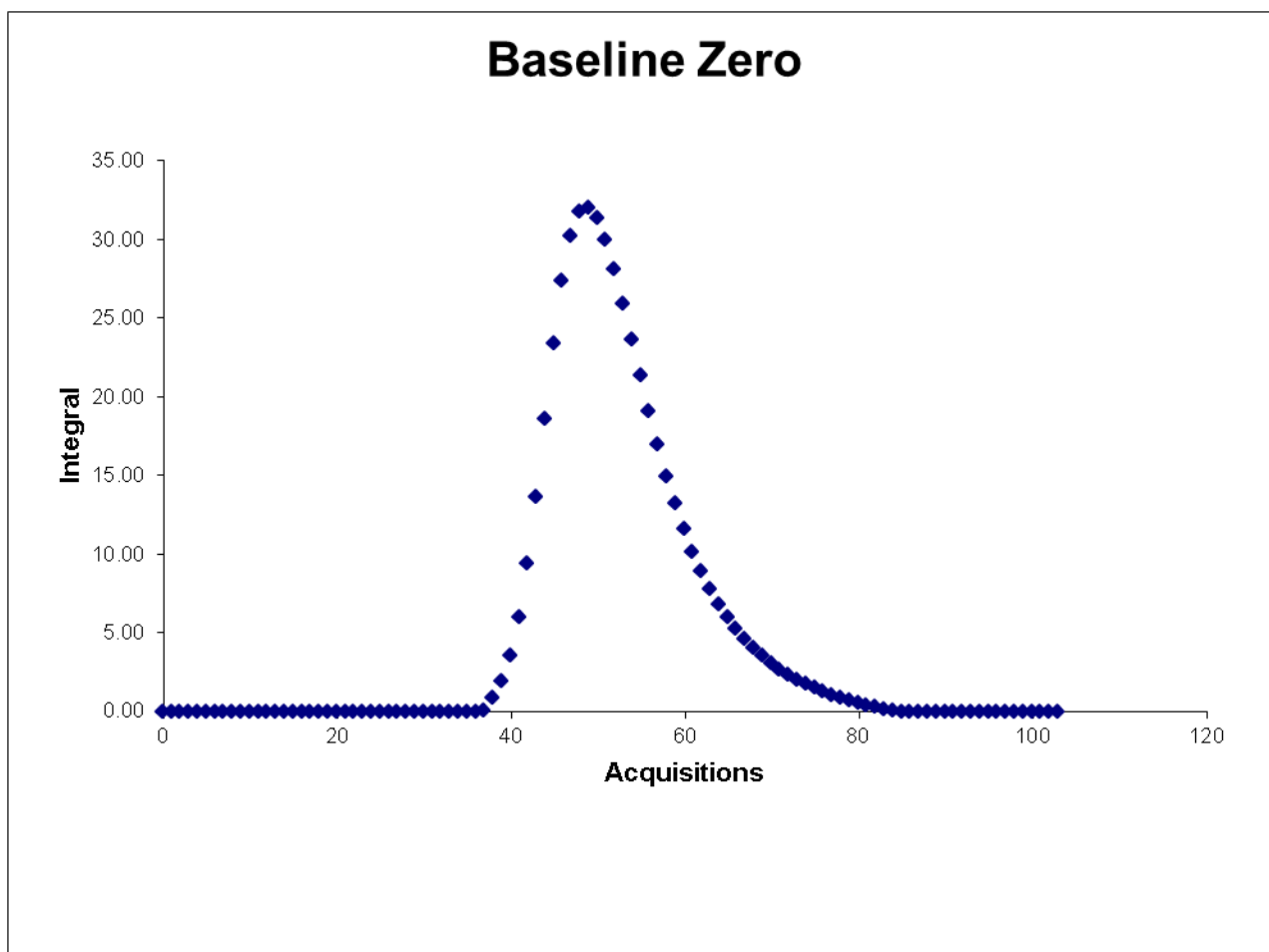


Figure 3.10: Bringing the baseline to zero to allow for the area under the graph to be determined in the integral method.

Step 6: The second integral is the sum of step 5.

Step 7: This step is to bring the baseline of the graph equal to zero. If the result of step 5 was negative then the value becomes zero, but if the value was positive it stays the same. This also takes the drift of the baseline into account and there is therefore no need for a drift correction.

Step 8: The positive intergral is the sum of all the values obtained in step 7.

Step 9: The blank is determined by the intercept obtained when loading the zero standard for five runs of 10s, three runs of 60s and three runs of 120s and plotted against the positive intergral of each respectively (Figure 3.6).

Step 10: The corrected intergral value depends on whether the positive intergral is positive or negative. If the value is negative then the value is equal to the positive intergral. If the value is positive then the blank is subtracted from the positive intergral.

Step 11: The calibration slope is the slope obtained when plotting the standard concetration against the corrected intergral values (Figure 3.11).

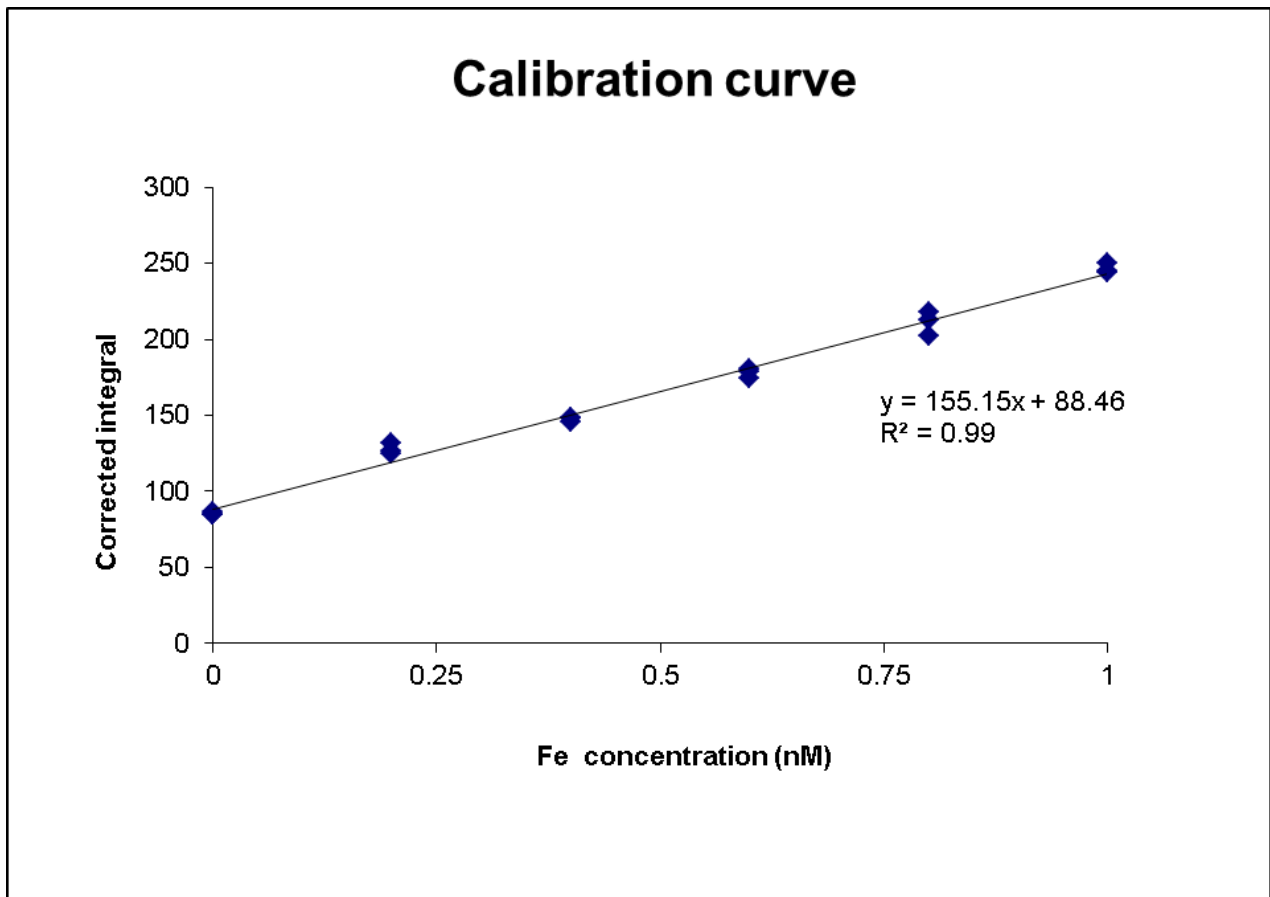


Figure 3.11: Calibration curve obtained in the integral method

Step 12: The final concentration is calculated by dividing the value obtained in step 10 by the calibration slope. As for the samples the mean of the set is then taken as the final concentration.

For both methods:

- The detection limit is three times the standard deviation of the zero standard divided by the calibration slope
- The concentration of the blank is determined by dividing the blank value by the calibration slope.
- The concentration of Fe in the seawater in which the standards have been prepared (referred to as the zero) is obtained by dividing the slope of the mean versus the standard concentration by the calibration slope. The zero correction is the addition of the sea water zero plus the added standard concentration.

3.2. Development of the method

The FIA-CL is the most common method used on ship's, however, it is not standardized method and requires some development and optimization of the system to suit individual laboratories. In this section the development of our system is discussed.

3.2.1 Length of the reaction coil

The reaction coil allows for the mixing of the reagents, i.e., for the chemiluminescence reaction to take place. The length of the coil is important and needs to be adjusted so that the chemiluminescence is highest in front of the PMT. Obata *et al.*, (1993) used a 1.9 m reaction coil. Nédélec (2006) used a 1.81 m reaction coil, and stated that it was close enough to that of Obata *et al.*, (1993) and that at that point a plateau was reached. Klunder *et al.*, (2011) made use of a 5m reaction coil to optimise the reaction. These discrepancies in length lead to the following experiment where various lengths for the reaction coil have been tested.

The experiment was set up as following: filtered seawater was pre-concentrated onto the resin column for two minutes, rinsed with MQ and then eluted for two minutes. The reaction coil was placed inside a water bath set at 30°C. The reaction coil (60 cm, 90 cm, 120 cm, 150 cm, 190 cm, 220 cm, 250 cm, 280 cm, 300 cm, and 330 cm) was replaced after every three runs. The results (Figure 3.12) showed a variance of 2.24 (ANOVA test) in the signal. The level of confidence (0.05) as determined by the standard deviation of three runs varied over the whole spectrum (Table 3.1). The 190 cm long reaction coil showed the best reproducibility, indicating that the reaction is stable and has its maximum peak in front of the PMT. This length corresponds to that of Obata *et al.*, (1993) and therefore was selected for our system.

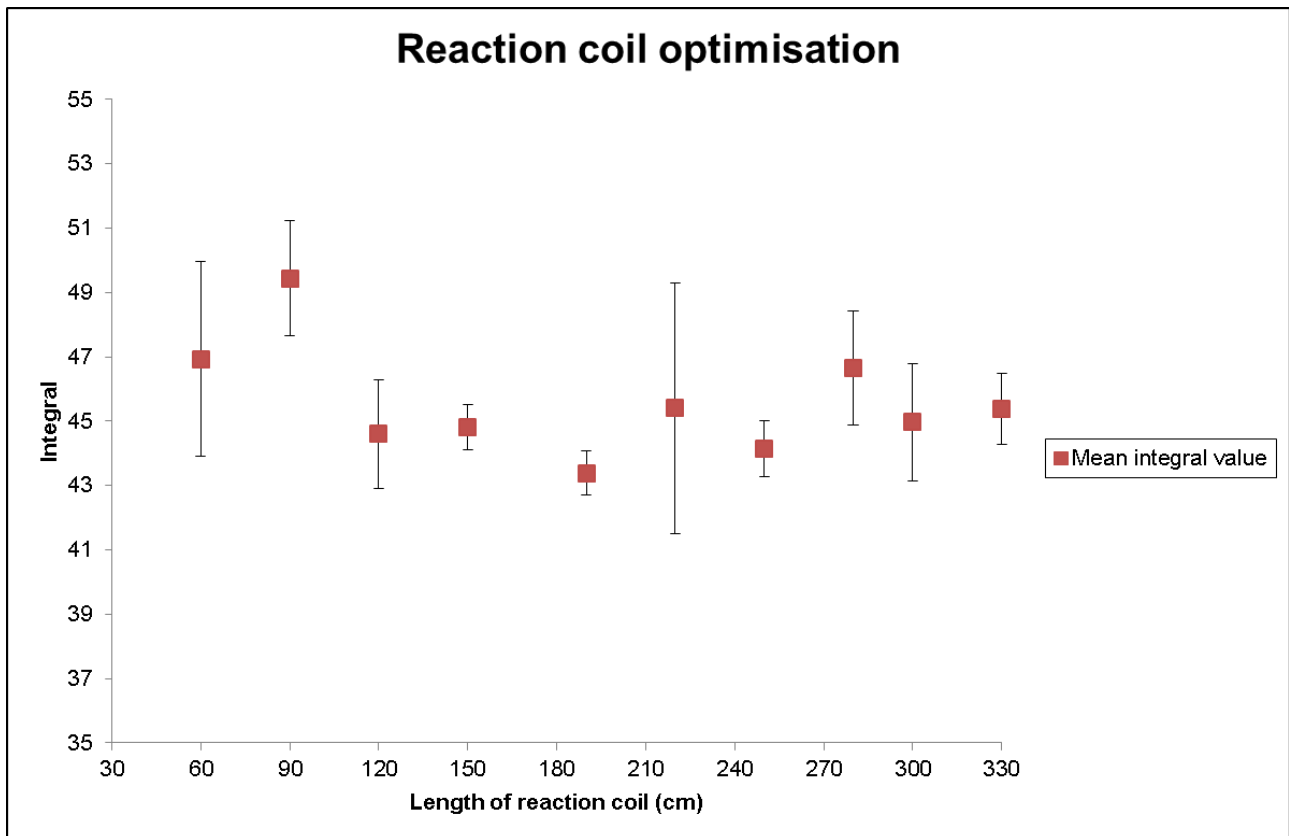


Figure 3.12: Represents the mean integral value of the length used for the optimization of the reaction coil. Error bars represent the standard deviation (n=3).

Table 3-1: Indicates the level of confidence from the lengths of the reaction coil

Length (cm)	60	90	120	150	190	220	250	280	300	330
Confidence interval (0.05)	3.43	2.04	1.91	0.79	0.77	4.41	0.98	2.00	2.05	1.25

3.2.2 Reaction temperature

The optimal temperature for the chemiluminescence reaction ranges from 27°C-35°C (Obata *et al.*, (1993); de Baar *et al.*, (1999); Johnson *et al.*, (2003); Nédélec (2006); Klunder *et al.*, (2011)). A higher temperature favours the decomposition of H₂O₂ (Nédélec, 2006), hence increases the signal. An increase in bubble formation was also noticed by Nédélec (2006) as temperature rose. For our system, temperatures between 25°C-35°C were tested. Bubble formation was observed above 30°C, hence the temperature was set at 30°C.

3.2.3 Luminol brands

There are a variety of suppliers of luminol: Merck, Fluka and Sigma. Luminol solutions of each supplier were prepared and tested to determine the cleanest supplied luminol to be used in the system. The luminol needed to be clean enough to prevent the PMT to overflow as well at the same time give the best sensitivity. This was done as following:

Luminol from Fluka and Merck were found to be heavily contaminated such that the PMT would overflow ($> 20\,000\,000$ photon counts s^{-1}). It was also observed that the Merck luminol had small black particles floating in the solution. This could cause potential contamination during analysis.

In order to purify the luminol; a 2 cm column of 8-HQ resin or IDA resin was placed inline of the luminol line prior to the t-connector. This caused the baseline to drop between 280 000-350 000 PMT counts and then rise over time. This lasted only for 3h on the IDA resin and 5h on the 8-HQ resin, until the PMT overflowed again, suggesting that the resins were saturated with iron. The IDA resin was found not to be as good as the 8-HQ resin to purify the luminol, hence the 8-HQ resin was used.

Five hundred millilitres of luminol was pre-purified through a 10cm long 8-HQ resin column. This was then introduced into the system, where the baseline was again back to the 280 000-350 000 PMT counts and slowly rose over time (never overflowing the PMT) until the whole purified 500 ml of luminol was empty.

The luminol obtained from sigma showed a baseline between 300 000-400 000 PMT counts without purification. The 2 cm IDA resin column inline brought the baseline down to 150 000 PMT counts and lasted for 2h until the baseline was back at 300 000 PMT counts. For the 2cm 8-HQ resin column it lasted for 4 hours before the counts were back at 300 000 PMT counts. 500ml was purified through a 10cm 8-HQ resin column, which gave stable PMT counts of 120 000-130 000. After 7 hours the PMT counts rose above 150 000.

Filtered (0.2 μm) seawater was loaded onto the system and eluted to see how the peaks would look for the purified Merck, Fluka and Sigma luminol as well as for the unpurified Sigma luminol (Figure 3.13). It was observed that the unpurified Sigma luminol showed the highest peaks. Therefore the Sigma luminol unpurified was used.

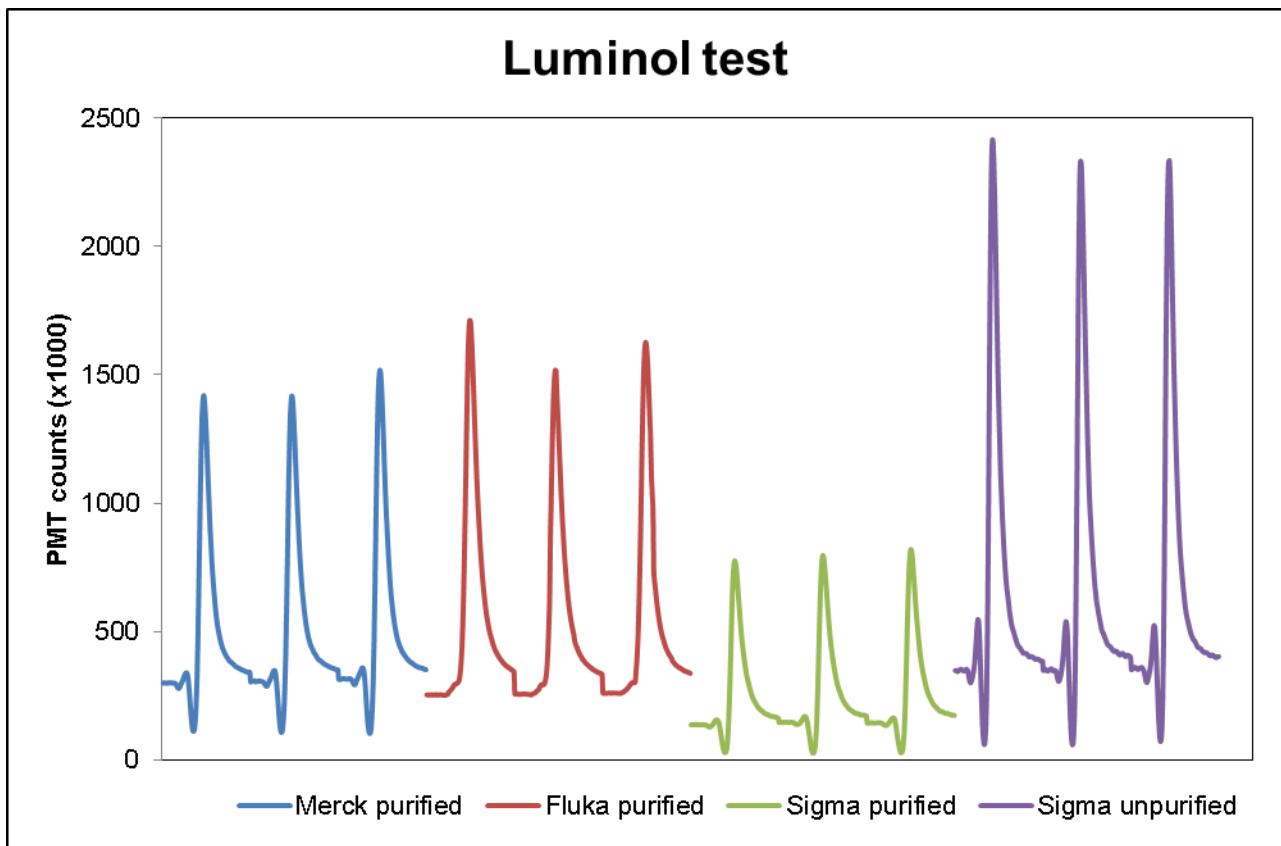


Figure 3.13: Indicates the curve obtained when running the different brands of luminol tested. Sigma unpurified gave the highest peak height (PH) difference (mean PH 2 011 092 with a RSD% of 2.4%). The worst results came from the Fluka purified (mean PH 1 362 563 and a RSD% of 7.2%).

3.2.4 Reagent concentrations

Literature states a variety of different reagent concentrations, see Table 3.2, therefore the original reagent concentrations were followed after LEMAR, Brest, France (2009), and were as follows: 0.4M HCl, 0.72M H₂O₂, 0.748M NH₄OH and 0.74mM Luminol. These concentrations gave a pH of 9.5 - 9.7. This agrees with the findings of Nédélec where the chemiluminescence reaction is optimal between pH 9.4-9.7, as well as the findings of Obata et al., (1993). One problem was that

Table 3-2: Shows the variety of concentration of the reagents used by different authors

	Obata <i>et al.</i> , 1993	de Jong <i>et al.</i> , 1998	Nédélec, 2006	Klunder <i>et al.</i> , 2012
HCl (M)	0.2	0.3	0.3	0.4
H ₂ O ₂ (M)	0.7	0.1	0.4	0.35
NH ₄ OH (M)	0.4	0.8	0.55	0.96
Luminol (mM)	0.74	0.1	0.1	0.305

the reaction was not sensitive enough (Figure 3.14a) After a visit at Plymouth University under the supervision of M. Lohan and A. Milne (2012) the concentrations were changed to 0.2M HCl, 0.3M H₂O₂, 0.5M NH₄OH and 0.25mM luminol. There was just a problem with the reaction pH which was observed at pH 9.9. Therefore the concentration of HCl was increased from 0.2M to 0.25M, giving a reaction pH of 9.6, which falls into the range observed by Nédélec (2006). The change in reagents increased the sensitivity (Figure 3.14b)

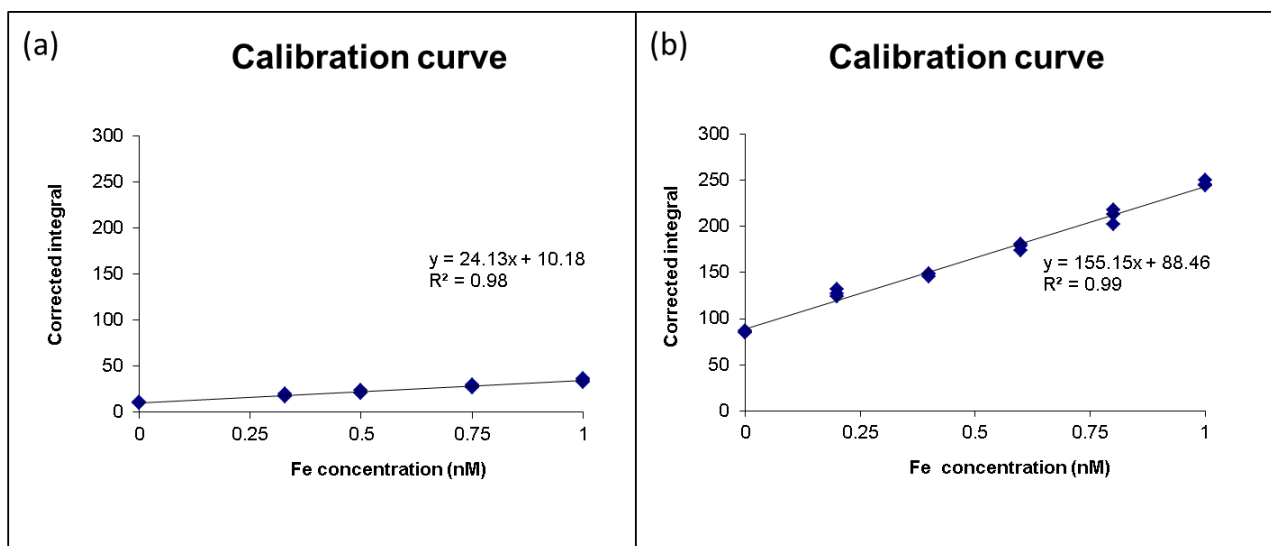


Figure 3.14: Sensitivity improvements, (a) indicates a poor sensitivity as the gradient is very low, (b) indicates a better sensitivity with a steeper gradient

3.2.5 Chelating pH

De Baar *et al.*, (2008) used IDA resin for its wide range of pH affinity and had the samples acidified to pH 1.8. Klunder *et al.*, (2011) also used the IDA resin, but buffered their samples to pH 4. We analysed acidified sweater buffered at different pH to optimize our own system. SAFe standard D1 was used as the base water for this experiment. Samples with a range of pH values (pH 1.7 – pH 4.8) were prepared. pH 1.7 looked like the optimum pH, but when looking at the peak heights individually one noticed that they are decreasing from analysis to analysis (Figure 3.15) and that the relative standard deviation (RSD) is at 15.4% (Table 3.3). Comparing the RSD from each individual pH, only pH 3.7 and pH 4.2 are below 1%. A higher peak was observed for the sample at pH 3.7 then at pH 4.2. A calibration curve with standard pH 3.7 was prepared and the samples analysed for the pH range. The mean concentration of 0.654 ± 0.012 nM for pH 3.7 (Figure 3.16) is also the only value which corresponds to that of SAFe D1 (Certified consensus values are 0.687 ± 0.041 nM) (www.geotraces.org). Therefore all samples were buffered to pH 3.7.

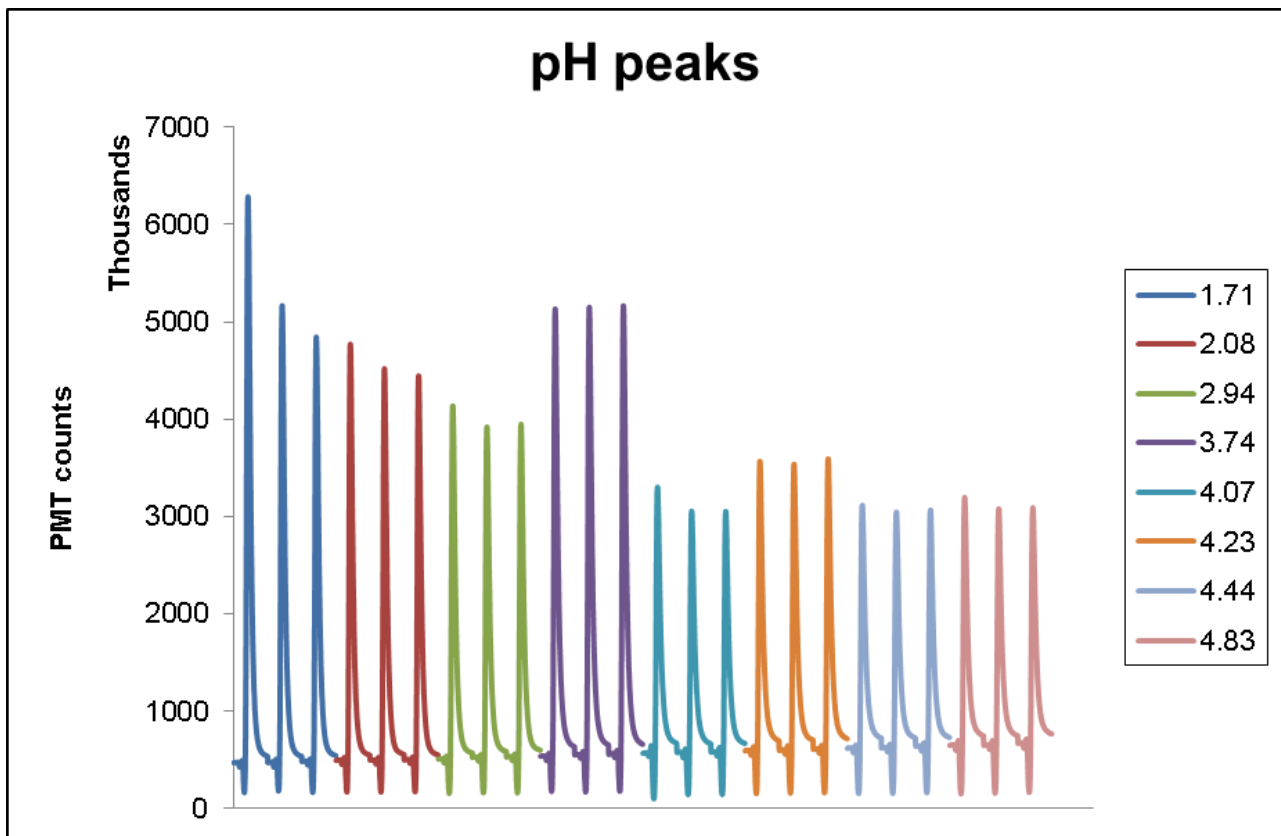


Figure 3.15: Indication of the peaks obtained by the various pH of the SAFe D1 sample used for the pH test. Each individual peak represents 120 acquisitions, which were stacked after each other for the visual comparison of each peak, and therefore there is no value on the x-axis.

Table 3-3: Indicates the pH values, the RSD%, concentration of Fe obtained as well as the standard deviation (STD)

pH	Concentration (nM)	RSD%	STD
1.71	0.819	15.362	0.144
2.08	0.629	4.246	0.027
2.94	0.504	3.649	0.030
3.74	0.654	0.127	0.012
4.07	0.345	5.83	0.029
4.23	0.382	0.800	0.006
4.44	0.297	1.702	0.013
4.83	0.282	2.855	0.010

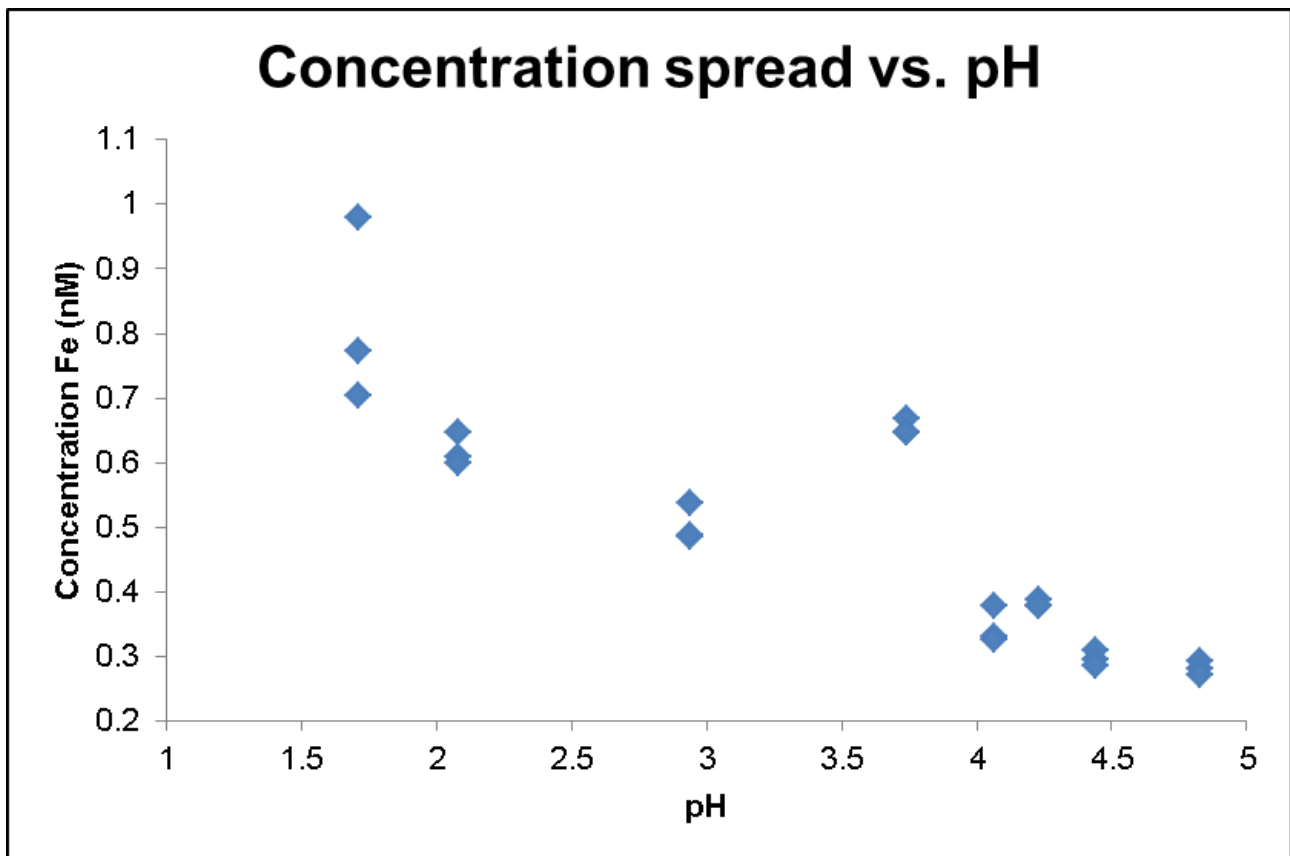


Figure 3.16: SAFe D1 concentrations obtained at various pH levels. pH 3.7 is the only pH at which the concentration is within the consensus value (0.687 ± 0.041 nM)

3.2.6 Buffer

An ammonium acetate buffer solution was prepared. Although the reagents were of suprapur grade and MQ water was used to prepare the buffer, the buffer needed to be tested for possible contamination of the sample. Filtered ($0.2\mu\text{m}$) – acidified (HCl up) ocean water was used with one time, two times and three times the addition of the buffer solution. The addition of ultrapur HCl was also increased to keep the samples at a similar pH 3.7. Without purification of the buffer there was a significant contamination of the sample (Figure 3.17). The buffer was then purified through a 10 cm 8-HQ resin column, and the experiment was repeated. It required 3 purification cycles for the contribution of the buffer to be negligible.

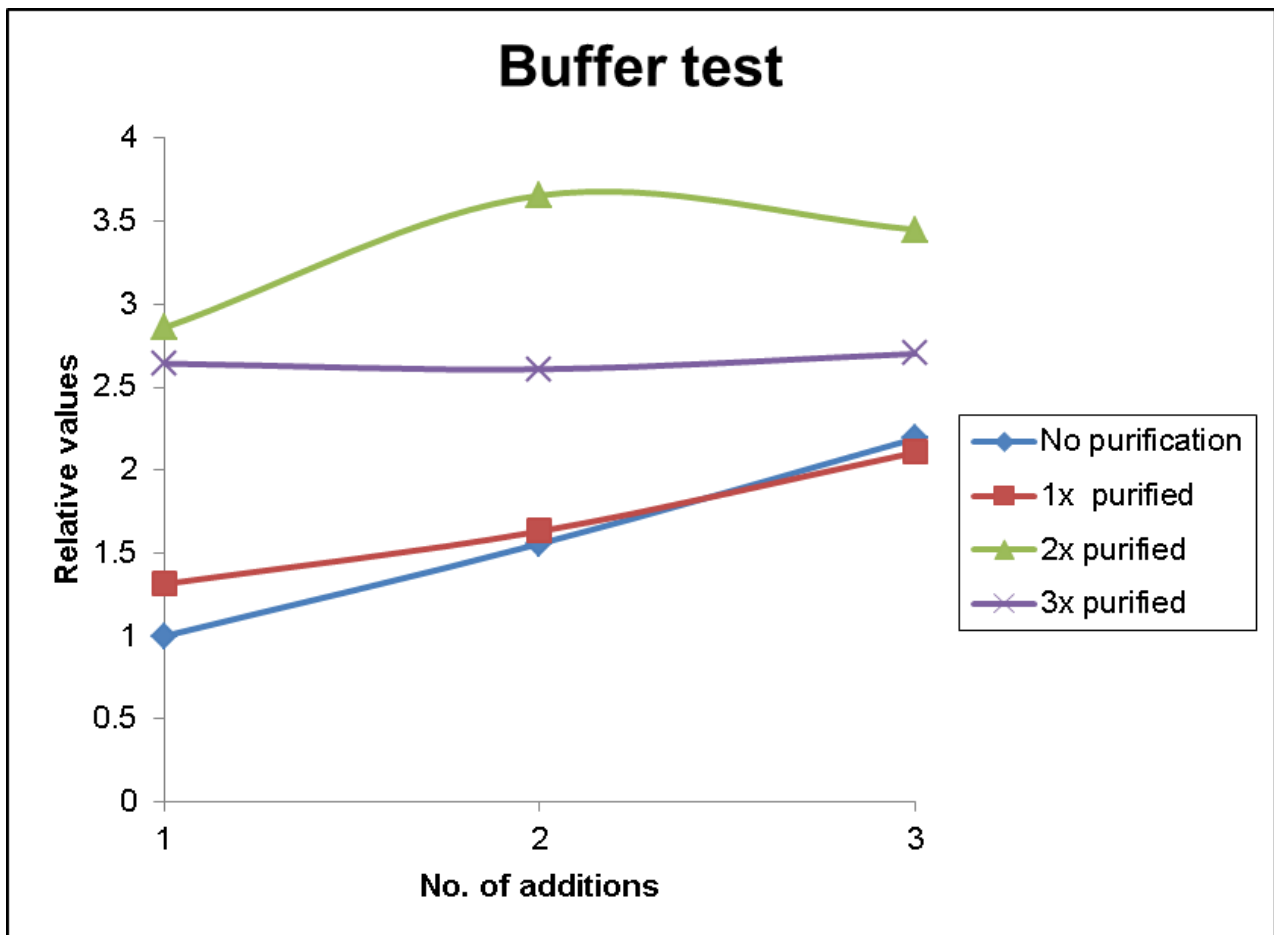


Figure 3.17: Displays the relative values (normalized to the no purification) of the buffer test for 0x, 1x, 2x, 3x purifications.

3.2.7 Accuracy

The accuracy of the system was tested by analysing the SAFe D1 and SAFe D2 reference material. This value was certified by 18 laboratories throughout the world using different analytical methods, including FIA-CL (Johnson *et al.*, 2007). Once the value fell within the certified range (after a number of attempts made within changes discussed previously), the method was considered to be accurate (Figure 3.18 & 3.19).

An average for the D1 SAFe standard has been observed as $0.667 \pm 0.046 \text{ nM}$ ($n=6$) for PH and $0.675 \pm 0.045 \text{ nM}$ ($n=6$) for Int. This is within the certified values for the calibration standards.

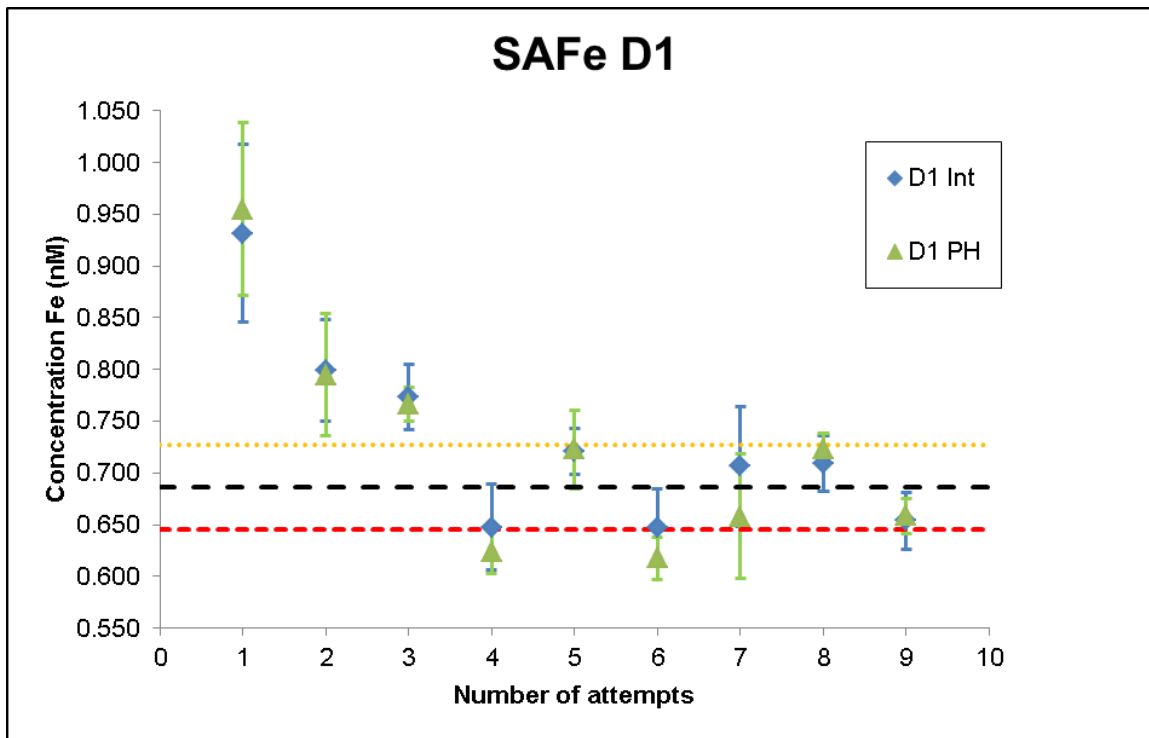


Figure 3.18: SAFe D2 reference material was used over several days during the development phase until a consistent result within the range of the certified value was achieved (only 2 were possible as the material ran out). The black dotted line indicates the mean SAFe value, the yellow and red dotted lines indicate the upper and lower limit of the SAFe value. (Each attempt refers to a different day after changes to the system have been made as discussed in the previous sections).

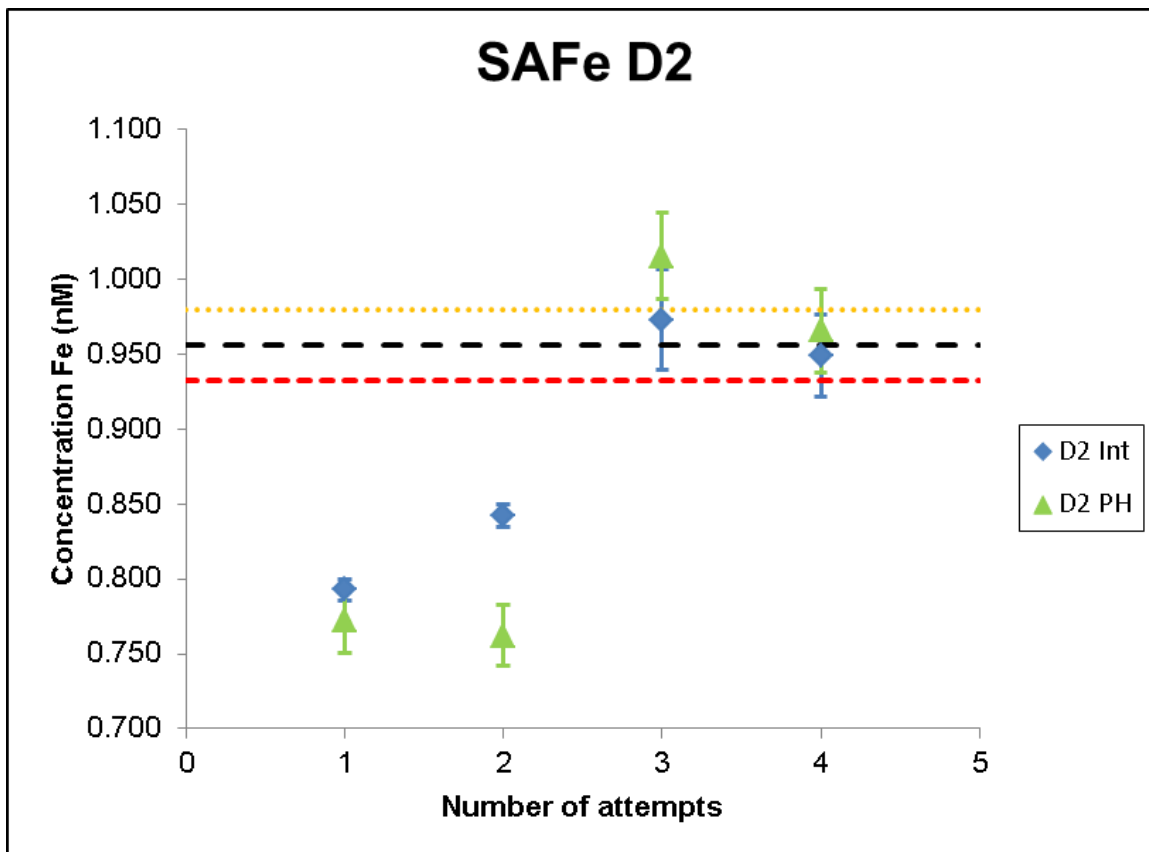


Figure 3.19: SAFe D1 reference material was used over several days during the development phase until a consistent result within the range of the certified value was achieved. The black dotted line indicates the mean SAFe value, the yellow and red dotted lines indicate the upper and lower limit of the SAFe value. (Each attempt refers to a different day after changes to the system have been made as discussed in the previous sections).

There are some differences noted between the PH and Int methods of calculating the concentration. A test was conducted running the D1 sample at the beginning and end of the day, and then both mathematical methods were used to calculate the concentrations. The Int method gave a slightly lower value at the end of the day as that of the start of the day. The PH method gave almost double the concentration at the end of the day compared to that of the start of the day. This indicates that there is an issue with the correction calculation for the PH method.

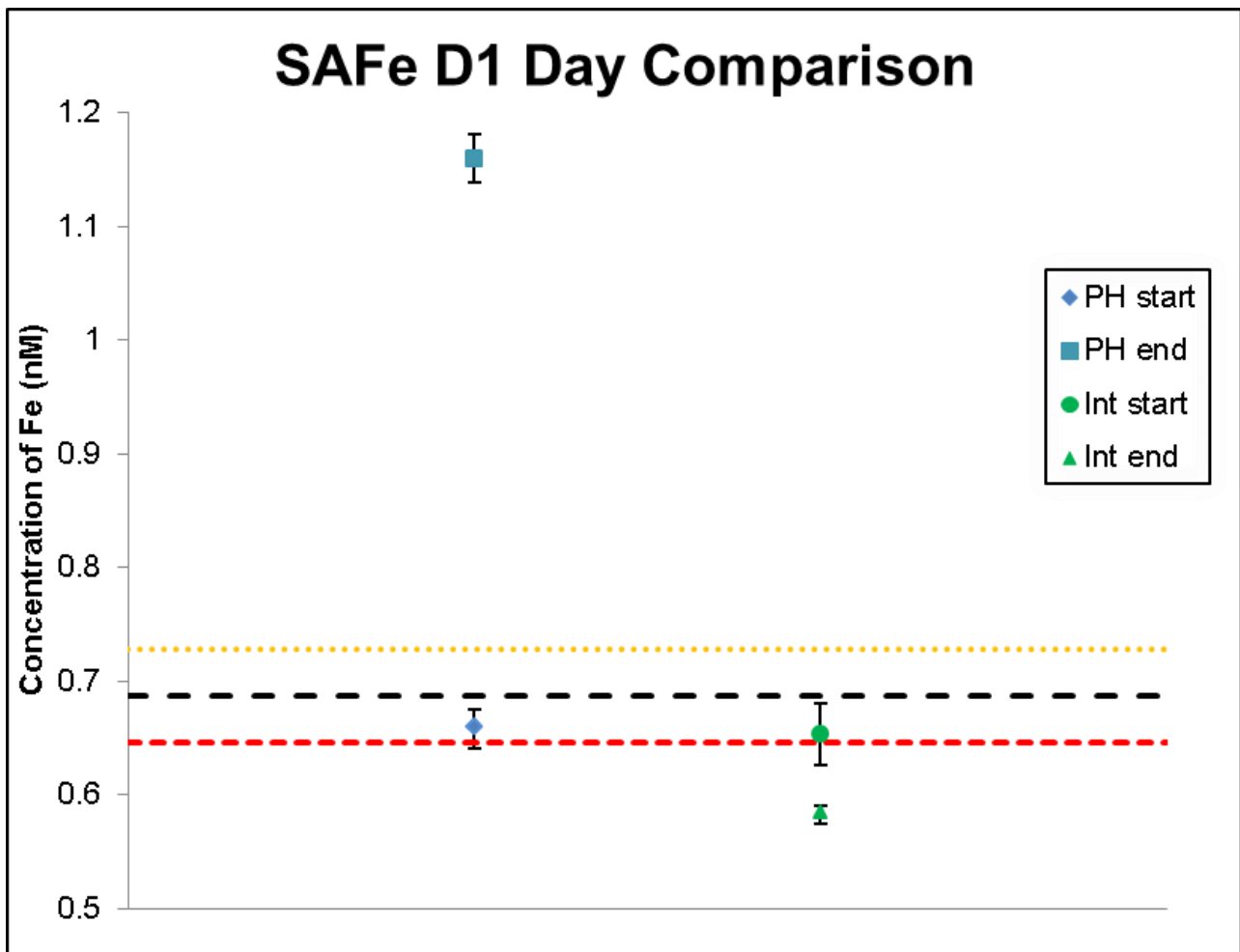


Figure 3.20: Shows the results for the SAFe D1 reference material run at the beginning and at the end of the day (15h later). Blue represents the PH method and green the Int method. The black dotted line indicates the mean SAFe value, the yellow and red dotted lines indicate the upper and lower limit of the SAFe value.

3.2.8 Precision

The precision test was conducted by running each standard ten times (n=10). All measurements are represented in Figure 3.21. From Table 3.3 it is evident that all the peak heights are below a RSD value of 5% and therefore are repeatable.

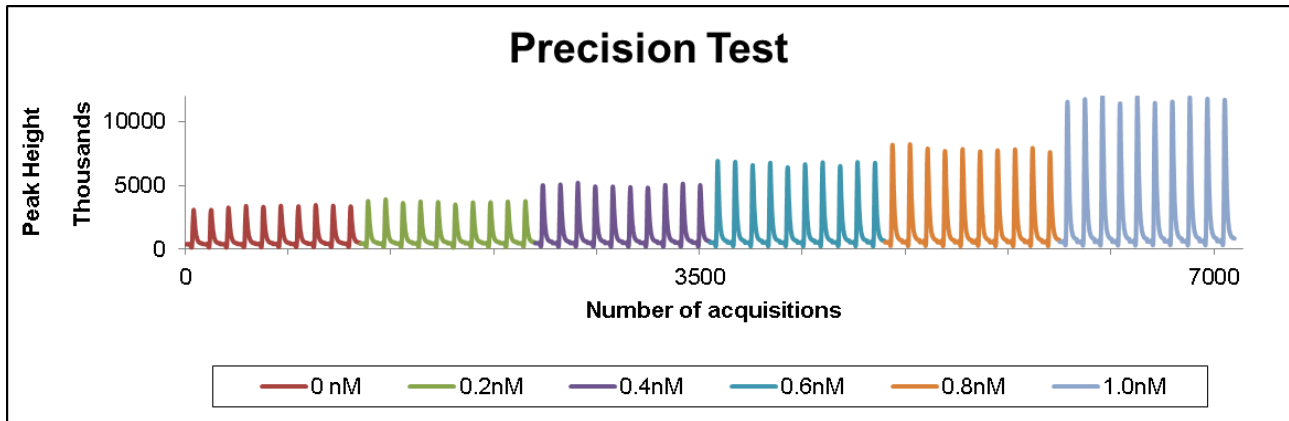


Figure 3.21: Standards were run for ten cycles each, to assess the precision of the system.

Table 3-4: Indicating the mean peak heights observed as well as the RSD% value

Standard addition concentration (nM)	Mean peak heights	RSD%
0.0	2901906	4.23
0.2	3250729	3.40
0.4	4506675	2.66
0.6	6181915	2.61
0.8	7304609	2.84
1.0	11105409	1.84

3.2.9 Internal Reference Material

Internal reference material was determined by analysing 0.2µm filtered low Fe seawater against the SAFe reference material. The seawater was obtained from the Southern Ocean during the SOSCEX1 cruise (2012). It was stored unacidified in a carboy. One litre was acidified with 2ml concentrated HCl ultrapur and was analysed after the calibration curve to verify the accuracy of the calibration. The advantages of having an internal reference material are to: i) save the SAFe reference material which is in limited access and ii) to have an internal reference material that has been acidified in the exact same way as the samples and standards.

3.3 Problems encountered during the development stage

During the development stage a variety of problems occurred. These problems involved back pressure, loss of resin and contamination.

3.3.1 Backpressure

Backpressure was the biggest problem for the setup of the manifold and originated from a variety of sources, which caused connection leakage and ultimately connection failure. These problems were solved by using connectors which are screwed together to keep the tubing in place. A rescuer build up caused the tubes to burst, which was solved by looking into the sources which could cause the pressure build up: i) the distance of the tubing, ii) the flow cell in front of the PMT, iii) the resin column and iv) the pump tubing to the flow tubing.

A decrease in the distance between each T-connector from 10 cm to 5 cm gave some relief but did not last long. A reduction in the distance between the pump tubing and the T-connectors was reduced to the minimum length possible to keep the system neatly in order. This resulted in some relief. Next was the flow cell. Under thorough investigation it was noticed that the tubing used was from a different internal diameter and therefore gave rise to the backpressure. This tubing was replaced with the same diameter as the rest of the system. After the flow cell a piece of 1.3 mm ID pump tubing was connected as the waste line. The change in diameter from 1/16" ID to 1.3 mm ID gave the relief that was needed. It was noticed there was still some back pressure in the sample/MQ line which was always relieved once the valve switched from load to inject, but now the HCl line would build up pressure. This could only be the resin column. Different lengths and types of columns were used to compensate for the pressure build up, with no result. A change in the frit size, from 0.2 μm pore size to 30 μm , gave finally the relief which was needed. This solved the final problem of back pressure. There was no need to change pump tubing.

3.3.2 Loss of resin

Due to the column design and the 0.2 μm frits which were first used, the resin flowed around the frits and leaked from the column. After the change of the frits from 0.2 μm pore size to 30 μm , and the back pressure being resolved, the resin stopped leaking.

3.3.3 Contamination

Iron being the fourth most abundant element on the earth's crust, it is found everywhere and great care must be taken during preparation of reagents, standards and sample handling. Ultra clean methods have been developed and a protocol to correctly measure iron (and other trace metals) in the ocean has been implemented within the international Geotraces program (www.geotraces.org). Therefore all work needed to be conducted in an ultra-clean laboratory under laminar flow. To reduce the risk of contamination, a frequent change of gloves policy was implemented.

During the beginning phase of the development there was no clean laboratory available. All work was done in a laminar flow chamber in a Geology laboratory. Even though great care was taken and reagents were prepared under the laminar flow hood, they were contaminated during preparation, as evidenced by high values of the baseline. This could only be solved by redoing all the reagents one by one to find the source of contamination.

After setting up the system in a class 1000 laboratory at Plymouth University it provided reproducible results, without any problems. This indicated that the working conditions were not clean enough at the Geology laboratory in Stellenbosch. The MQ system, for example, was found to be polluted by a rusty filter. Once the class 100 laboratory was constructed at Stellenbosch University (May 2013) and the system was setup inside, the problems of contamination were solved, which was proven by obtaining the certified SAFe reference values have been obtained.

During the visit to Plymouth the FIA was setup with a PMT from their laboratory, which could connect to a chart recorder. This allowed for real time visualization of the baseline and peaks, as the program which captures the data does not display any visual output. The advantage gained is that one would see changes on the graph immediately and did not have to wait for the program to finish operating until looking at the processed data.

The following changes and tests, as presented above, were conducted:

- Luminol brands and concentration changes.
 - Luminol from Merck, Fluka, and Sigma were used. The concentration of the luminol was changed, which eliminated the cleaning step, giving a lower baseline.
- Reagent concentrations
 - Reagent concentrations have been lowered from those used originally
- Buffer solution.

- Originally a buffer solution was made up and then the pH was adjusted by addition of either NH₄OH conc. sp. or HCl con. sp. A stronger buffer solution was prepared which eliminated the step of extra additions which could introduce contamination.
- Chelating resin
 - The chelating resin was changed from 8-HQ to IDA. This gave rise to consistent data acquisition.
- Calibration curve and calculations
 - Introduction of the Peak Height method. This was optimal for the peaks obtained on the chart recorder. This method could be transferred to the digital data obtained.

All these changes have been repeated at the new Stellenbosch clean laboratory, and forms part of the development section previously discussed.

Chapter 4: Application of the FIA-CL to measure iron in Southern Ocean Samples

This chapter represents a variety of implementations of the system in at sea as well as on land. Each section represents a different scenario and as that each section as its own results and discussions.

4.1 Discovery samples

During the 2010 austral spring (October-November) 12 samples from a vertical profile were collected aboard the R/V Discovery at Station 3 on the Goodhope line (Geotraces cruise D357, 36°20' S; 13°07' E). This station corresponds closely to station S1 (36°50' S; 13°10' E) previously sampled by Chever *et al.*, (2010) during the BONUS – GoodHope cruise (February-March 2008).

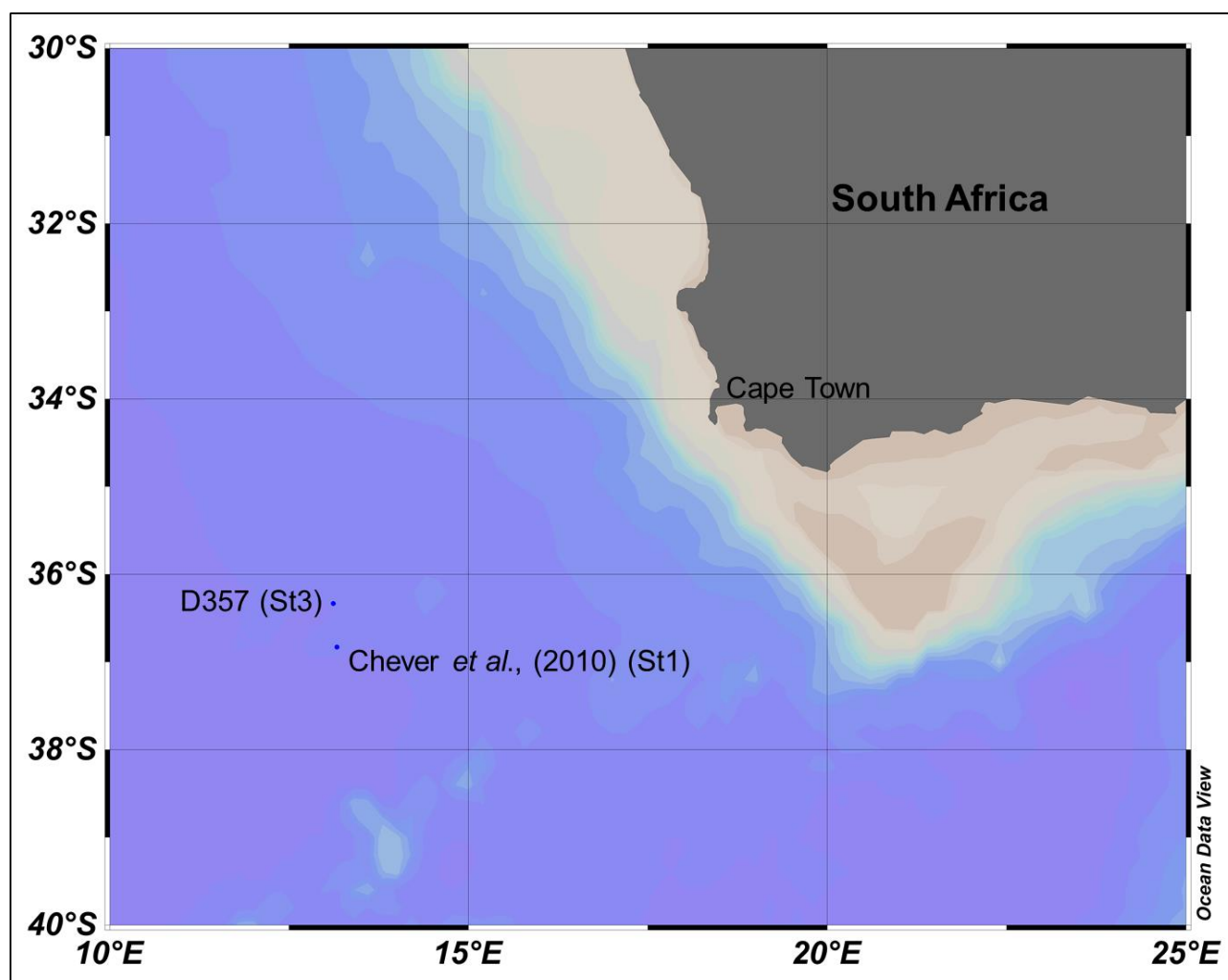


Figure 4.1: Indicates sample location of D357 and Chever *et al.*, (2010)

These samples were collected for an inter-laboratory comparison between Southampton University (which had an established FIA-CL system up and running) and Stellenbosch University (newly developed system), as well as for comparison with data from Chever *et al.*, (2010).

4.1.1 Sampling

Samples were collected with 10L OTE (Ocean Technology Equipment) sampling bottles with external springs, mounted on a titanium rosette. A towed fish was used for the collection of surface waters, which was pumped into the clean van using a diaphragm pump connected to clean oil free compressed air compressor. Samples were filtered and collected within a clean container laboratory and were acidified to < pH 1.7 by addition of UpA HCl (Romil, Cambridge, UK) Cruise report D357/GA10 UK-Geotraces 40°S (2010). A total of 12 samples were collected (surface, 30 m, 50 m, 100 m, 200 m, 300 m, 500 m, 750 m, 1500 m, 2000 m, 3000 m, 4000 m).

4.1.2 Analytical method

The samples were analysed by the newly developed FIA-CL at Stellenbosch University. The PH and Int methods were used to calculate the dissolved Fe (dFe) concentrations. SAFe D1 reference material was used to verify the accuracy of these results. All samples including reference material were analysed in one run from surface to deep.

4.1.3 Results and Discussion

Figure 4.2 shows data calculated using both methods, PH and Int. The SAFe D1 results obtained were 0.640 ± 0.035 nM (n=3) for the PH and 0.609 ± 0.044 nM (n=3) Int, which corresponds to the certified values.

Unfortunately the results obtained from Southampton are not published, therefore cannot be represented in this thesis. Our results obtained were in general lower than measured at Southampton. However, note that samples were collected 20 days apart at the same site.

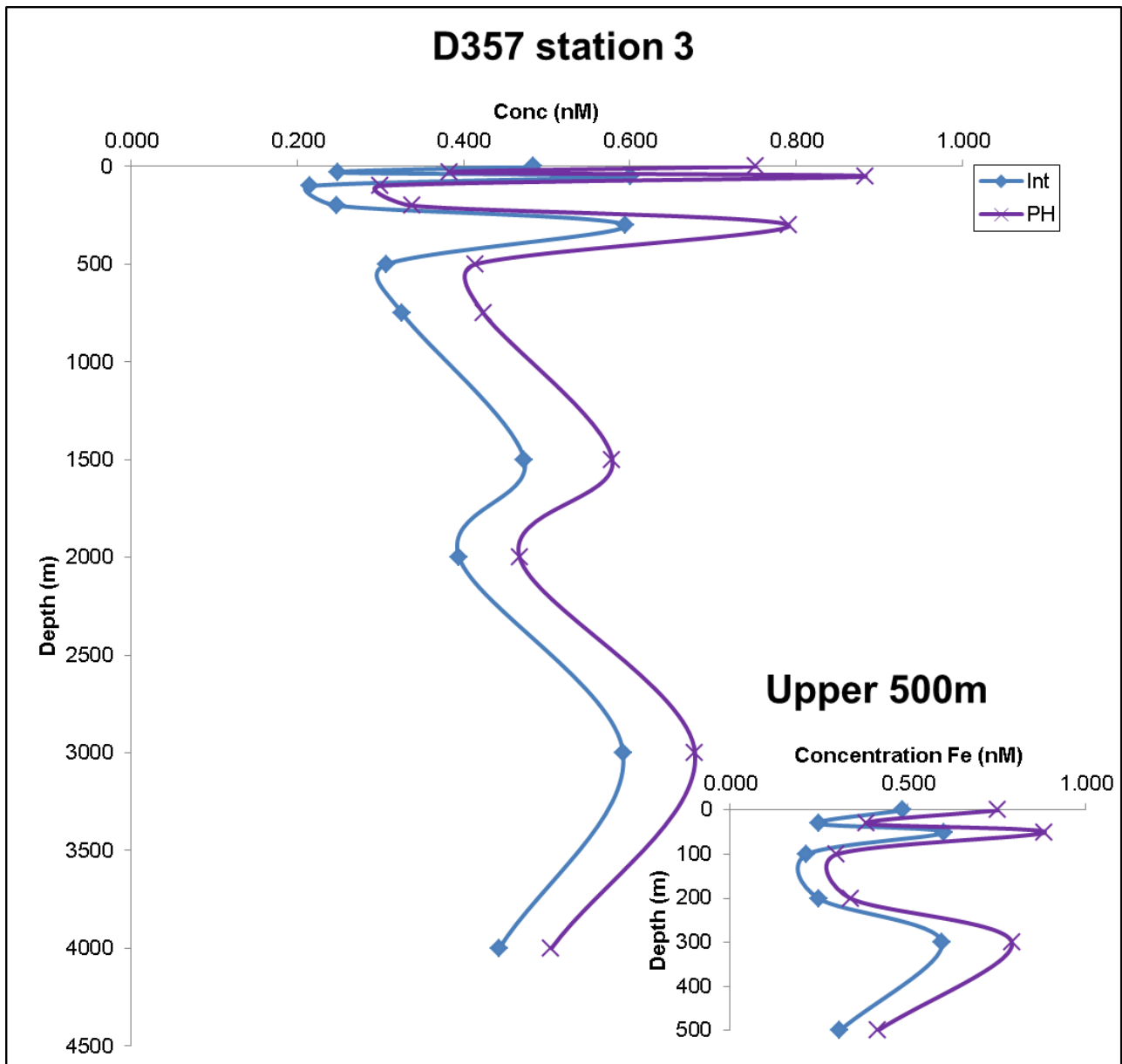


Figure 4.2: Displays the values obtained from the D357 cruise at station 3 for both methods. The insert shows the upper 500m Data presented in Appendix 3.

There are differences between the two methods. In general the Int method reports lower concentrations than that of PH. Data calculated with both methods follow the same trend and shape of the graph. The drift in the baseline does tend to give higher values for the PH even taking the drift into account.

The data were also compared to those of Chever *et al.*, (2010) Figure 4.3.

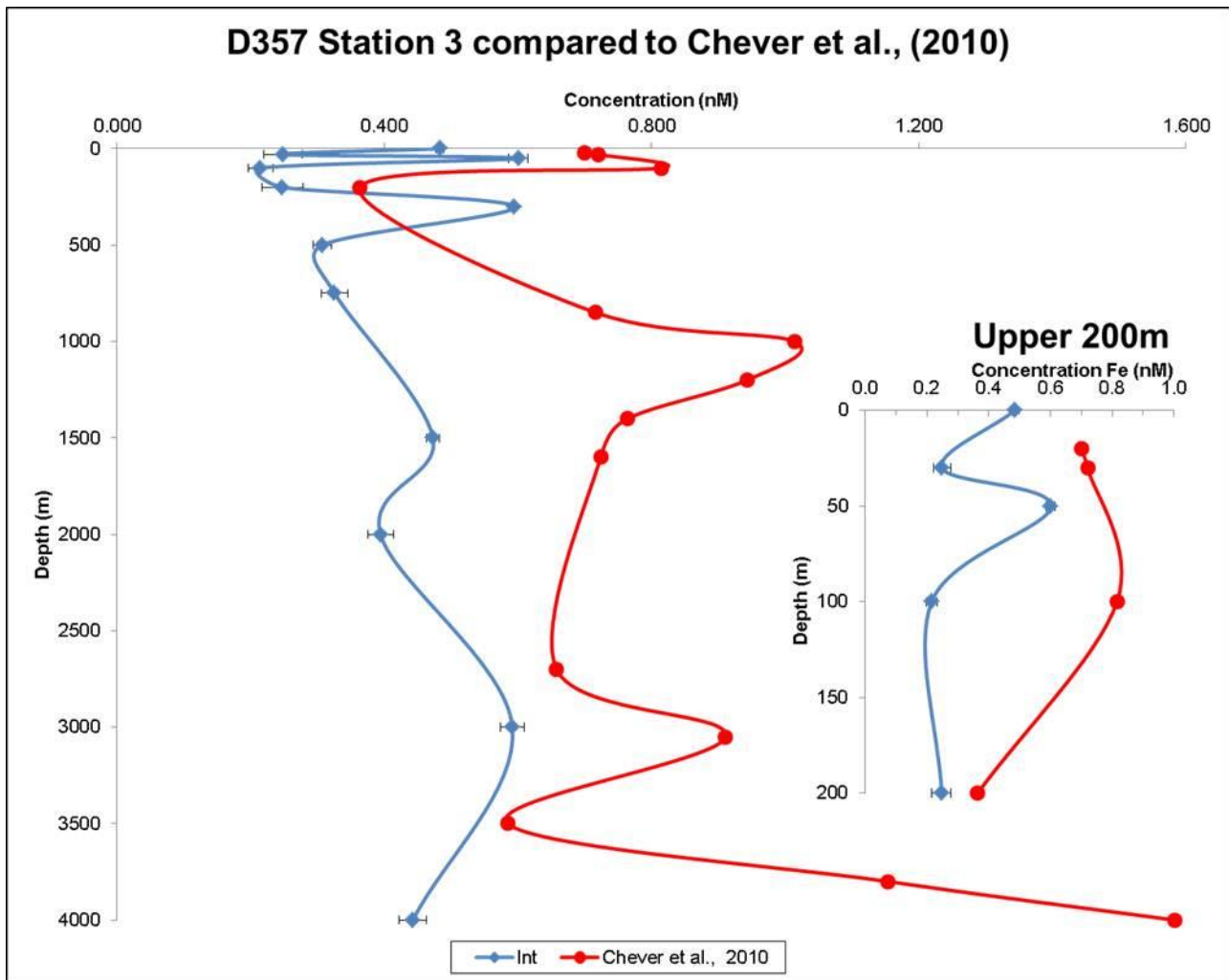


Figure 4.3: Comparison of the D357 data with that of Chever *et al.*, 2010. The insert shows the upper 200m.

The data were in general lower than those of Chever *et al.*, (2010). At 50m and 300m depth we observed an increase in Fe concentration, which indicated a shallow and deeper ferricline. This was not detected by Chever *et al.*, (2010) who did not collect samples at those depths. Chever *et al.*, (2010) reported only a ferricline at 1000m. The Discovery samples have been collected at the end of spring, whereas Chever *et al.*, (2010) collected samples at the end of summer, when dFe in surface waters could have been taken up by phytoplankton. Chever *et al.*, (2010) reported ~1.6nM of dFe at 4000m depth, which is four times higher than our results. This could be due to a change in the water masses in the deep water resulting in different deep concentrations (Klunder, 2012).

4.2 SANAE 51 samples

During the austral summer 2011/12 surface water samples were collected on the return leg from Antarctica to Cape Town in February 2012. The cruise track did not follow the normal Goodhope line, but took the shortest route back to Cape Town, passing downstream of Bouv t Island (Figure 4.4).

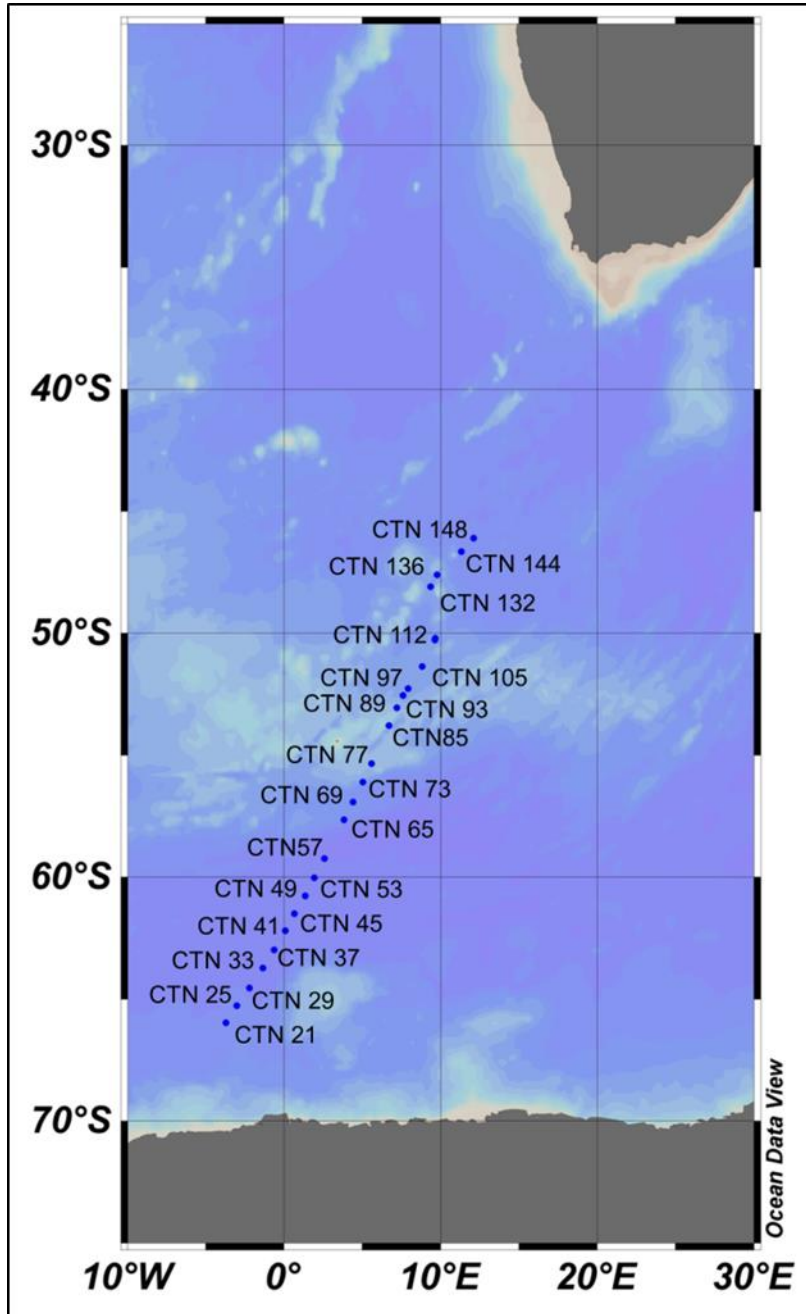


Figure 4.4: Indication of the cruise track where the samples have been collected

4.2.1 Sampling

Surface water was collected using an epoxy coated torpedo fish. The towed torpedo fish system is described by Vink *et al.*, (2000), with slight modifications. The torpedo fish did not have a bathythermograph. It was one meter long and weighted 80kg. It had a tunnel from the top to the nose where a Teflon funnel was connected. A Teflon tube (10 mm ID) was connected to the nozzle and ran through the tunnel, up along the winch line into the plastic covered laboratory. A diaphragm pump was connected to the other end of tubing. A tube was connected to the other side of the pump with a Y-connection, one side led into a class 100 laminar flow and the other towards the wet laboratory as runoff water.

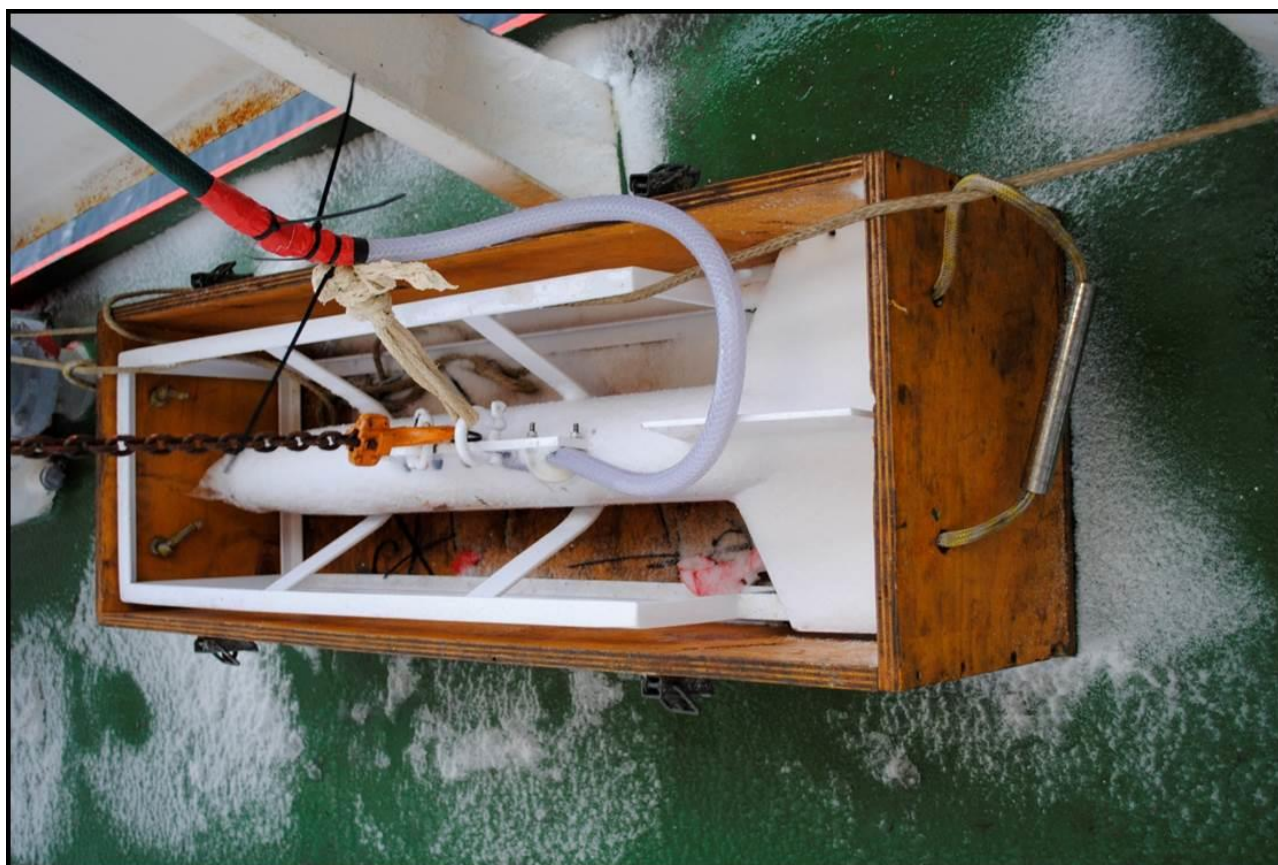


Figure 4.5: The torpedo fish used for the sampling of the surface waters during the SANAE 51 cruise.

Samples were collected in 125ml PFA grade bottles, every four hours inside a class 100 laminar flow. Five minutes of free flowing water through the pipe was allowed to flush the piping as well as the 0.2 μm Sartobran filter before samples were collected. All bottles for collection have been rinsed three times with seawater prior to collection. Unfiltered samples (total dissolvable Fe, TdFe) and filtered samples (dFe) were collected. All samples were spiked with 200 μl HCl conc. ultrapur (Merck). Samples were double bagged and stored in the dark at ambient room temperature before analysis 20 months later.

4.2.2 Analysis

The samples were analysed by the newly developed FIA-CL at Stellenbosch University. The Int method of calculation was used for these samples. The internal reference was used for the validation of these results. All TdFe samples have been analysed from south to north, and the same is true for dFe samples.

4.2.3 Results

TdFe and dFe data is displayed in Figure 4.6 and Figure 4.7 (Data Table in Appendix 4). This excludes CTN 61 and CTN 143, which display extra ordinary high concentrations, and should not be taken into account. Measurements range from 0.271-3.107 nM for dFe (mean 0.635 ± 0.552 nM (n=21)) and 0.292-4.928 nM for TdFe (mean 0.834 ± 0.663 nM (n=21)).

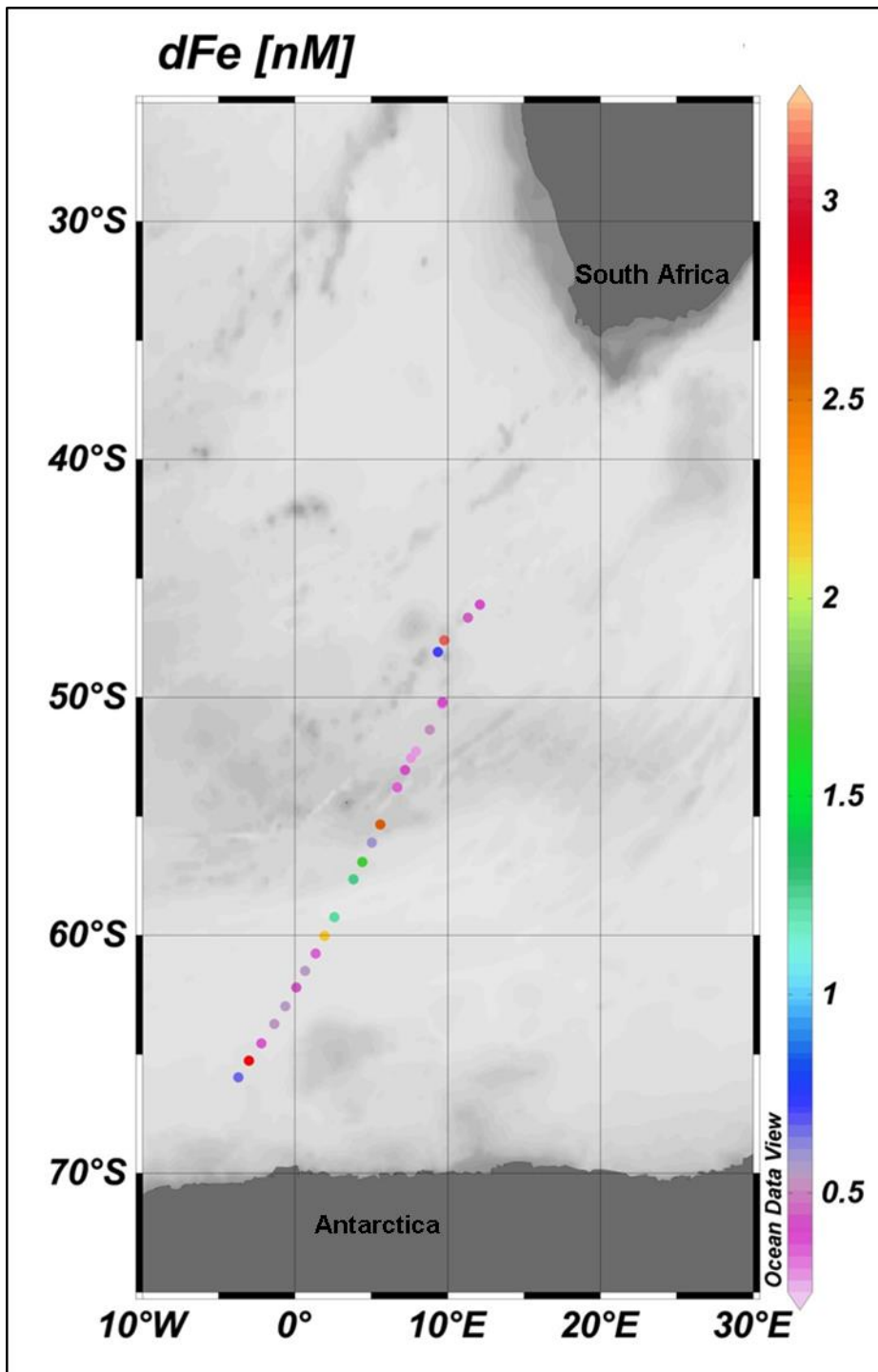


Figure 4.6: Display of the dFe concentrations for surface water samples from the SANAE 51 cruise.

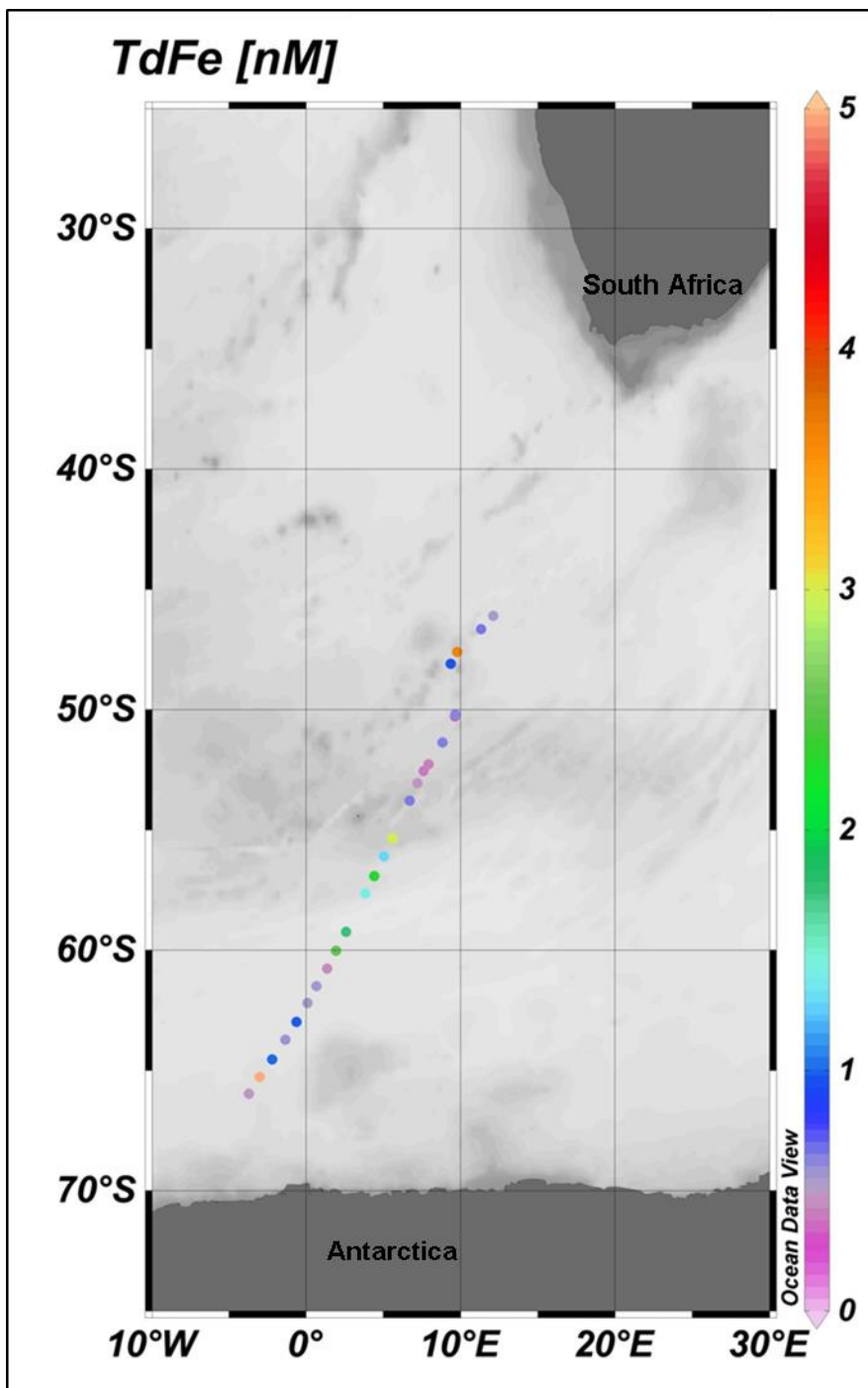


Figure 4.7: Display of the TdFe concentrations for surface water samples from the SANA 51 cruise.

4.2.4 Discussion

CTN 61 and CTN 143 concentrations are so high that they can be considered as contaminated. All samples where the dFe value is higher than the TdFe value, or above 1nM should also be regarded as contaminated (except for sample CTN 77, see below). Samples CTN 112 has the same concentration for TdFe and dFe, indicating that during sampling no filter was used or that the filter had a leak/tear in its membrane. This cannot be confirmed as the sampling was not conducted by the author of this thesis. The rest of the data can be considered for oceanographic interpretation. The TdFe results are comparable with those of Landing and Powell

(1998) (0.5-2.6nM), de Jong et al., (1999) (0.05-0.90nM), Croot et al., (2004) (0.18-2.69nM) and Chever et al., (2010) (0.265-1.231 nM) for the same sector.

CTN 77 was taken in the island wake of Bouv et Island. Therefore this sample could have a higher Fe concentration due to addition of Fe from the island (Boyd and Ellwood, 2010).

The values reported in Appendix 4 are proof that the system is capable of analysing for picomolar concentrations of Fe in open ocean waters. The low values also state that we are able to sample cleanly enough to get acceptable results. The next step was to perform deep casts on the SANAE 53 cruise and analyse them, to contribute to the international effort to collect oceanic Fe data.

4.3 Optimization of on-board sampling protocol: SANAE 53

Samples were collected during the annual austral summer cruise of the SA Agulhas II to Antarctica (February 2014) (Figure 4.8). This was also the first time for the clean container sampling and analytical laboratory on-board the vessel. The greatest obstacle was to prevent any contamination to occur during the on-board transportation of the Go-Flo bottles (General Oceanics) from the container to the CTD and back. Therefore transport protocols had to be developed.

During this voyage the new, ultra-clean, sampling equipment and procedures were tested in order to obtain clean, uncontaminated samples that could be analysed directly on board by our FIA-CL system.

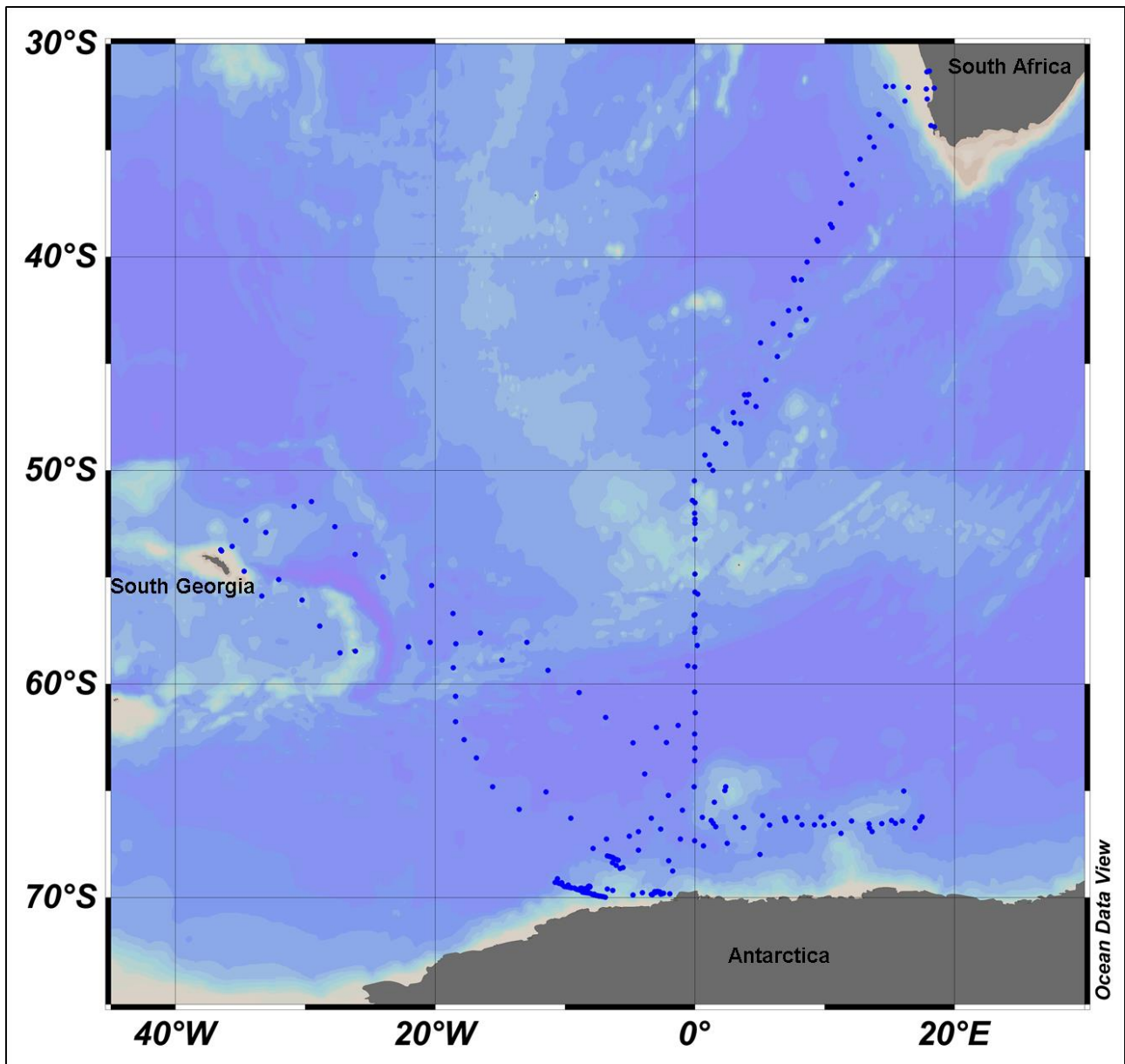


Figure 4.8: SANA E 53 cruise track

4.3.1 Transportation of Go-Flo bottles

All the Go-Flo bottles were armed inside the clean container sampling laboratory. Then the tap and valve of each Go-Flo bottles was covered with a shower cap. The whole Go-Flo bottle was then covered with a plastic sheath which was sealed at the bottom. The top was closed by putting in a temporary knot. The bottles were carried from the container sampling laboratory to the CTD. One person at the CTD was responsible to receive the bottle, who also loaded the bottle onto the CTD. Prior to loading the Go-Flo bottle onto the CTD another person removed the plastic sheath (Figure 4.9). The shower caps were removed immediately prior to deployment after the doors have been opened. Each person handling the Go-Flo bottles, CTD and plastic sheathing wore gloves at

all times. Great care was taken to prevent the sheaths and shower caps from coming into contact with any part of the ship and were stored in a plastic bag if not in use.

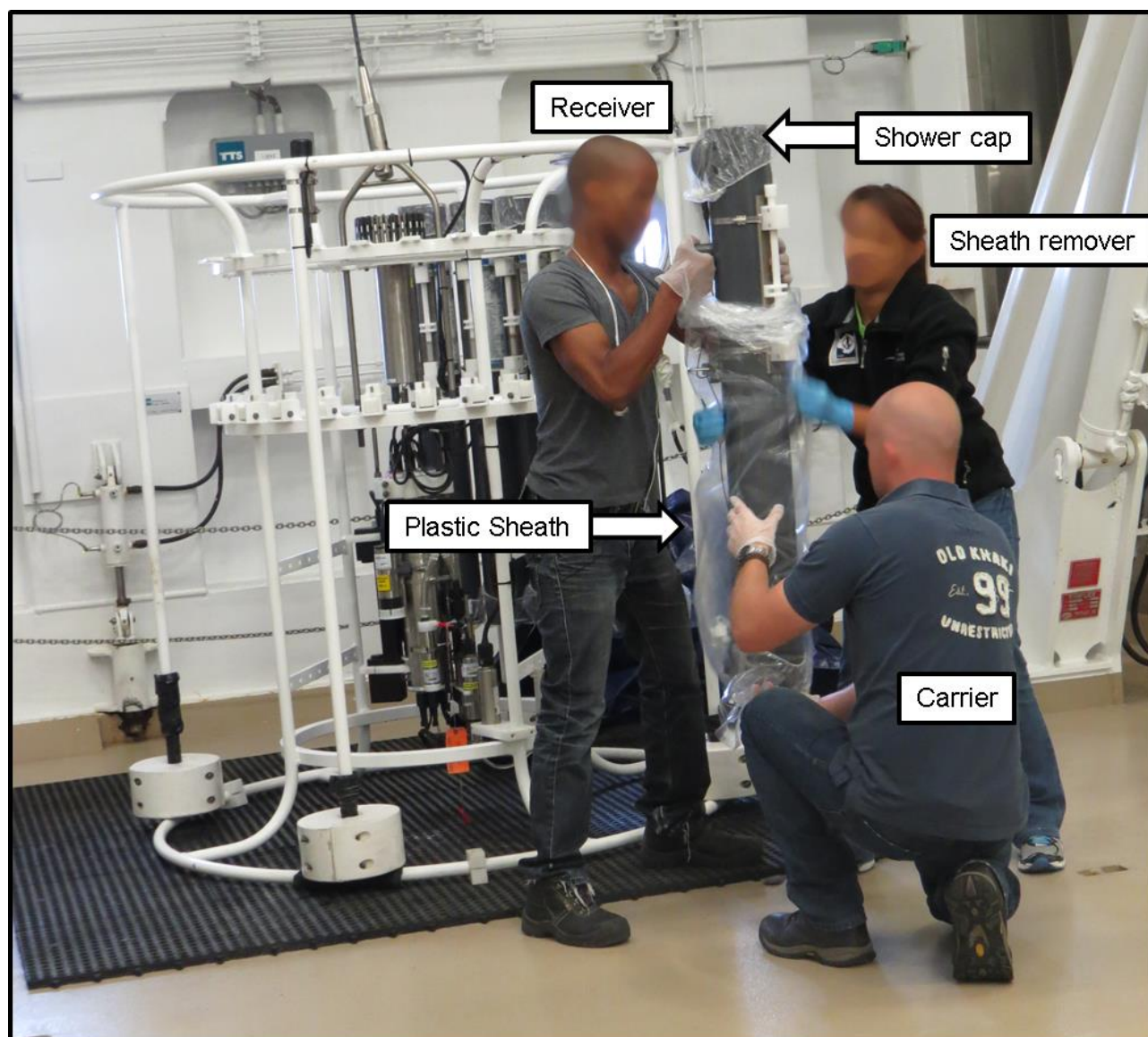


Figure 4.9: Transfer of Go-Flo bottle from carrier to receiver, including the person responsible for the removal of the plastic sheath (Foto by N. Knox).

4.3.2 Sampling Procedure

24 Go-Flo bottles were used to collect trace metal clean samples. Prior to sampling, the Go-Flo bottles were cleaned according to de Baar *et al.*, (2008) and Cutter and Bruland (2012) except that the O-ring was not exchanged as suggested by those authors. The bottles were cast to a depth of 250 m for rinsing purposes. Seawater collected just under the chlorophyll max was used to condition them. Conditioning was done over several days. This was repeated until results showed that the bottles were clean (Figure 4.10). The Go-Flo bottles were transported from the clean container sampling laboratory to the trace metal rosette in plastic sleeves. There they were unwrapped and mounted onto the trace metal rosette, which was painted with epoxy and connected to an optical Kevlar cable. A CTD was mounted permanently at the base of the rosette.

Once all the bottles were loaded and ready for deployment the starboard side door was opened. The rosette was lowered to a depth of five meters below surface for all for the bottles to be activated (opened). The rosette was lowered manually up to 30 m and back to surface for the assessment of sea conditions. Once the ship's crew was satisfied with the sea conditions, the rosette stayed at the surface for 10 minutes allowing for the sensors of the CTD to calibrate. The rosette was lowered manually up to 30 m again where the automatic deployment system was activated. The rosette was lowered down to 50 m below the bottom depth sampled. Bottles were triggered on the way up by manually overriding the automatic system five meters before the acquisition depth to allow a slower speed for the sampling (closing of bottles). Once the rosette was back on board the bottles head and foot including the taps were covered with plastic shower caps and zip lock bags. After demounting, the bottles were put back into the plastic sleeves for transportation between the rosette and sampling laboratory. Once all the bottles had been mounted inside the clean sampling container a 15 min break was taken to allow for the air in the container to re-circulate properly.

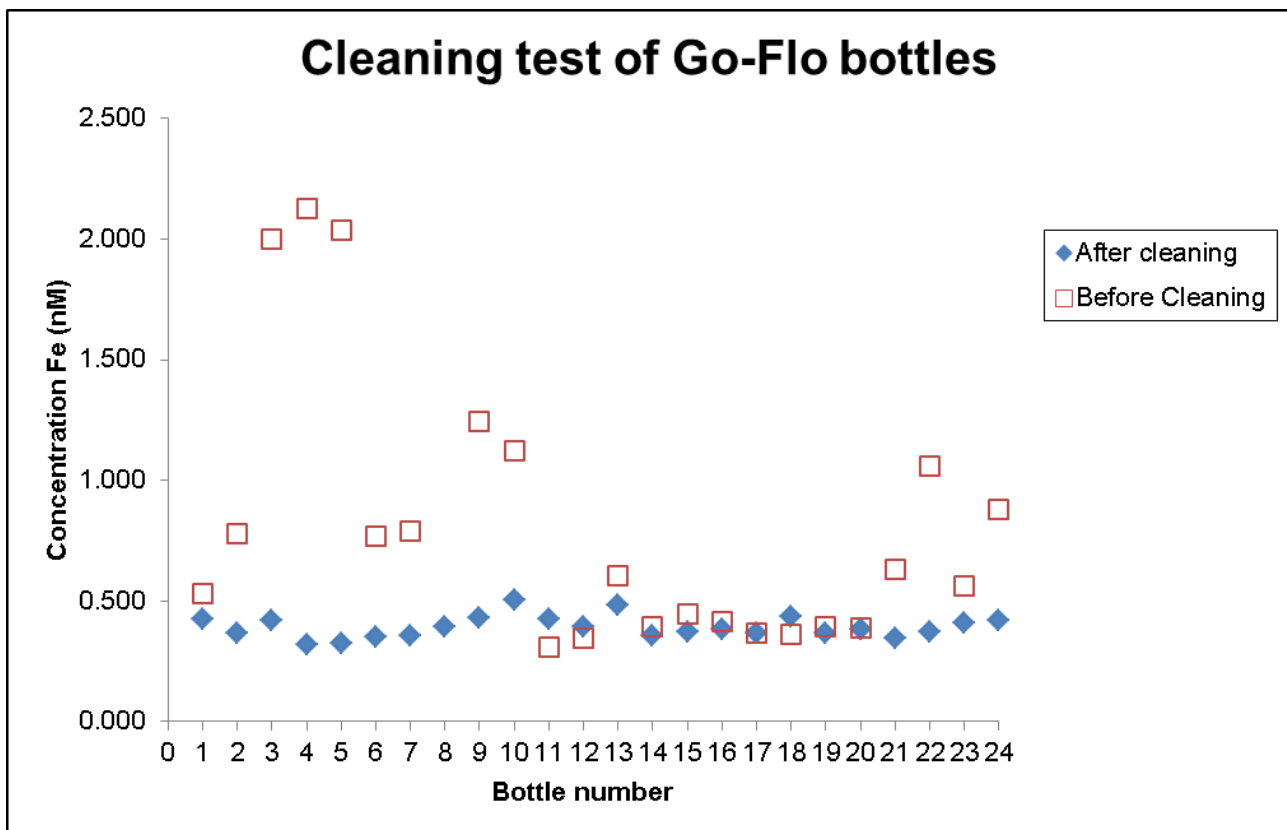


Figure 4.10: Represents the concentration of the 24 Go-Flo bottles before cleaning and after the final cleaning and soaking step.

Samples from the Go-Flo bottles were collected in either low density polyethylene (LDPE) or polycarbonate (PC) bottles. LDPE and PC bottles were cleaned as described in Appendix 5. A test was done between the two types of bottles to see which were the cleanest to use (see below). They were further rinsed three times with seawater before sample was collected. For dFe 0.2 μm Sartobran filters were used. These were cleaned by filtering 500 ml of a 0.1M HCl suprapur

solution, followed by one litre of MQ and then one litre of seawater. Filters were double bagged if not in use and stored in a fridge. Clean laboratory protocols were adhered to at all times while sampling.

Two LDPE bottles and one polycarbonate bottle were filled from 2 different Go-Flo bottles, bottle 6 and 12. Results are presented in Figure 4.11.

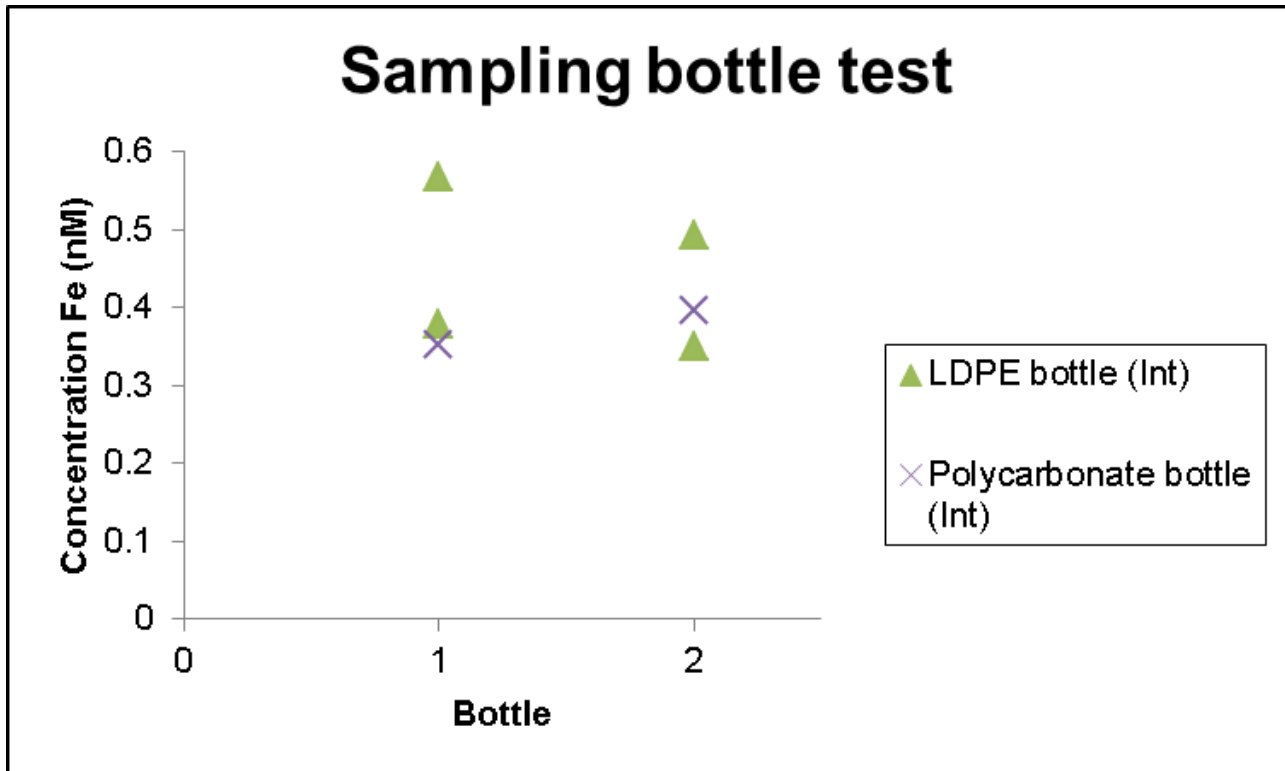


Figure 4.11: Comparison between the LDPE bottles and the polycarbonate bottles, showing that there is not a great difference in the two results.

The results show no difference between PC and LDPE sampling bottles. Due to availability of samples taken no further confidence tests could be conducted. PC bottles were then used to sample all 24 Go-Flo bottles as they showed the overall lower value. The dFe concentration was $0.392 \pm 0.45 \text{ nM}$ ($n=24$). A further test using LDPE and PC bottles was conducted for a vertical profile which is presented in the next section (Mega station 2).

4.3.3 Mega Station 2

The Mega station 2 (5 February 2014, $50^{\circ}0.08' \text{ S}$, $1^{\circ}23.08' \text{ E}$) corresponds to a station also sampled by Klunder *et al.*, (2011)(February 2008, $50^{\circ}16.2' \text{ S}$, $1^{\circ}27.00' \text{ E}$) (Figure 4.12). Samples were analysed on board and on land two months after the voyage. Samples for total dissolvable Fe (TdFe), dissolved Fe (dFe), soluble Fe (sFe) as well as for macro nutrients had been collected from the trace metal rosette. Data for dFe is displayed as by the time of completion the TdFe samples have not been analysed.

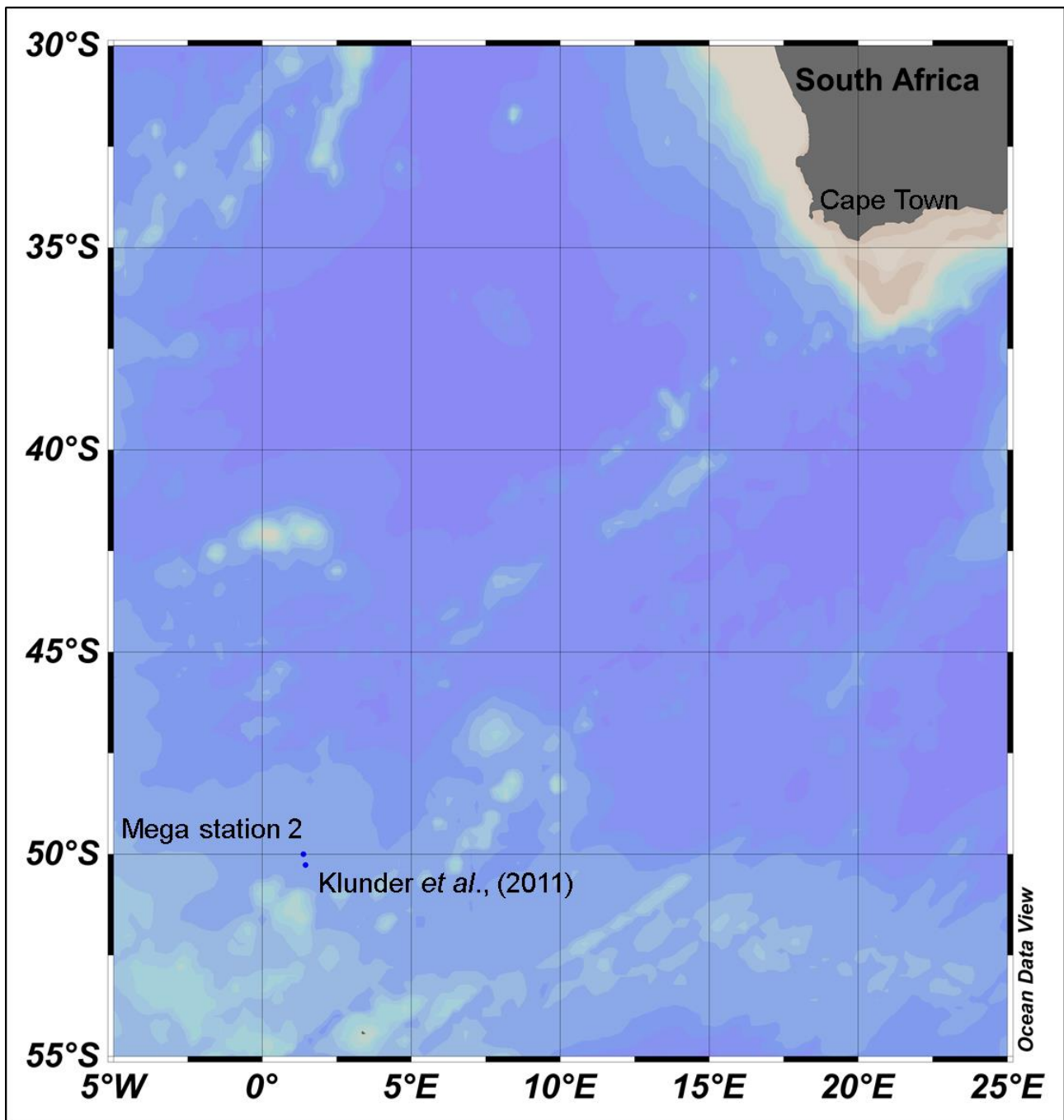


Figure 4.12: Indication where Mega station 2 has been sampled compared to that of Klunder et al., (2011)

4.3.3.1 Results

The samples collected with polycarbonate bottles showed the lowest concentrations, compared to those in LDPE bottles (Figure 4.13). Two LDPE bottles were so badly contaminated that they could not be measured due to the PMT overflowing, and represent the missing data on Figure 4.13.

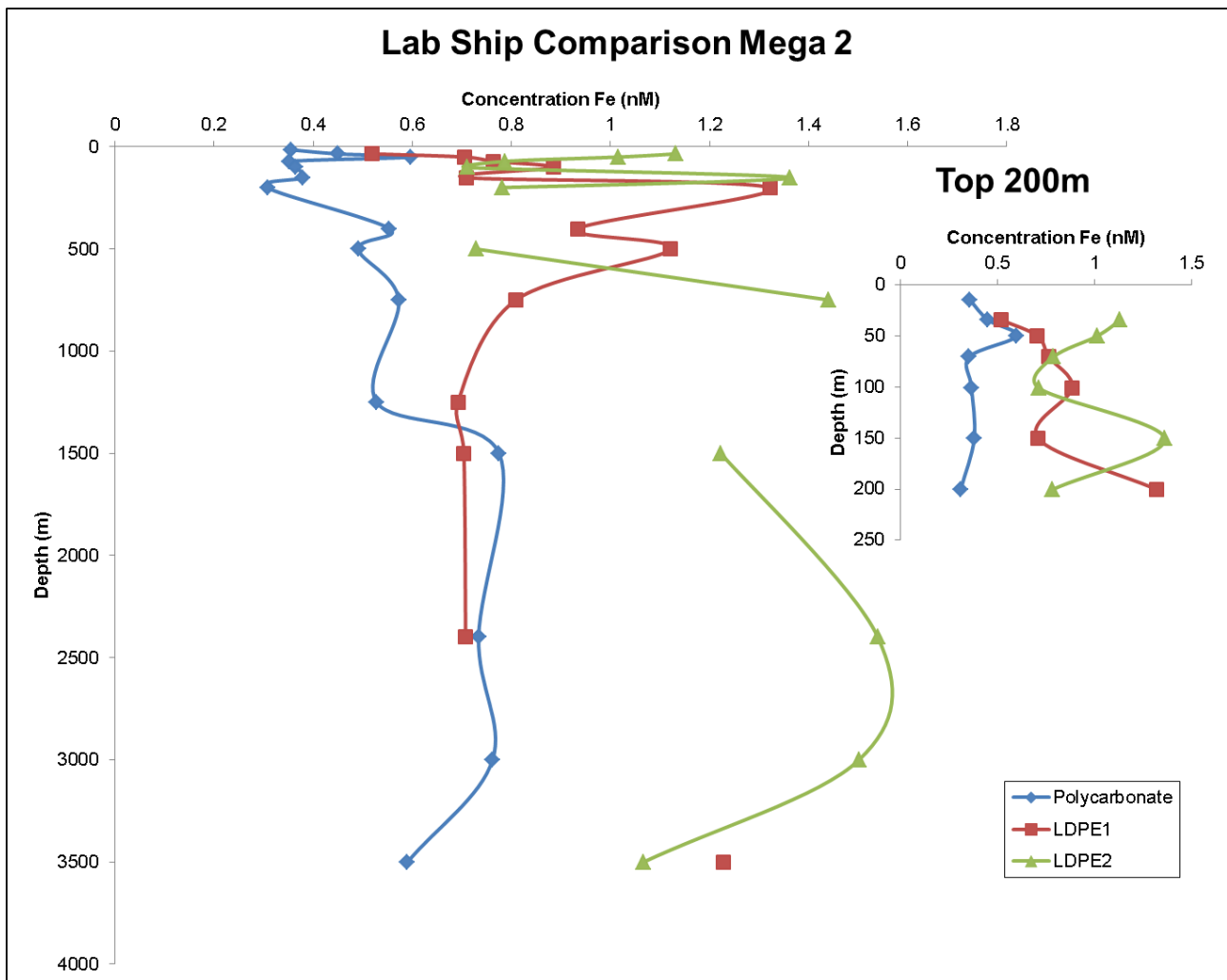


Figure 4.13: Comparison of the LDPE and PC bottles on a profile, clearly indicating that the sampling in LDPE bottles leads to contamination.

The dFe concentrations from the PC bottles were generally higher than those of Klunder *et al.*, (2011), except at the deeper sampling (Figure 4.14). The mixed layer depth for this profile was 140 m. Maximum fluorescence was observed at 70 m.

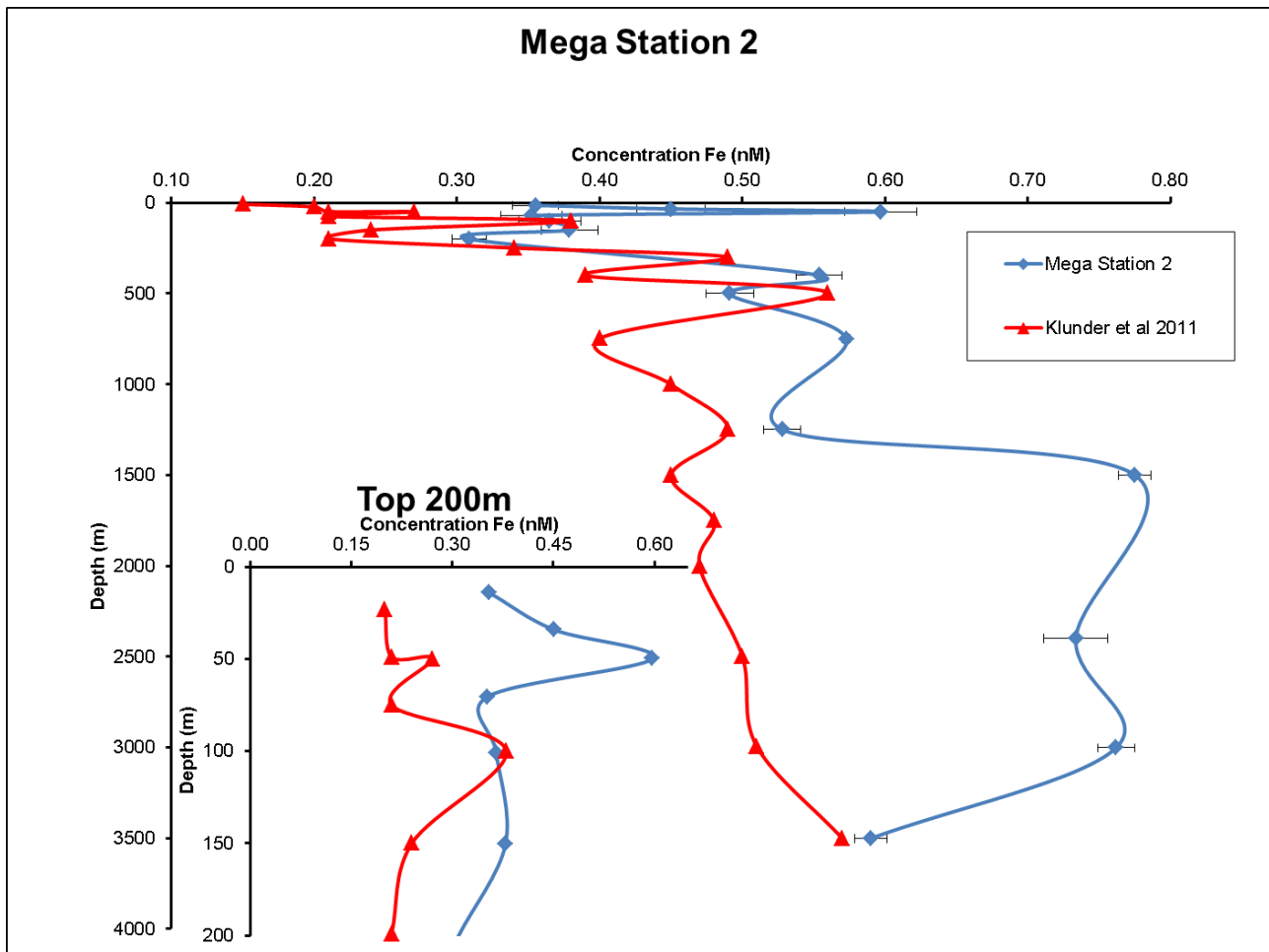


Figure 4.14: Comparison between our data and Klunder et al., (2011). Klunder et al (2011) is in general lower than our data.

4.3.3.2 Discussion

It is evident from our results that the LDPE bottles were not clean enough, giving a clear indication that there is a problem with the sampling procedure or the bottles, because PC bottles were cleaned following the same protocol as the LDPE bottles, one can deduce that the LDPE bottles are the problem. Hence the LDPE data cannot be used.

The concentrations obtained from the polycarbonate bottles are higher than those from Klunder *et al.*, (2011), as well as global mean surface concentrations (Achterberg *et al.*, (2001). This could be due to the ship standing still over a long period at one position, which may have introduced some contamination from the ship.

Fe concentration increased from the surface to 50m depth, with a sharp decline to 70m. This low concentration equals the depth of maximum fluorescence, hence most productivity. This increase to 50m and decrease to 70m is also observed in the data of Klunder *et al.*, (2011). Klunder *et al.*, (2011) data displays a Fe max at 500 m depth and from there the Fe concentrations decrease with depth. In the upper waters, the Fe maximum was observed at 400 m and 750 m (excluding the one at 50 m). This would indicate two ferriclines compared to the one from Klunder

et al., (2011). Concentrations decreased down to 1250 m with a steep increase from there to 1500 m depth. Data displayed below 1500m are higher than those of Klunder *et al.*, (2011). The reason for this might be contribution from the area sampled, which is downstream of a mid ocean ridge. During our sampling the hydrothermal vent located in that area could have injected new Fe into the ocean. The deepest values are similar indicating a consistent Fe concentration close to the seafloor.

Chapter 5: Conclusion

The aim of this project was to develop and optimize an analytical method to analyse seawater samples for Fe(III) at picomolar concentrations. The objective was to have a system which is mobile and can be used in a laboratory as well as in a ship based laboratory.

A Flow injection analyser with chemiluminescence detection was the choice of analytical method to be implemented. The reason for this was the mobility of the system, allowing for it to be used on land and at sea. Many attempts and re-runs of calibration curves have gone through the development phase for the optimization of the system. Development was hampered due to contamination in the laboratory in which conditions the system was developed until the ultra-clean laboratory was finally completed. The bad working conditions allowed for a visit to Plymouth University to assess if the system was in a working condition or more development had to be done. This was also the first test if the system could easily be transported and re-assembled. The visit proved to be a success for assessing laboratory issues as well as the mobility of the system.

The visit to Plymouth University also introduced a different method of calculating the results, resulting in new tests to be developed around the calculations for the concentrations of Fe. In this work it was found that the peak height method used produces higher concentrations compared to that of the integral method, even with certified reference material. Therefore all final results have been reported based on the integral method of calculation.

Based on various test conducted, the method is now described in Appendix 6 is setup and working at Stellenbosch Universities ultra-clean laboratory.

The system was used to analyse samples collected during the Geotraces cruise D357. It was to be an inter-laboratory calibration study, which was not completed as the other laboratory has not yet analysed the samples from the same day of collection from that site. Despite that, samples were compared to those of the first visit to that sampling station during that cruise. The results obtained by our FIA-CL were lower than those of the first visit, which had been analysed by the laboratory in Southampton. Therefore this cannot be used as a basis, that our system is in order, never the less it was regarded that the system is working accurately, due to the results obtained were lower than the D357 results and that the SAFe reference materials concentrations had been obtained.

Samples collected during the SANAE 51 cruise were successfully analysed in the land based clean laboratory. The results gave a clear indication that it was possible to sample cleanly in a plastic covered laboratory on board a very old vessel. Some samples though were still contaminated. Source for that could not be determined.

In order to optimize clean sampling protocols aboard the new South African research vessel, the system was taken on board SA. Agulhas II and was setup inside a clean class 100 container laboratory. The system was used to test the cleanliness of the Go-Flo bottles and the sampling procedure. The system was also used to analyse the Mega station 2 on board. This proved that the system could easily be implemented in a clean container laboratory and had no interference from the ship. Samples are at an acceptable range at deeper waters. Slightly elevated results at the surface indicate that there was still some contamination. Elevated deeper waters indicated a possible hydrothermal event which was captured during sampling.

To conclude a mobile system able to analyse for picomolar concentrations of Fe(III) has been successfully developed and implement in a laboratory as well as on board a vessel. Further work is required to automate the system as well as the introduction of an online buffer injection. This would reduce sample prepping leading to a decrease chance of contamination. Re-writing the software into a newer format, as this is accepted by modern computers. The current software can only run on PC with Windows XP and older versions of Windows on. The software should also display the peaks obtained in real time. This could indicate earlier any problems that might occur.

References

- Achterberg E.P., Holland T.W., Bowie A.R., Mantoura R.F.C., and Worsfold P.J., 2001. Determination of iron in seawater. *Analytica Chimica Acta*, 442(1): 1-14.
- Al-Gailani B.R.M., Greenway G.M. and McCreedy T. 2007. A miniaturized flow-injection analysis(μ FIA) system with on-line chemiluminescence detection for the determination of iron in estuarine water. *International Journal of Environmental Analytical Chemistry* 87: 637-646
- Aldrich A.P and van den Berg C.M.G., 1998, Determination of Iron and Its Redox Speciation in Seawater Using Catalytic Cathodic Stripping Voltammetry. *Electroanalysis*, 10(6): 369-373
- Barnola J.-M., Raynaud D., Korotkevich Y.S. and Lorius C., 1987. Vostok ice core provides 160,000-year record of atmospheric CO₂. *Nature* 329: 408-414
- Barnola J.-M., Raynaud D., Lorius C., and Barkov N.I.. 2003. Historical CO₂ record from the Vostok ice core. In Trends: A Compendium of Data on Global Change. *Carbon Dioxide Information Analysis Center, Oak Ridge National Laboratory, U.S. Department of Energy, Oak Ridge, Tenn., U.S.A.*
- Beck N.G., Franks R.P. and Bruland K.W., 2002. Analysis for Cd, Cu, Ni, Zn, and Mn in estuarine water by inductively coupled plasma mass spectrometry coupled with an automated flow injection system. *Analytica Chimica Acta* 455: 11–22
- Behrenfeld M.J., Bale A., Kolber Z., Aiken J. and Falkowski P., 1996 Confirmation of iron limitation of phytoplankton photosynthesis in the equatorial Pacific Ocean. *Nature* 383:508–511
- Blain S. and Tréguer P., 1995. Iron (II) and iron (III) determination in sea water at the nanomolar level with selective on-line preconcentration and spectrophotometric determination. *Analytica Chimica Acta* 308: 425-432
- Boukhalfa H. and Crumbliss A.L., 2001 Kinetics and mechanism of a catalytic chloride ion effect on the dissociation of model siderophore hydroxamate-iron(III) complexes. *Inorganic Chemistry* 40: 4183-4190
- Bowie A.R., Achterberg E.P., Mantoura R.F.C. and Worsfold P.J., 1998. Determination of sub-nanomolar levels of iron in seawater using flow injection with chemiluminescence detection. *Analytica Chimica Acta* 361: 189-200
- Bowie A.R., Achterberg E.P., Sedwick P.N., Ussher S. and Worsfold P.J., 2002(b). Real-Time Monitoring of Picomolar Concentrations of Iron(II) in Marine Waters Using Automated Flow Injection-Chemiluminescence Instrumentation. *Environmental Science Technology* 36: 4600-4607
- Bowie A.R., Sedwick P.N. and Worsfold P.J., 2004. Analytical intercomparison between flow injection-chemiluminescence and flow injection-spectrophotometry for the determination of picomolar concentrations of iron in seawater. *Limnology and Oceanography: Methods* 2: 42-54
- Bowie A.R., Achterberg E.P., Ussher S. and Worsfold P.J., 2005. Design of an Automated Flow Injection-Chemiluminescence Instrument Incorporating a Miniature Photomultiplier Tube for the Monitoring Picomolar Concentrations of Iron in Seawater. *Journal of Automated Methods & Management in Chemistry* 2: 37-43
- Boyd P.W. and Ellwood M.J., 2010. The biogeochemical cycle of iron in the ocean. *Nature Geoscience* 3: 675-682

- Brita J-F., Dubos C. and Gerard F., 2014. Iron nutrition, biomass production and plant production quality. *Trends in Plant Science* 1207: 1-8
- Broecker W.S., 1982a, Ocean chemistry during glacial time. *Geochimica et Cosmochimica Acta* 46: 1689-1705
- Broecker W.S., 1982b, Glacial to Interglacial Changes in Ocean Chemistry. *Progress in Oceanography* 11: 151-197
- Bruland K. W., Franks R. P., Knavery G. A. and Martin J. H., 1979, Sampling and analytical methods for the determination of copper, cadmium, zinc and nickel at the nanogram per liter level in sea water. *Analytica Chimica Acta*, 105,223-245.
- Bruland K.W. and Rue E.L., 2001. Analytical Methods for the Determination of Concentrations and Speciation of Iron, In: *The Biogeochemistry of Iron in Seawater*. Turner D.R., and Hunter K.A., Chichester, John Wiley & Sons, IUPAC 7: 123-253.
- Bucciarelli E., Blain S. and Tréguer P., 2001. Iron and manganese in the wake of the Kerguelen Island (Southern Ocean). *Marine Chemistry* 73: 21-36
- de Baar H.J.W., Timmermans K.R. Laan P., De Porto H.H., Ober S., Blom J.J. Bakker M.C. Schilling J., Sarthou G., Smit M.G. and Klunder M., 2008. Titan: A new facility for ultraclean sampling of trace elements and isotopes in the deep oceans in the international Geotraces program. *Marine Chemistry* 111: 4-21
- Chever F., Bucciarelli E., Sarthou G., Speich S., Arhan M., Penven P. and Tagliabue A., 2010. Physical speciation of iron in the Atlantic sector of the Southern Ocean along a transect from the subtropical domain to the Weddell Sea Gyre. *Jnr of Geophysical Research* 115: C10059
- Chisholm S.W., 2000. Stirring times in the Southern Ocean. *Nature* 407: 685-687
- Croot P.L., and Johansson M., 2000. Determination of iron speciation by cathodic stripping voltammetry in seawater using the competing ligand 2-(2-thiazolylazo) - p-cresol (TAC). *Electroanalysis*, 12(8): 565-576
- Croot P.L. and Laan P. 2002. Continuous shipboard determination of Fe(II) in polar waters using flow injection analysis with chemiluminescence detection. *Analytica Chimica Acta* 466: 261-273
- Croot P.L., Andersson K., Öztürk M., and Turner D.R., 2004. The distribution and speciation of iron along 6°E in the Southern Ocean. *Deep-Sea Research II*, 51: 2857-2879.
- Cutter G.A. and Bruland K.W., 2012. Rapid and noncontaminating sampling system for trace elements in global ocean surveys. *Limnology and Oceanography: Methods* 10: 425-436
- Danielsson L-G. Magnusson B. and Westerlund S., 1985. Cadmium, Copper, Iron, Nickel and Zinc in the North-East Atlantic Ocean. *Marine Chemistry* 17: 23-41
- de Jong J.T.M., den Das J., Bathmann U. Stoll M.H.C., Kattner G., Nolting R.F. and de Baar H.J.W. 1998. Dissolved iron at subnanomolar levels in the Southern Ocean as determined by ship-board analysis. *Analytica Chimica Acta* 377: 113-124
- de Jong J. T. M., Croot P. L. and de Baar H. J. W., 1999, Distribution of iron in the surface and deep waters of the Southern Ocean along 20°E, *Eos, Transactions American Geophysical Union*, 80(49), 161.
- Dierssen H., Balzer W., and Landing W.M., 2001. Simplified synthesis of an 8- hydroxyquinoline chelating resin and a study of trace metal profiles from Jellyfish Lake, Palau. *Marine Chemistry*, 73(3-4): 173-192.

- Elrod V.A., Johnson K.S. and Coale K.H., 1991. Determination of Subnanomolar Levels of Iron(II) and total Dissolved Iron in Seawater by Flow Injection Analysis with Chemiluminescence Detection. *Analytical Chemistry* 63: 893-898
- Falkowski P.G., Scholes R.J., Boyle E., Canadell J., Canfield D., Elser J., Gruber N., Hibbard K., Högberg P., Linder S., Mackenzie F.T., Moore (III) B., Pedersen T., Rosenthal Y., Seitzinger S., Smetacek V. and Steffen W. 2000. The Global Carbon Cycle: A Test of Our Knowledge of Earth as a System. *Science* 290: 291-296
- Flajnik C., and Delles F., 2010, Evaluation of Deuterium and Zeeman Background Correction with the presence of Spectral Interferences Determinations of Arsenic in an Aluminium Matrix and Selenium in an Iron Matrix by GFAAS. www.agilent.com/chem
- Gledhill M. and Van den Berg C.M.G., 1994. Determination of complexation of iron(III) with natural organic complexing ligands in seawater using cathodic stripping voltammetry. *Marine Chemistry* 47: 41-54
- Gledhill M. and van den Berg C.M.G., 1995. Measurement of the redox speciation of iron in seawater by catalytic cathodic stripping voltammetry. *Marine Chemistry*, 50(1-4): 51-61.
- Hirata S., Yoshihara H. and Aihara M., 1999. Determination of Fe(II) and total iron in environmental water samples by flow injection analysis with column preconcentration of chelating resin functionalized with N-hydroxyethylethylenediamine ligands and chemiluminescence detection. *Talanta* 49: 1059-1067
- Johnson K.S., Boyle E., Bruland K., Measures C., Moffett J., Aquilarislas A., Barbeau K., Cai Y., Chase Z., Cullen J., Doi. T., Elrod V., Fitzwater S., Gordon M., King A., Laan P., Laglera-Baquer L., Landing W., Lohan M., Mendez J., Milne A., Obata H., Ossiander L., Plant J., Sarthou G., Sedwick P., Smith G.J., Sohst B., Tanner S., Van Den Berg S., and Wu, J., 2007. Developing Standards for Dissolved Iron in Seawater. *Eos Transactions of the AGU* 88 (11), 131.
- Khrycheva A.D., Nedosekin D.A., Proskurnin M.A., Kononets M.Y., Pakhomova S.V. and Faubel W., 2008. Photothermal Deflection Determination of Iron(II) with Ferrozine with Sorption Preconcentration on Silufol Plates. *Applied Spectroscopy* 62(4): 450-457
- King D.W., Lin J. and Kester D.R., 1991. Spectrophotometric determination of iron (II) in seawater at nanomolar concentrations. *Analytica Chimica Acta* 247: 125-132
- King D.W., Lounsbury H.A. and Millero F.J., 1995. Rates and Mechanism of Fe(II) Oxidation at Nanomolar Total Iron Concentrations. *Environmental Science Technology* 29: 818-824
- Klunder M.B., 2012. Distribution and Sources of Dissolved Iron in the Polar Oceans. PhD thesis.
- Laës A., Blain S., Laan P., Achterberg E.P. Sarthou G. and de Baar H.J.W., 2003. Deep dissolved iron profiles in the eastern North Atlantic in relation to water masses. *Geophysical Research Letters* 30(17):OC 8
- Laës A., Vuillemin R., Leilde B., Sarthou G., Bournot-Marec C. and Blain S., 2005. Impact of environmental factors on in situ determination of iron in seawater by flow injection analysis. *Marine Chemistry* 97: 347-356
- Landing W.M., Haraldsson C., and Paxeus N., 1986. Vinyl polymer agglomerate based transition metal cation chelating ion-exchange resin containing the 8- hydroxyquinoline functional group. *Analytical Chemistry*, 58(14): 3031-3035.
- Landing W.M. and Bruland K.W., 1987. The contrasting biogeochemistry of iron and manganese in the Pacific Ocean. *Geochimica et Cosmochimica Acta* 51: 29-43
- Landing W. M., and Powell R. T., 1998, Vertical profiles of dissolved and particulate iron in the southern and equatorial Atlantic: Relationships between atmospheric deposition,

biogeochemical cycling, and inorganic scavenging, *Eos, Transactions American Geophysical Union*, 79(1), 137.

- Lannuzel D., de Jong J., Schoemann V., Trevena A., Tison J. And Chou L., 2006. Development of a sampling and flow injection analysis technique for the determination in the sea ice environment. *Analytica Chimica Acta* 556: 476-483
- Lohan M.C., Aguilar-Islas A.M., Franks R.P., and Bruland K.W., 2005. Determination of iron and copper in seawater at pH 1.7 with a new commercially available chelating resin, NTA Superflow. *Analytica Chimica Acta* 530: 121-129
- Löscher B.M., de Baar H.J.W., de Jong J.T.M., Veth C. And Dehairs F. 1997. The Distribution of Fe in the Antarctic Circumpolar Current. *Deep-Sea Research II* 44: 143-187
- Martin J. H., Bruland K. W. and Broenkow W. W. 1976 Cadmium transport in the California Current. In: *Marine pollutant transfer*, Windom H. and Duce R., (D.C. Heath, Lexington, MA,) pp.159-184.
- Martin J.H. and Gordon R.M. 1988. Northeast Pacific iron distributions in relation to phytoplankton productivity. *Deep-Sea Research* 35: 177-196
- Martin J.H., Gordon R.M., Fitzwater S.E. and Broenkow W.W., 1989. VERTEX: phytoplankton/iron studies in the Gulf of Alaska. *Deep-Sea Research* 36: 649-680
- Martin J.H., 1990. Glacial-interglacial CO₂ change: The iron hypothesis. *Paleoceanography*, 5: 1-13
- Martin J.H., Gordon R.M. and Fitzwater S.E., 1990. Iron in Antarctic Waters. *Nature* 345: 156
- Measures C.I., Yuan J. and Resing J.A., 1995. Determination of iron in seawater by flow injection analysis using in-line preconcentration and spectrophotometric detection. *Marine Chemistry* 50: 3-12
- Milne A., Landing W., Bizims M., and Morton P., 2010. Determination of Mn, Fe, Co, Ni, Cu, Zn, Cd and Pb in seawater using high resolution magnetic sector inductively coupled mass spectrometry (HR-ICP-MS). *Analytica Chimica Acta*, 665: 200-207
- Morel, F. M. M., and Price N. M., 2003, The Biogeochemical Cycles of Trace Metals in the Oceans, *Science*, 300(5621), 944-947.
- Nédélec F., 2006. Implementation of a method to determine sub-nanomolar concentrations of iron in seawater and its application to the study of marine iron biogeochemistry at the ocean – shelf interface. PhD Thesis, University of Southampton,
- O'Sullivan D.W., Hanson A.K., Miller W.L. and Kester D.R., 1991. Measurements of Fe(II) in surface water of the equatorial Pacific, *Limnology and Oceanography* 36(8): 1727-1741
- O'Sullivan D.W., Hanson Jr. A.K. and Kester D.R., 1995. Stopped flow luminol chemiluminescence determination of Fe(II) and Reducible iron in seawater at subnanomolar levels. *Marine Chemistry* 49: 65-77
- Obata H., Karatani H., and Nakayama E., 1993. Automated determination of iron in seawater by chelating resin concentration and chemiluminescence detection. *Analytical Chemistry*, 65: 1524-1528.
- Obata H., Karatani H., Matsui M. and Nakayama E., 1997. Fundamental studies for chemical speciation of iron in seawater with an improved analytical method. *Marine Chemistry* 56: 97-106
- Obata H. and van den Berg C.M.G., 2001. Determination of Picomolar Levels of Iron in Seawater Using Catalytic Cathodic Stripping Voltammetry. *Analytical Chemistry* 73: 2522-2528

- Pachauri, R.K. & Reisinger, A. 2007. Climate Change 2007: Synthesis Report. Contribution of Working Groups I, II and III to the Fourth Assessment Report of the Intergovernmental Panel on Climate Change. *Cambridge, UK: Cambridge University Press.*
- Páscoa R.N.M.J., Tóth I.V. and Rangel A.O.S.S., 2009. A multi-syringe flow injection system for the spectrophotometric determination of trace levels of iron in waters using a liquid waveguide capillary cell and different chelating resins and reaction chemistries. *Microchemical Journal* 93: 153-158
- Petit J.R., Jouzel J., Raynaud D., Barkov N.I., Barnola J-M., Basile I., Bender M., Chappellaz J., Davisk M., Delaygue G., Delmotte M., Kotlyakov V.M., Legrand M., Lipenkov V.Y., Lorius C., Pépin L. Ritz C., Saltzman E. and Stievenard M. 1999. Climate and atmospheric history of the past 420,000 years from the Vostok ice core, Antarctica. *Nature* 399: 429-436
- Powell R.T., King D.W. and Landing W.M., 1995. Iron distributions in surface waters of the south Atlantic *Marine Chemistry* 50:13-20
- Qin W., Zhang Z. and Zhang C., 1998. Chemiluminescence Flow sensor with Immobilized Reagents for the Determination of Fe(III). *Mikrochimica Acta* 129: 97-101
- Rakestraw N.W., Mahncke H.E. and Beach E.F., 1936. Determination of Iron in Sea Water. *Industrial and Engineering Chemistry* 8(2): 136-138
- Rose A.L. and Waite T.D., 2001. Chemiluminescence of luminol in the presence of iron(II) and oxygen: Oxidation mechanism and implications for its analytical use. *Analytical Chemistry*, 73: 5909-5920.
- Rue E.L. and Bruland K.W., 1995. Complexation of iron(III) by natural organic ligands in the Central North Pacific as determined by a new competitive ligand equilibration/adsorptive cathodic stripping voltammetric method. *Marine Chemistry* 50: 117-138
- Ruth E.W., 2005, What is ICP-MS? ... and more importantly, what can it do? <http://crustal.usgs.gov/laboratories/icpms/intro.html>
- Saager P.M., de Baar H.J.W. and Burkill P.H., 1989. Manganese and iron in Indian Ocean. *Geochimica et Cosmochimica Acta* 53: 2259-2267
- Saito M.A., and Schneider D.L., 2006. Examination of precipitation chemistry and improvements in precision using the Mg(OH)₂ preconcentration inductively coupled plasma mass spectrometry (ICP-MS) method for high-throughput analysis of open-ocean Fe and Mn in seawater. *Analytica Chimica Acta*, 565: 222-233
- Sarthou G. and Jeandel C., 2001. Seasonal variations of iron concentrations in the Ligurian Sea and iron budget in the Western Mediterranean Sea. *Marine Chemistry* 74: 115-129
- Sarthou G., Baker A.R., Blain S., Achterberg E.P., Boye M., Bowie A.R. Croot P., Laan P., de Baar H.J.W., Jickells T.D and Worsfold P.J. 2003. Atmospheric iron deposition and sea-surface dissolved iron concentrations in the eastern Atlantic Ocean. *Deep-Sea Research I* 50: 1339-1352
- Sarthou G., Baker A.R. Kramer J., Laan P., Laës A., Ussher S., Achterberg E.P., de Baar H.J.W., Timmermans K.R. and Blain S., 2007. Influence of atmospheric inputs on iron distribution in the subtropical North-East Atlantic Ocean. *Marine Chemistry* 104: 186-202
- Sedwick P.N., DiTullio G.R. and Mackey D.J., 2000. Iron and manganese in the Ross Sea, Antarctica: Seasonal iron limitation in Antarctic shelf waters. *Jnr of Geophysical Research* 105: 11321-11336
- Segura R., Toral M.I. and Arancibia V., 2008. Determination of iron in water samples by adsorptive stripping voltammetry with a bismuth film electrode in the presence of 1-(2-pyridylazo)-2-naphthol. *Talanta* 75: 973-977

- Sunda W.G., 2001. Bioavailability and bioaccumulation of iron in the sea. In: *The Biogeochemistry of Iron in Seawater*. Turner D.R., and Hunter K.A., Chichester, John Wiley & Sons, IUPAC 7: 41-84.
- Thermal Elemental 2001, AAS, GFAAS, ICP or ICP-MS? Which technique should I use? An elementary overview of elemental analysis. www.thermalelemental.com
- Thompson T.G., Bremner R.W. and Jamieson I.M., 1932. Occurrence and Determination of Iron in Sea Water. *Industrial and Engineering Chemistry* 4(3): 288-290
- Ussher S.J., Yaqoob M., Achterber E.P., Nabi A. and Worsfold P.J., 2005. Effect of Modal Ligands on Iron Redox Speciation in Natural Waters Using Flow Injection with Luminol Chemiluminescence Detection. *Analytical Chemistry* 77: 1971-1978
- Ussher S.J., Milne A., Landing W.M., Attiq-ur-Rehman K., Séguret M.J.M., Holland T., Achterberg E.P., Nabi A., and Worsfold P.J., 2009. Investigation of iron(III) reduction and trace metal interferences in the determination of dissolved iron in seawater using flow injection with luminol chemiluminescence detection. *Analytica Chimica Acta* 652: 259-265
- Vink S., Boyle E.A., Measures C.I., and Yuan J., 2000. Automated high resolution determination of the trace elements iron and aluminium in the surface ocean using a towed Fish coupled to flow injection analysis. *Deep-Sea Research I*, 47(6): 1141-1156.
- Warnken K.W., Tang D., Gill G.A. and Santschi P.H., 2000 Performance optimization of a commercially available iminodiacetate resin for the determination of Mn, Ni, Cu, Cd and Pb by on-line preconcentration inductively coupled plasma-mass spectrometry. *Analytica Chimica Acta* 423: 265–276
- Watson A.J., 2001. Iron Limitation in the Oceans. In: *The biogeochemistry of iron in seawater*. Turner D.R., and Hunter K.A., Chichester, John Wiley & Sons, IUPAC 7: 9-39
- Weeks D.A. and Bruland K.W., 2002. Improved method for shipboard determination of iron in seawater by flow injection analysis. *Analytica Chimica Acta* 453: 21-32
- Witter A.E. and Luther III, G.W., 1998. Variation in Fe-organic complexation with depth in the North-western Atlantic Ocean as determined using a kinetic approach. *Marine Chemistry* 62: 241-258
- Wu J. and Bolye E.A., 1998. Determination of iron in seawater by high-resolution isotope dilution inductively coupled plasma mass spectrometry after Mg(OH)₂ coprecipitation. *Analytica Chimica Acta* 367: 183-191
- Wu J., 2007. Determination of picomolar iron in seawater by double Mg(OH)₂ precipitation isotope dilution high-resolution ICPMS. *Marine Chemistry* 103: 370-381
- Wu J., Wells M.L., and Rember R., 2011. Dissolved iron anomaly in the deep tropical-subtropical Pacific: Evidence for long-range transport of hydrothermal iron. *Geochimica et Cosmochimica Acta* 75: 460-468
- Xiao C., King D.W., Palmer D.A., and Wesolowski D.J., 2000. Study of enhancement effects in the chemiluminescence method for Cr(III) in the ng.l⁻¹ range. *Analytica Chimica Acta*, 415: 209-219.
- Xiao C., Palmer D.A., Wesolowski D.J., Lovitz S.B. and King D.W., 2002. Carbon Dioxide Effects on Luminol and 1, 10-Phenanthroline Chemiluminescence. *Analytical Chemistry* 74: 2210-2216
- Zhang J., Kelble C. and Millero F.J., 2001. Gas-segmented continuous flow analysis of iron in water with a long liquid waveguide capillary flow cell. *Analytica Chimica Acta* 438: 49-57

Appendices

Appendix 1

8-hydroxyquinoline preparation (after Dierssen *et al.*, (2001))

Reagents used:

Toyopearl TSK HW-65F (particle size 30 μ m) (Sigma Aldrich)

Epichlorohydrin (Merck)

5-amino-8-hydroxyquinoline (Sigma Aldrich)

Sodium hydroxide pellets (Merck)

Hydrochloric acid suprapur (Merck)

Procedure

10g wet Toyopearl TSK HW-65F (Toyopearl) was washed three times with MilliQ and allowed to dry at room temperature.

Epoxy activation

25ml of 10M NaOH added to 37ml MQ and then added to 38ml epichlorohydrin

Add 5g dried Toyopearl to the mixture

Allowed to react at 50°C for 2h while stirring slowly (avoid damage of particles)

Wash epoxy-activated resin with MQ by making use of a vacuum filtration system.

Acid washed glass fibre filter (GF/F, Whatman) was used to collect the resin.

8-HQ resin preparation

5g of 5-amino-8-hydroxyquinoline is added to 25ml MQ

10M NaOH is added slowly until pH 12

2.5g epoxy-activated resin was added and allowed to react at 80°C for 6h by making use of a rotovap.

Rinsing of the resin was done as follows:

The resin is washed by making use of a vacuum filtration system. An acid washed 20 μ m filter (Millipore) was used to retain the resin.

- 4x 25ml 0.5M NaOH, resin turned green
- 5x 25ml MQ

- 4x 25ml 1M HCl sp., resin turned red
- 5x 25ml MQ

If the resin was still bleeding the rinsing cycle was repeated until bleeding stopped.

Appendix 2

Output text file

Each column represents an individual .txt file of data acquired by the PMT associated with each elution time. Each individual number represents the amount of photos counted by the PMT and is known as the PMT counts.

429824	426992	447196	467140	472368	467224	495432	512660	523176
434260	431592	448132	467840	473492	470044	500124	515304	521084
435420	434544	447368	466216	472560	474068	502472	517812	520396
434568	435308	446516	467432	469716	474280	502172	518644	520516
433520	435252	447260	469448	468364	476412	500972	520236	523104
434516	434912	447616	470020	469280	473312	501176	517944	525264
435852	435820	448728	473884	472624	473040	502792	518760	527116
435036	435196	450272	472880	476228	472472	504952	515216	530360
437116	435564	450644	472668	479296	471356	506424	514704	528520
437756	436504	449052	471552	478020	474724	506172	516528	527260
440564	438272	446516	471208	478276	479076	507912	517748	525604
439108	441564	446648	472104	476740	479836	505560	520280	525864
438772	439352	448032	474860	474840	479656	504928	524192	527644
437052	440976	449896	475520	475072	478644	505648	524248	530628
437120	440144	453184	475848	478368	476220	508988	527048	531572
438608	439460	453868	476128	479628	476112	512368	527552	532148
439312	437296	454248	474240	479260	476896	515032	525884	529352
439432	436772	450272	470360	477380	474620	514132	524428	524324
432484	430072	442552	465664	471532	468964	506868	515252	518592
424844	421508	432264	458884	462104	464120	494088	501456	512964
418628	414888	421392	452888	457876	458624	483148	489388	506880
414488	415028	412996	450192	454336	461248	476896	482768	503172
412336	421640	409508	453792	455568	468872	473764	487392	501992
408912	429360	413416	460788	457776	472220	474076	497060	505856
410612	434928	425480	470008	461700	475028	476788	508084	513972
414032	435860	438932	481944	467924	474420	481944	519892	526700
427816	436464	453360	493352	481324	474288	496100	524604	543056
445712	436820	465308	499580	496544	479496	519684	530784	559984
466280	447100	472932	506148	512308	490480	549660	540900	571184
481472	464500	475512	514664	522636	503264	572996	559076	580872
489000	483344	479324	525324	525068	512612	586252	578436	587716
485316	494756	483672	529920	518444	514908	579164	592724	589500
474084	487220	486116	522896	504480	499744	551232	587060	581096
451924	458040	474116	494244	478744	467224	510080	549580	552984
425068	408864	444852	435164	436104	422468	459148	483024	501192
386440	350176	391960	362040	378792	372252	401180	401512	428928
334492	296280	324740	288360	313800	319628	338344	324896	347156
279024	248580	261996	230508	249028	271368	281904	267844	276020
223280	210720	214456	194120	199628	231448	234516	227940	228420
182132	185900	186836	175396	173128	205116	210728	211716	211460
163680	172700	179420	176520	172284	198856	220332	219504	224268
169100	178652	189288	198404	202704	222568	269628	257316	279464
201908	211200	224064	252892	271640	290360	380372	345648	386064

267852	285512	294396	356104	393732	418764	574712	510480	573812
377560	414836	412484	527956	595684	639268	8.81E+05	788608	864032
551200	627624	608940	7.98E+05	8.92E+05	9.68E+05	1.33E+06	1.23E+06	1.28E+06
7.93E+05	9.38E+05	9.00E+05	1.18E+06	1.28E+06	1.40E+06	1.89E+06	1.83E+06	1.84E+06
1.11E+06	1.34E+06	1.29E+06	1.68E+06	1.73E+06	1.89E+06	2.52E+06	2.55E+06	2.50E+06
1.51E+06	1.78E+06	1.79E+06	2.24E+06	2.23E+06	2.36E+06	3.16E+06	3.30E+06	3.25E+06
1.95E+06	2.20E+06	2.30E+06	2.77E+06	2.75E+06	2.77E+06	3.77E+06	3.95E+06	3.96E+06
2.44E+06	2.55E+06	2.76E+06	3.18E+06	3.21E+06	3.12E+06	4.31E+06	4.44E+06	4.54E+06
2.89E+06	2.85E+06	3.08E+06	3.45E+06	3.55E+06	3.43E+06	4.74E+06	4.78E+06	4.90E+06
3.24E+06	3.10E+06	3.26E+06	3.59E+06	3.73E+06	3.65E+06	4.99E+06	5.01E+06	5.02E+06
3.43E+06	3.29E+06	3.33E+06	3.67E+06	3.73E+06	3.76E+06	5.04E+06	5.13E+06	4.98E+06
3.47E+06	3.42E+06	3.36E+06	3.68E+06	3.63E+06	3.74E+06	4.91E+06	5.13E+06	4.87E+06
3.43E+06	3.40E+06	3.36E+06	3.64E+06	3.49E+06	3.60E+06	4.68E+06	5.00E+06	4.71E+06
3.36E+06	3.29E+06	3.31E+06	3.50E+06	3.34E+06	3.38E+06	4.43E+06	4.74E+06	4.53E+06
3.28E+06	3.09E+06	3.20E+06	3.29E+06	3.19E+06	3.15E+06	4.18E+06	4.41E+06	4.30E+06
3.18E+06	2.90E+06	3.01E+06	3.03E+06	3.04E+06	2.96E+06	3.95E+06	4.08E+06	4.02E+06
3.04E+06	2.73E+06	2.77E+06	2.79E+06	2.84E+06	2.79E+06	3.71E+06	3.79E+06	3.70E+06
2.83E+06	2.59E+06	2.53E+06	2.59E+06	2.63E+06	2.65E+06	3.45E+06	3.54E+06	3.38E+06
2.60E+06	2.46E+06	2.34E+06	2428904	2.40E+06	2.49E+06	3.17E+06	3.32E+06	3.11E+06
2366348	2.31E+06	2190392	2293104	2216320	2.31E+06	2.89E+06	3.10E+06	2.88E+06
2186976	2141568	2074844	2156284	2060216	2120052	2.66E+06	2.87E+06	2.69E+06
2049832	1965028	1967900	2000616	1938848	1953348	2.47E+06	2.63E+06	2533180
1944616	1803208	1843088	1837192	1839020	1817464	2.33E+06	2406548	2368760
1844200	1683484	1708024	1693780	1729832	1715184	2.20E+06	2227376	2194912
1729848	1590960	1576924	1578668	1616088	1635388	2069504	2082420	2024288
1593044	1519664	1462016	1493476	1501380	1555200	1919588	1966204	1866600
1460000	1448224	1381724	1426168	1394084	1465828	1767392	1855376	1745780
1348864	1361584	1318116	1361592	1310968	1373276	1632644	1740064	1652468
1271532	1264116	1263800	1294792	1247948	1284996	1530256	1608080	1573024
1215304	1176068	1202536	1213812	1196752	1210032	1452836	1484808	1498172
1166504	1104328	1134932	1132896	1148656	1159984	1393512	1383784	1409616
1116600	1058648	1064024	1066960	1095704	1118960	1337868	1313980	1318140
1050932	1019800	1003080	1021280	1034604	1079228	1270576	1264384	1232508
979720	986340	961672	990684	977556	1030416	1196076	1223436	1166844
916992	945032	928400	962980	931880	972072	1125084	1176588	1120988
873432	894220	905080	933072	898600	919972	1072308	1118260	1089496
847764	842212	875976	892912	878696	874924	1036304	1054120	1060816
831504	803020	837168	848416	860632	849876	1012988	1000784	1022652
815844	777288	797956	810924	837364	833468	990572	963952	982608
789036	764016	760400	786804	806404	818476	960284	941344	935212
752672	751092	734548	774584	771624	801024	915716	925408	899604
715064	733444	721084	763744	743944	768684	875544	907752	876592
687076	706632	711696	754308	728884	735988	838020	881320	861488
671328	675140	703044	732464	718908	709292	819600	842532	850776
668568	649820	685104	707740	710776	696128	808932	807260	838884
663980	634056	657620	682740	703940	692908	806376	786148	816812
653264	630484	631220	670132	685660	691000	798904	775156	791976
635188	630184	609920	662320	661960	687368	779864	774552	768332
611704	626632	604020	661064	644840	672092	752648	772552	754716
592164	614156	604668	657756	634580	650392	728828	761932	748012

586996	594444	607232	647804	631504	629936	714448	742844	748240
587868	576424	606620	631512	631740	619060	711076	721168	745528
590644	563544	592216	614988	631504	617872	712936	703736	735152
589780	563520	577064	602724	628116	622360	711052	698104	720568
579416	568736	562232	601880	612524	626584	701648	697752	704552
562072	569424	561260	605808	600696	620632	682536	702528	693640
545700	565748	568640	609528	591108	606312	664052	700848	692460
539420	553200	578072	607724	590804	591952	652424	690464	694456
540960	536300	583888	599312	594380	580624	654104	672844	697296
548180	527836	578252	582976	599140	578220	658560	656288	691084
550984	525944	563948	569684	594700	584960	667288	648672	679500
545020	531116	545692	565932	585036	590732	664820	651088	663740
531992	536984	535452	568376	573588	593020	651776	659896	652164
515908	539432	534092	574920	562388	587212	634064	663392	650680
507000	532788	539692	580736	561832	574320	622048	659196	656104
509196	519948	542648	578776	564680	565040	620668	643280	661756
516616	506988	540992	570140	571716	560756	626180	627944	661064
523800	505268	531736	554020	573544	566240	636496	617248	655348
524196	509368	522416	548972	569276	571652	642212	618680	641048
518256	516252	515644	549852	560008	575412	634280	625604	629580
500080	521628	514552	557996	549472	573268	621876	638184	624896
485628	519360	523136	564552	546516	563256	606976	640996	629996
484572	508508	528152	567400	550160	553696	604116	635380	636728
491016	497672	529860	560144	556548	547624	605192	622724	641512
501244	492420	525840	551452	562848	550532	615556	610648	642232
509524	495256	513900	543616	561044	558808	622356	606700	633460

Appendix 3

Table 1: Representing the data for Figure 4.2.

Depth (m)	Peak height		Integral	
	Conc. (nM)	Std	Conc.(nM)	Std
0	0.751	0.014	0.484	0.006
30	0.383	0.036	0.249	0.029
50	0.884	0.046	0.601	0.015
100	0.299	0.020	0.215	0.019
200	0.338	0.037	0.248	0.031
300	0.791	0.006	0.595	0.002
500	0.391	0.007	0.307	0.014
750	0.400	0.016	0.326	0.019
1500	0.547	0.004	0.473	0.010
2000	0.441	0.015	0.395	0.019
3000	0.641	0.023	0.592	0.018
4000	0.477	0.019	0.443	0.020

Appendix 4

Table 1: Displays all the concentrations which have been measured for the SANAE 51 cruise (dFe & TdFe). Values in bold indicate values which show contamination.

Sample #	Latitude	Longitude	dFe (nM)	Std	TdFe (nM)	Std
CTN 21	-65.9805	-3.6905	0.641	0.069	0.427	0.038
CTN 25	-65.2802	-2.9981	2.778	0.098	4.928	0.104
CTN 29	-64.5439	-2.1941	0.352	0.006	0.982	0.041
CTN 33	-63.7285	-1.345	0.512	0.015	0.553	0.066
CTN 37	-62.9873	-0.6182	0.537	0.064	0.937	0.059
CTN 41	-62.2045	0.0957	0.421	0.029	0.520	0.031
CTN 45	-61.5025	0.6605	0.531	0.015	0.534	0.025
CTN 49	-60.7655	1.357	0.335	0.031	0.400	0.027
CTN 53	-60.0247	1.9337	2.144	0.882	2.487	0.314
CTN 57	-59.2356	2.5885	1.204	0.021	1.714	1.009
CTN 61	-58.416	3.1843	244.490		287.813	
CTN 65	-57.6588	3.8292	1.248	0.016	1.370	0.150
CTN 69	-56.9297	4.4184	1.652	0.137	2.236	0.148
CTN 73	-56.1113	5.047	0.580	0.026	1.257	0.014
CTN 77	-55.3553	5.5877	2.561	0.034	2.958	0.286
CTN 85	-53.7859	6.715	0.338	0.046	0.617	0.024
CTN 89	-53.0587	7.2146	0.401	0.035	0.430	0.011
CTN 93	-52.5613	7.6092	0.276	0.037	0.364	0.021
CTN 97	-52.2667	7.923	0.271	0.021	0.373	0.016
CTN 105	-51.3619	8.8338	0.490	0.005	0.611	0.005
CTN 112	-50.2867	9.631	0.290	0.039	0.292	0.029
CTN 113	-50.2067	9.67	0.394	0.011	0.594	0.027
CTN 132	-48.104	9.3729	0.693	0.053	0.918	0.011
CTN 136	-47.6032	9.79	3.107	0.195	3.621	0.170
CTN 143	-46.7919	11.1405	28.018		190.995	
CTN 144	-46.6585	11.3366	0.432	0.046	0.626	0.029
CTN 148	-46.1031	12.1169	0.378	0.011	0.515	0.022

Appendix 5

Cleaning protocol for LDPE bottles

(BOTTLE W/N PE, 50ml, Grad 10ml, Mouth I.D. 24mm; Plastpro Scientific)

- Bottles were soaked for one week in detergent (phosphors free) (Extran MA03(Merck)).
- Bottles rinsed seven times with MQ
- Bottles soaked in 6M HCl analytical grade for one month
- Bottles rinsed five times with MQ
- Bottles transported in double bag to clean laboratory
- Bottles soaked in 1M HCl sp. for one week
- Bottles rinsed three times in a class 100 laboratory with MQ
- Bottles stored with 0.1M HCl sp. in double zip lock bags

The polycarbonate (Thermo Fisher Scientific) bottles followed the same protocol.

Appendix 6

Operations protocol

Running a sample and operating the program

Sample preparation

- 1) 30ml sample is volumetrically determined and decanted into the sampling bottle (this is to prevent contamination from a new bottle used for analysis)
- 2) 30µl 0.1%_o H₂O₂ sp. solution is added to the sample (oxidizes all Fe species to Fe(III))
Shake well
 - a. Allow to equilibrate for at least 1h
- 3) Add buffer (Xµl as pre-determined to obtain final pH 4.7 for the sample) (Note: buffer weakens over time, and therefore needs to be regularly determined the volume added to the sample). Shake well.
- 4) Insert sample tubing into sample (take note that this can only be done during the rinsing or elution phase)
- 5) Repeat for next sample and replace sample bottle.

Software operation (this is a dos program)

- 1) Enter the program called QBasic
- 2) Press **Spacebar** twice
- 3) Press **ALT + F** and then **O**, (this will open a new window)
- 4) Press **Tab** and use the **Arrow keys** to highlight the IronBase file, press **Enter**
- 5) Press **F5** this will execute the program used to operate the valves and PMT.
- 6) Pressing **1** will allow to change the time duration for each position on the sample valve
 - a. Position 1 sample
 - b. Position 6 rinse
- 7) Pressing **2** will allow to change the elution time
- 8) Pressing **3** will give the option under which file name the data should be saved (this should not be longer than five characters)
- 9) Pressing **4** allows for the data to be printed
- 10) Pressing **5** executes the operation (Runs the program)
- 11) Pressing **6** exits program
- 12) During a cycle the program can be stopped by hitting **Any Key**. It will though finish that acquisition.
- 13) Record the baseline and the max value for each file name as well as the sample number.

Table 1: Record sheet example

File Name	e.g.Meg1	e.g.Meg2	e.g.Meg3
Sample #	e.g.123	e.g.123	e.g.123
Baseline	325010	326005	325091
Max value	1009638	1010631	1010023

Cleaning the system

- 1) Inset all the tubing into a 1M HCl sp.
- 2) Run the program for three cycles named "clean"
- 3) Insert all the tubing into MQ (rinse phase)
 - a. Store all the tubing in the MQ
- 4) Run program for one cycle named "MQ"

Once finished cleaning release the clamps on the pump, and bring the waste line tubing above the pump.

Excel sheet

All data is added into the excel sheet, with the standards under the standard columns, and the samples under the sample section. This excel sheet has a macros imbedded which give the concentrations on sheet 3 when activated.